OCT 20 1995

ENGINEERING DATA TRANSMITTAL

Page 1 of 1

1. EDT 603711

2. To: (Receiving Organization)	3. From: (Originating Organization)	4. Related EDT No.:
TWRS Design Basis Integration	Analytical Services	N/A
5. Proj./Prog./Dept./Div.:	**6. Cog. Engr.:**	**7. Purchase Order No.:**
TWRS	C. J. Moore	N/A
8. Originator Remarks: Approval/Release		**9. Equip./Component No.:** N/A
		10. System/Bldg./Facility: N/A
11. Receiver Remarks:		**12. Major Assm. Dwg. No.:** N/A
		13. Permit/Permit Application No.: N/A
		14. Required Response Date: N/A

15. DATA TRANSMITTED

(A) Item No.	(B) Document/Drawing No.	(C) Sheet No.	(D) Rev. No.	(E) Title or Description of Data Transmitted	(F) Approval Designator	(G) Reason for Transmittal	(H) Originator Disposition	(I) Receiver Disposition
1	WHC-SD-WM-DA-208		0	Soil Structural Analysis Tools and Properties for Hanford Site Waste Tank Evaluation	N/A	1	1	1

16. KEY

Approval Designator (F)	Reason for Transmittal (G)	Disposition (H) & (I)
E, S, Q, D or N/A (see WHC-CM-3-5, Sec 12.7)	1. Approval 4. Review 2. Release 5. Post-Review 3. Information 6. Dist. (Receipt Acknow. Required)	1 Approved 4 Reviewed no/comment 2 Approved w/comment 5 Reviewed w/comment 3 Disapproved w/comment 6 Receipt acknowledged

17. SIGNATURE/DISTRIBUTION (See Approval Designator for required signatures)

(G) Reason	(H) Disp.	(J) Name	(K) Signature	(L) Date	(M) MSIN	(J) Name	(K) Signature	(L) Date	(M) MSIN	(I) Reason	(I) Disp
1	1	Cog.Eng. C... Moore									
1	1	Cog. Mgr. R. N. Boger			H5-57						
		QA									
		Safety									
		Env.									
1	1	M.A. Scott			H5-52						

18.	19.	20.	21. DOE APPROVAL (if required) Ctrl. No.
C.J. Moore 10/3/95 Signature of EDT Originator Date	K.V. Scott 10-11-95 Authorized Representative for Receiving Organization Date	B.N. Boger Cognizant Manager Date	☐ Approved ☐ Approved w/comments ☐ Disapproved w/comments

THIS PAGE INTENTIONALLY
LEFT BLANK

RELEASE AUTHORIZATION

Document Number:	WHC-SD-WM-DA-208, Rev. 0
Document Title:	Soil Structure Analysis Tools and Properties for Hanford Site Waste Tank Evaluation
Release Date:	10/19/95

This document was reviewed following the procedures described in WHC-CM-3-4 and is:

APPROVED FOR PUBLIC RELEASE

WHC Information Release Administration Specialist:

James B. Bishop — 10/19/95

THIS PAGE INTENTIONALLY
LEFT BLANK

SUPPORTING DOCUMENT

1. Total Pages 147

2. Title	3. Number	4. Rev No.
Soil Structure Analysis Tools and Properties for Hanford Site Waste Tank Evaluation	WHC-SD-WM-DA-208	0

5. Key Words

Soil
Sand
Soil Springs
Drucker-Prager

6. Author

Name: C. J. Moore

Signature

Organization/Charge Code N1531 5A620/~~E47026~~

7. Abstract

As Hanford Site contractors address future structural demands on nuclear waste tanks, built as early as 1943, it is necessary to address their current safety margins and ensure safe margins are maintained. Although the current civil engineering practice guidelines for soil modeling are suitable as preliminary design tools, future demands potentially result in loads and modifications to the tanks that are outside the original design basis and current code based structural capabilities. For example, waste removal may include cutting a large hole in a tank.

The Hanford Site engineering staff requires accurate soil evaluation tools (best estimate plus accurate understanding of Hanford Site soil variability) that are suitable to compliment nonlinear analytical tools that have been developed to model reinforced concrete. This document is a first effort by the authors to bring together and integrate past Hanford Site structural analysis methods, past Hanford Site soil testing, public domain research testing, and current soil research directions. This document, including future revisions, will become the structural engineering overview (or survey) for a consistent accurate approach to soils structural modeling for Hanford Site waste storage tanks.

This report addresses both spring modeling of site soils and finite-element modeling of soils. Additionally seismic dynamic modeling of Hanford Site soils is also included. Of new and special interest is Section 2.2 that Prof. Robert D. Holtz of the University of Washington wrote on plane strain soil testing versus triaxial testing with Hanford Site application to large buried waste tanks.

8. RELEASE STAMP

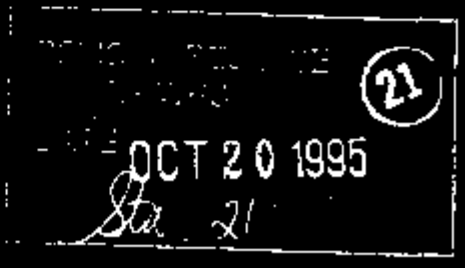

THIS PAGE INTENTIONALLY
LEFT BLANK

WHC-SD-WM-DA-208
Revision 0

SOIL STRUCTURAL ANALYSIS TOOLS AND PROPERTIES

for HANFORD SITE WASTE TANK EVALUATION

September 1995

PREPARED BY:

C. J. Moore, Principal Engineer
Analytical Services — Date: 10/2/95

R. D. Holtz, Professor
University of Washington — Date: 29 Sept 95

G. R. Wagenblast, Principal Engineer — Date: 10/2/95

REVIEWED BY:

K. C. Tu, Principal Engineer — Date: 10/3/95

APPROVED BY: — Date: 10/13/95

Prepared by: ICF Kaiser Hanford Company
Richland, Washington
for
Westinghouse Hanford Company
Richland, Washington

THIS PAGE INTENTIONALLY
LEFT BLANK

WHC-SD-WM-DA-208
Revision 0

SOIL STRUCTURAL ANALYSIS TOOLS AND PROPERTIES for HANFORD SITE WASTE TANK EVALUATION

September 1995

C. J. Moore
R. D. Holtz
G. R. Wagenblast
with contributions by: E. O. Weiner and R. S. Marlow

Prepared by: ICF Kaiser Hanford Company
Richland, Washington
for
Westinghouse Hanford Company
Richland, Washington

THIS PAGE INTENTIONALLY
LEFT BLANK

CONTENTS

LIST OF FIGURES

LIST OF FIGURES (continued)

LIST OF TABLES

SOIL STRUCTURAL ANALYSIS TOOLS AND PROPERTIES for HANFORD SITE WASTE TANK EVALUATION

1.0 INTRODUCTION

As Hanford Site contractors address future structural demands on nuclear waste tanks, built as early as 1943, it is necessary to address their current safety margins and ensure safe margins are maintained. Although the current civil engineering practice guidelines for soil modeling are suitable as preliminary design tools, future demands potentially result in loads and modifications to the tanks that are outside the original design basis and current code based structural capabilities. For example, waste removal may include cutting a large hole in a tank.

The Hanford Site engineering staff requires accurate soil evaluation tools (best estimate plus accurate understanding of Hanford Site soil variability) that are suitable to compliment nonlinear analytical tools that have been developed to model reinforced concrete. This document brings together and integrates past Hanford Site structural analysis methods, past Hanford Site soil testing, public domain research testing, and current soil research directions. This document, including future revisions, provides the structural engineering overview (or survey) for a consistent accurate approach to soils structural modeling for Hanford Site waste storage tanks.

Included in this document are examples of past Hanford Site soil modeling. Although the examples provide valuable historical information, application of older analyses of record in evaluating new load applications should consider the soil responses to applied loads addressed in this report. A single soil stiffness, that provides conservatism in the evaluation of structural integrity for all the regions of every tank, cannot be selected. The data must be evaluated for suitability and reduced, if necessary, for structural model input using the tools described herein. The Hanford Site has historical soil test data that might be applicable to a specific application (Giller 1992).

This page intentionally left blank.

2.0 STATIC MODELING OF HANFORD SITE SOIL

2.1 TRIAXIAL SOIL TESTING PROPERTIES

All soil constitutive models contain parameters that must be calibrated from test data. Dames & Moore (1988) conducted triaxial compression tests for the Grout Vault Project soil and provided graphs of stress versus strain at three different confining pressures (see Figures 2-1, 2-2 and 2-3).

2.1.1 Soil Moduli and Power Equation Variation with Depth

The University of California at Berkeley has done considerable research on soil constitutive modeling (Wong and Duncan 1974, Duncan et al. 1980, Seed and Duncan 1983). The goal has been to develop a model suitable for finite-element analysis that properly models the soil-structure interaction as well as the lateral loads introduced by soil compaction. The Berkeley research employed the existing soil triaxial test procedures with confining pressures and developed the hyperbolic model for the soil stress-strain relation and bulk moduli (Wong and Duncan 1974, Duncan et al. 1980).

The Berkeley hyperbolic model has been used at the Hanford Site to interpolate and extrapolate limited triaxial test data to provide soil moduli and strength data at various depths and confining pressures. The hyperbolic model was also recommended for similar use for foundation design in a Cornell University report funded by the Electric Power Research Institute (Kulhawy and Mayne 1990).

The model assumes that stress-strain curves for soils can be approximated as hyperbolae, shown in Figure 2-4. The local slope of the hyperbolic stress-strain curve is the tangent modulus E_t. The hyperbolic model is really a family of hyperbolic stress-strain curves that shift with confining pressure or stress (σ_3) and the axial compression stress minus the confining pressure (σ_1-σ_3):

$$E_t = (1-R_f\ SL)^2\ K\ P_a \left(\frac{\sigma_3}{P_a}\right)^n, \qquad (2\text{-}1)$$

where

R_f = constant (0.6 to 0.9)
SL = ratio of deviatoric stress to deviator stress at Mohr-Coulomb failure
K, n = material constants
P_a = atmospheric pressure (normalization factor).

Figure 2-1. Consolidated - Drained Triaxial Test Data.

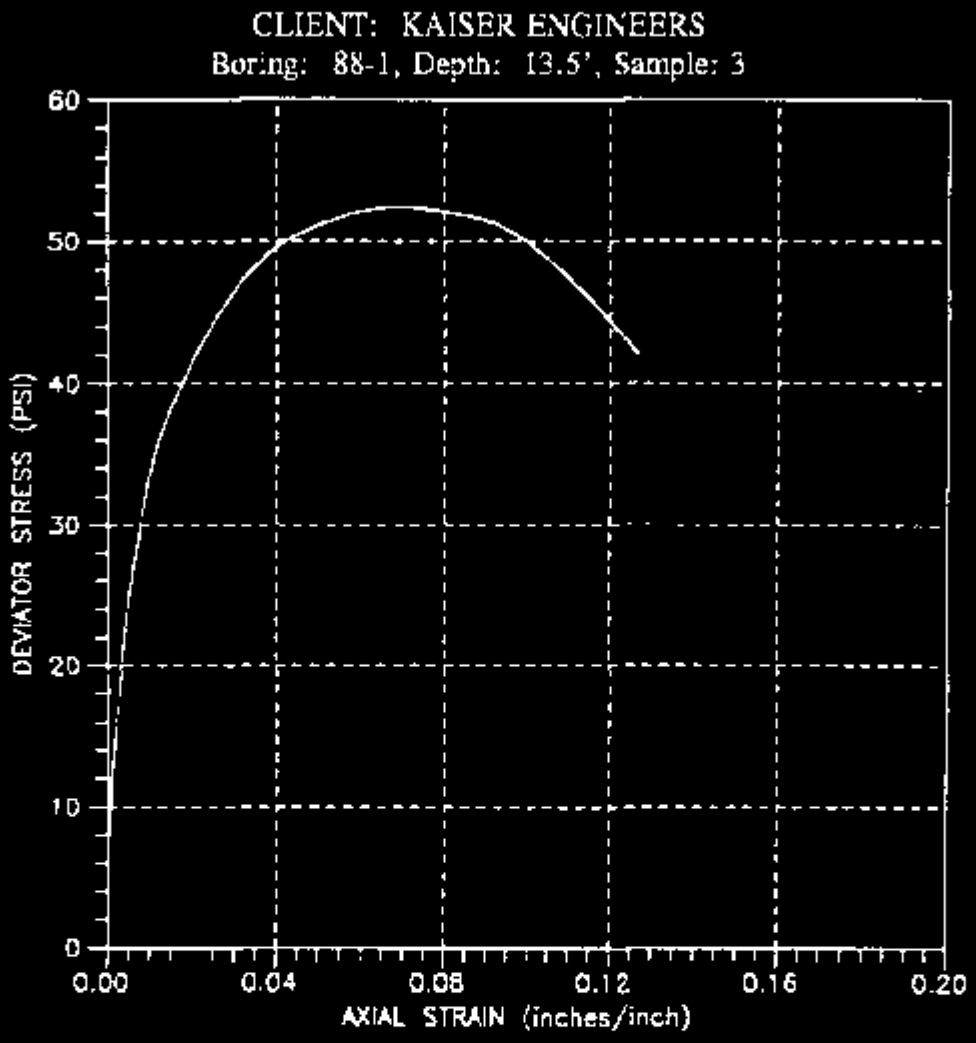

SUMMARY OF SAMPLE DATA:					
Moisture Content	=	9.5 %			
Wet Density	=	100.9 pcf	Initial Height	=	5.00 in
Dry Density	=	94.3 pcf	Final Height	=	4.37 in

SUMMARY OF TEST DATA:
Confining Pressure = 13.9 psi
Peak Deviator Stress = 52.0 Psi
Tangent Modulus = 7570 psi (No. of Cycles - 0)

DESCRIPTION: LIGHTLY CEMENTED BROWN FINE SAND W/TRACE SILT (SP/SM)

October 10, 1988 DAMES & MOORE

Figure 2-2. Consolidated - Drained Triaxial Test Data.

CLIENT: KAISER ENGINEERS
Boring: 88-1, Depth: 19.5', Sample: 4

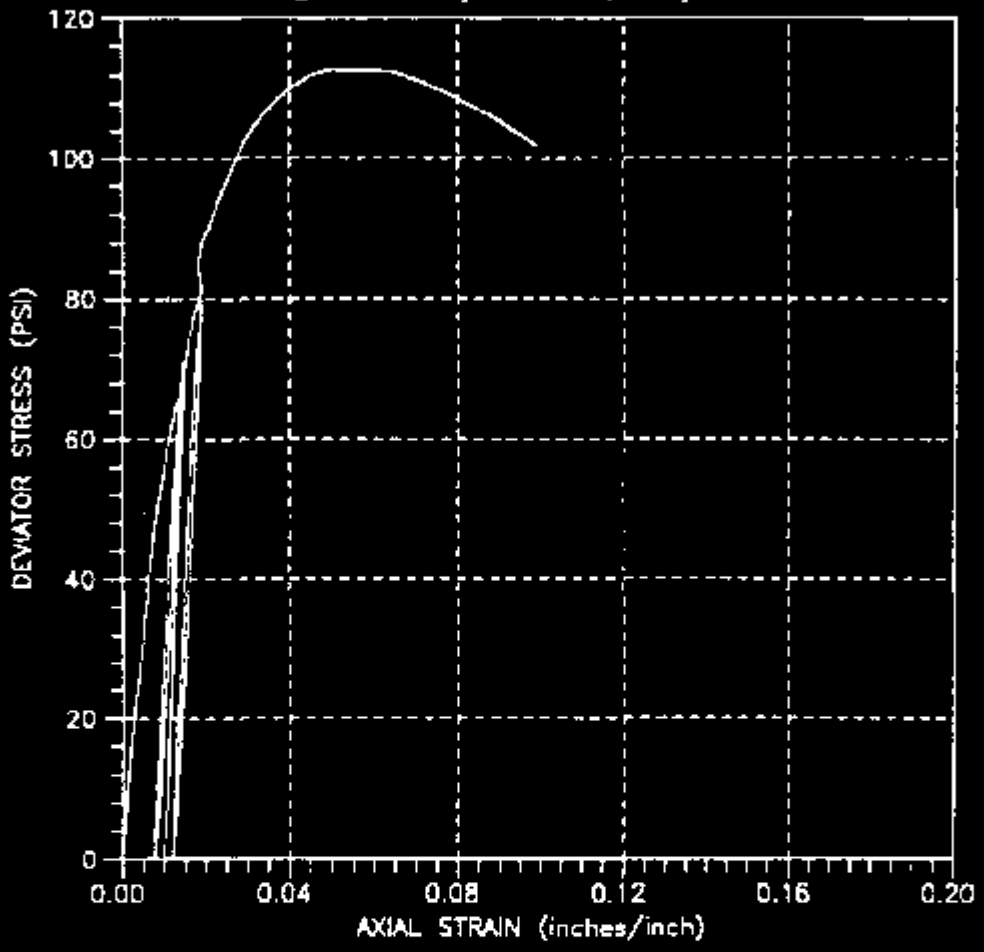

SUMMARY OF SAMPLE DATA:					
Moisture Content	=	11.5 %			
Wet Density	=	112.2 pcf	Initial Height	=	5.10 in
Dry Density	=	100.5 pcf	Final Height	=	4.60 in

SUMMARY OF TEST DATA:
Confining Pressure = 27.8 psi
Peak Deviator Stress = 116.0 Psi
Tangent Modulus = 17,000 psi (No. of Cycles = 3)

DESCRIPTION: LIGHTLY CEMENTED BROWN FINE SAND W/TRACE SILT (SP/SM)

October 10, 1988 DAMES & MOORE

Figure 2-3. Consolidated - Drained Triaxial Test Data.

CLIENT: KAISER ENGINEERS
Boring: 88-1, Depth: 33.5', Sample: 7

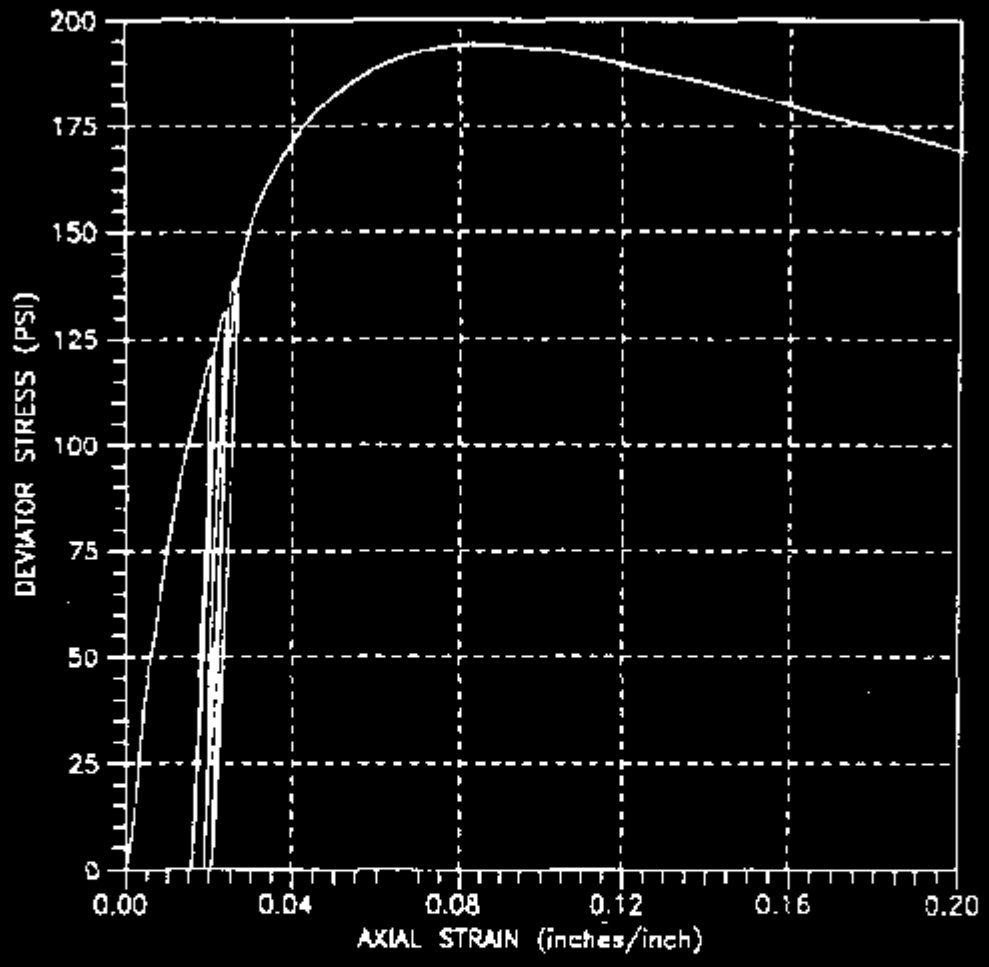

SUMMARY OF SAMPLE DATA:					
Moisture Content	=	12.7 %			
Wet Density	=	109.8 pcf	Initial Height	=	5.00 in
Dry Density	=	99.3 pcf	Final Height	=	4.00 in

SUMMARY OF TEST DATA:
Confining Pressure = 55.6 psi
Peak Deviator Stress = 190.0 Psi
Tangent Modulus = 28,200 psi (No. of Cycles - 3)

DESCRIPTION: LIGHTLY CEMENTED BROWN FINE SAND W/TRACE SILT (SP/SM)

October 10, 1988 DAMES & MOORE

The modulus modeled in this manner increases with increasing confining pressure and decreases with increasing deviatoric stress. The hyperbolic model uses this tangent modulus to model primary loading where the loading occurs at a stress level equal to or higher than all previous stress levels.

Triaxial test data from the Grout Vault soil show that, when the stress unloaded level is less than the previous maximum stress, the soil no longer follows the primary load curve. The soil responds along the unload-reload path (Figure 2-1b) that is defined by the unload-reload modulus as follows:

$$E_{ur} = K_{ur}\, P_a \left(\frac{\sigma_3}{P_a}\right)^n, \qquad (2\text{-}2)$$

where

E_{ur} = unload-reload elastic modulus in consistent units
K_{ur} = nondimensional constant = 726.2
p_a = atmospheric pressure in consistent units
p_3 = confining pressure in consistent units
n = power constant = .730.

The original hyperbolic model assumes that the bulk modulus, B, of the soil is independent of the deviatoric stress and depends on confining pressure as follows:

$$B = K_B\, P_a \left(\frac{\sigma_3}{P_a}\right)^m, \qquad (2\text{-}3)$$

where K_B and m are nondimensional material constants.

2.1.2 Sandy Soil Poisson's Ratio

To complete the Hanford Site soil properties description requires volume-change data to determine the dilation angle and Poisson's ratio. Such data are not included in the Dames & Moore report. However, the test reports do contain enough information to define the internal angle of friction, Young's modulus, and the material yield stress. These parameters, along with Poisson's ratio, completely describe the classical material properties.

Figure 2-4. Hyperbolic Soil Model (a) Stress-Strain Curve for Primary Loading and (b) Linear Unloading-Reloading Stress-Strain Relationship.

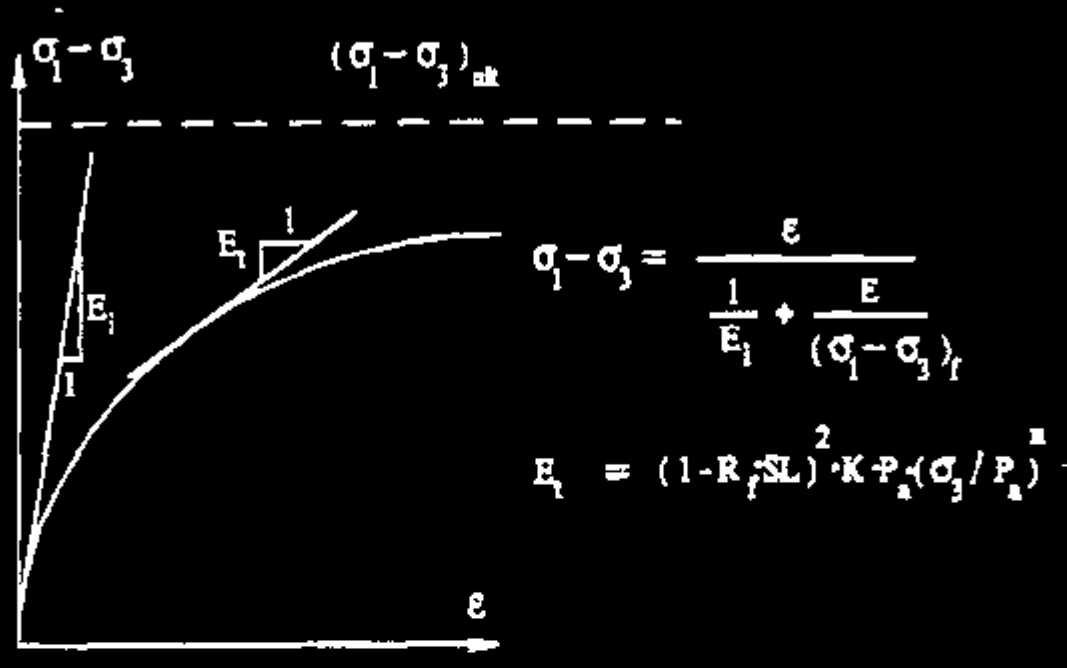

(a) Hyperbolic Representation of Stress-Strain Curve for Primary Loading.

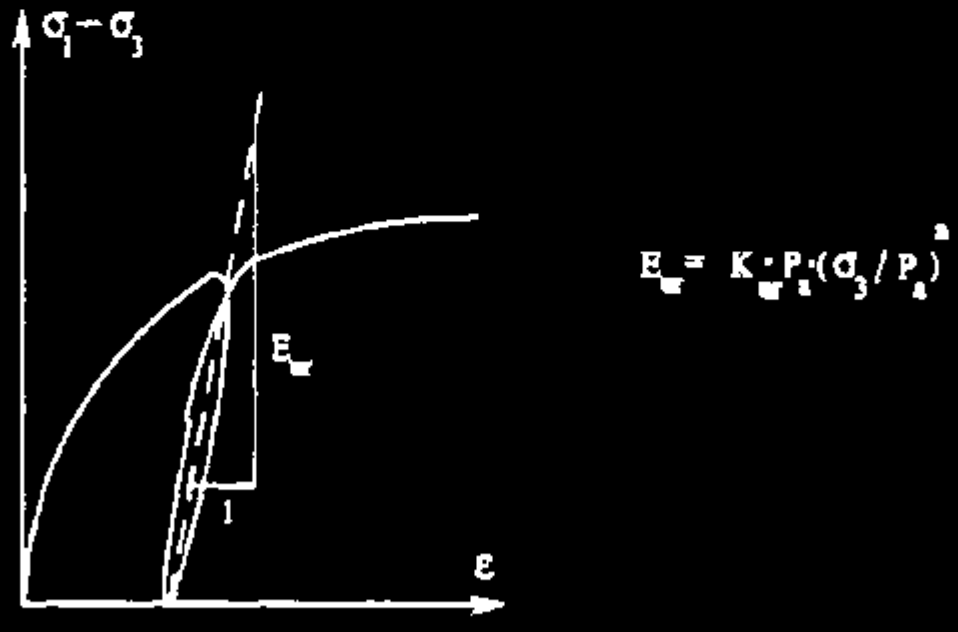

(b) Linear Unloading-Reloading Stress-Strain Relationship.

Although volume-change data were not recorded for the Hanford Site triaxial testing, volume-change data have been found for triaxial testing of sandy soil in Japan (Kitamura and Haruyama 1988). The trends of stress-strain behavior for the Japanese sandy soil are similar to the trends from the Hanford Site Grout Vault sandy soil tests. The volumetric data for high confining pressures from the Japanese sandy soil tests exhibit the classic behavior with a Poisson's ratio of 0.27 at zero strain and approaches 0.5 at plastic failure. The data for low confining pressures of approximately 28 lbf/in^2 showed a significant shift in Poisson's ratio approaching the plastic failure value during the triaxial compression test.

2.2 PLANE STRAIN TESTING SOIL PROPERTIES

2.2.1 Introduction

In the 241-C-106 report (Julyk et al. 1993), the loading conditions on the tanks were "defined as axisymmetric because the in situ loads are essentially axisymmetric." However, there is some question as to whether the soil loading conditions on the sidewalls of the tanks are in fact axisymmetric, and therefore, whether it is appropriate to conduct all the proposed analyses within an axisymmetric framework. Because the diameter of most of the tanks is 75 ft, conditions at the sides of the tanks are approaching plane strain conditions (the actual plane strain test sample is closer to the condition including confinement, than the small cylinder of the triaxial test). This can be seen in Figure 2-5, in which an arc of a circle 37.5 ft in radius has been drawn. The arc appears to be almost a straight line. The soil element sketched near the tank wall can only undergo movement in the direction of the tank wall, and not laterally. Thus, the element when subjected to in situ loads will be essentially in plane strain, not axisymmetric.

For this reason, a review of plane strain soils testing was carried out. The objective was to see if and how much the basic soil properties are different when tested in plane strain rather than conventional triaxial compression testing. An additional consideration was to determine how plane strain soil properties might be implemented in the Drucker-Prager constitutive models being used for the finite-element analyses of the tank-soil interaction.

Figure 2-5. Plan View of Tank Wall.

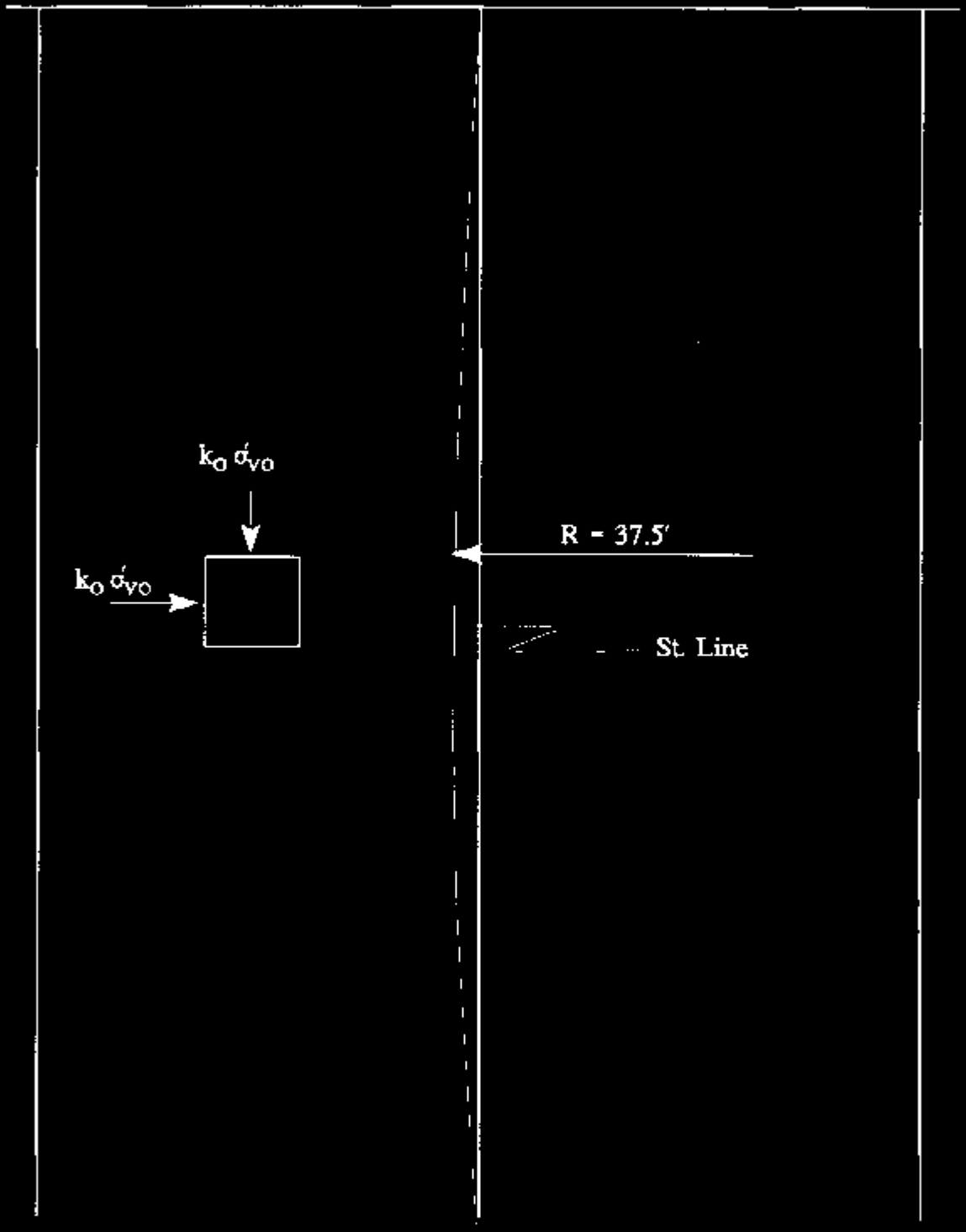

2.2.2 Background on Plane Strain Testing

Saada and Townsend (1980) reviewed the test devices designed primarily for plane strain testing, that have been developed by several researchers since the 1950s. The devices test a cube or parallelepiped of soil, in which the two opposite faces of the prism are prevented from moving while pressures are applied to the other two sets of faces. The end platens are either lubricated or the dimensions of the prism are large enough so that the stationary faces can be assumed to be the intermediate principal planes. Figure 2-6 shows the stress conditions in plane strain, while Figure 2-7 shows a plane strain test specimen in the University of California, Berkeley, device.

2.2.3 Review of Plane Strain Testing on Sands

A review of the soil mechanics literature on plain strain testing granular materials was conducted, and the following is a summary of pertinent work. Emphasis is on the strength and modulus properties in plain strain (PS) versus triaxial compression (TC).

Cornforth (1964) reported on a comprehensive testing program of PS and TC on a rather uniform medium sand over a wide range of densities. Results of interest to this project are shown in Figures 2-8 and 2 9. The angle of internal friction in plane strain is somewhat higher than in triaxial compression, especially at higher densities (lower void ratios and porosities). That the axial strain at failure is being significantly lower in plane strain (Figure 2-8c) indicates that the PS modulus is likely to be much greater than the TC modulus, and this is indeed the case, as indicated by the test results shown in Figure 2-9. In addition, the peak strengths are markedly greater, especially at higher densities. Because of the small size of the figures as published, no attempt was made to determine initial target moduli, but estimates of the peak secant moduli could be scaled from the figures. The ratios of this modulus in plane strain to the corresponding triaxial modulus was between 3 and 4.6; the lower values were for the higher densities.

Sultan and Seed (1967), in a study of the stability of sloping core earth dams, reported on the results of some PS and TC compression tests on two sands over a range of void ratios (Figure 2-10).

Green and Reades (1975) conducted a wide range of both TC and PS tests on sand, and their results essentially confirmed earlier work on the PS versus TC friction angle (Figure 2-11). These results were confirmed by Oda et al. (1978) who studied anisotropy in sands by PS tests (Figure 2-12).

Figure 2-6. Stresses in Plane Strain Conditions.
(Saada and Townsend 1981)

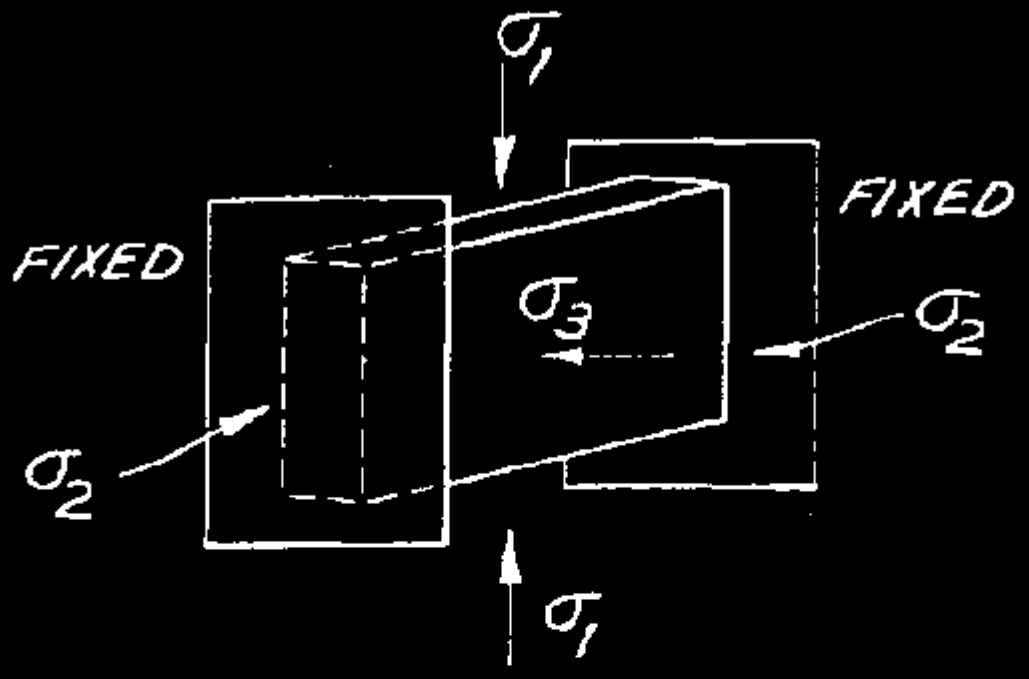

Figure 2-7. Plane Strain Specimen.
2.6 cm wide by 21.6 cm long by 10.1 cm high (Marachi et al. 1981)

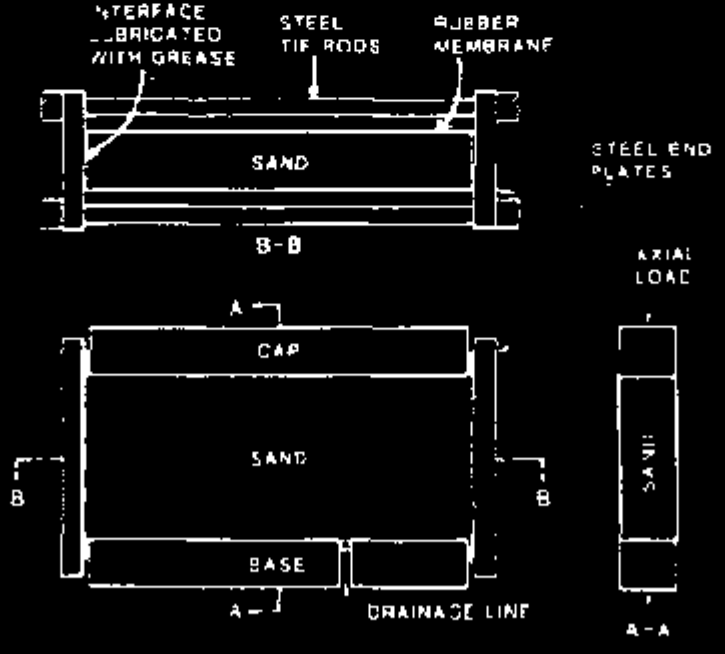

Figure 2-8. Comparison of Plane Strain and Triaxial Failure Characteristics. (Cornforth 1964)

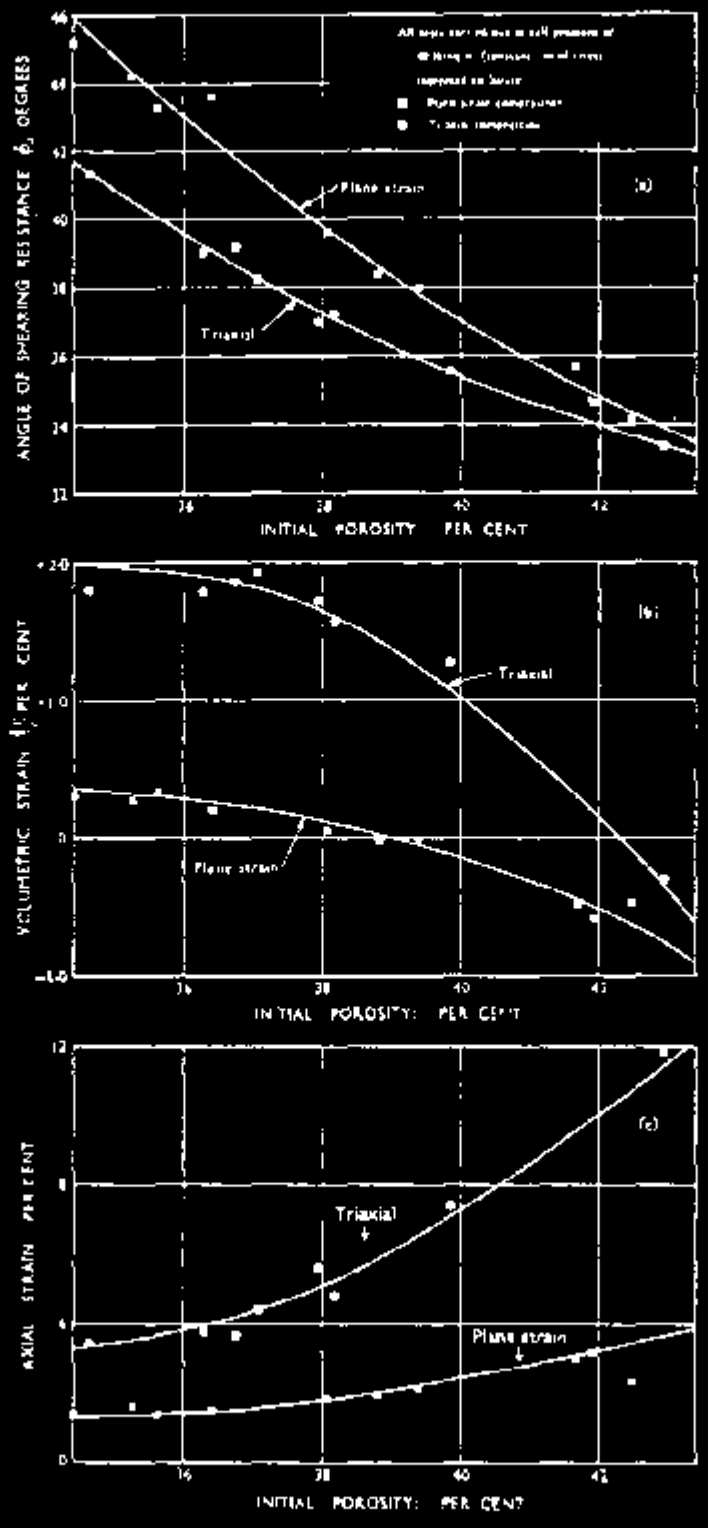

Figure 2-9. Comparison of Plane Strain and Triaxial Compression Tests at Different Sand Densities.

(a) Dense: Relative Property 80 percent, (b) Medium Dense: Relative Porosity 63 percent, (c) Loose Medium: Relative Porosity 40 percent, (d) Loose: Relative Porosity 15 percent (Cornforth 1964).

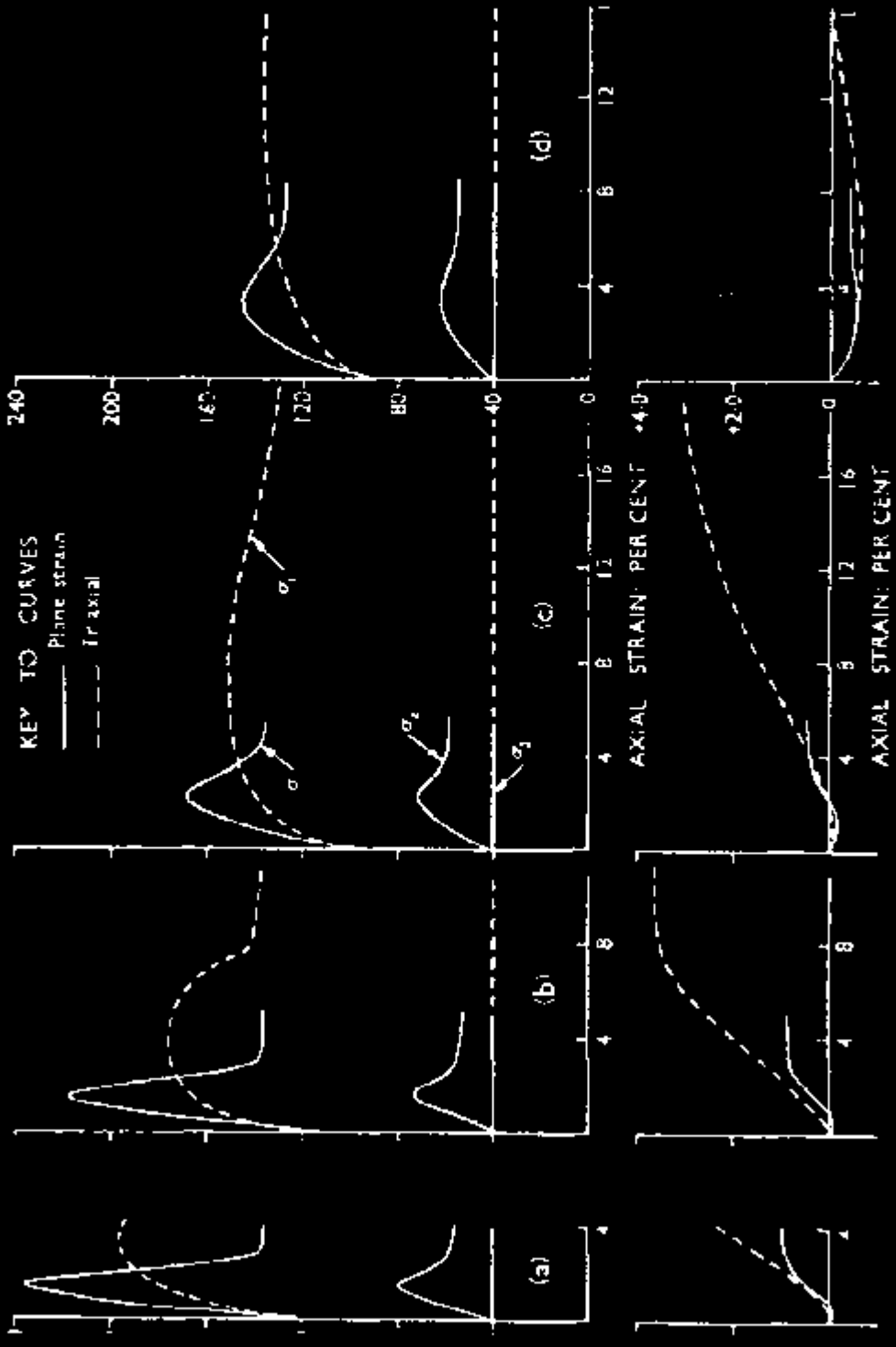

Figure 2-10. Relationship Between Angle of Internal Friction and Void Ratio For Monterey and Ottawa Sands. (Sultan and Seed 1967)

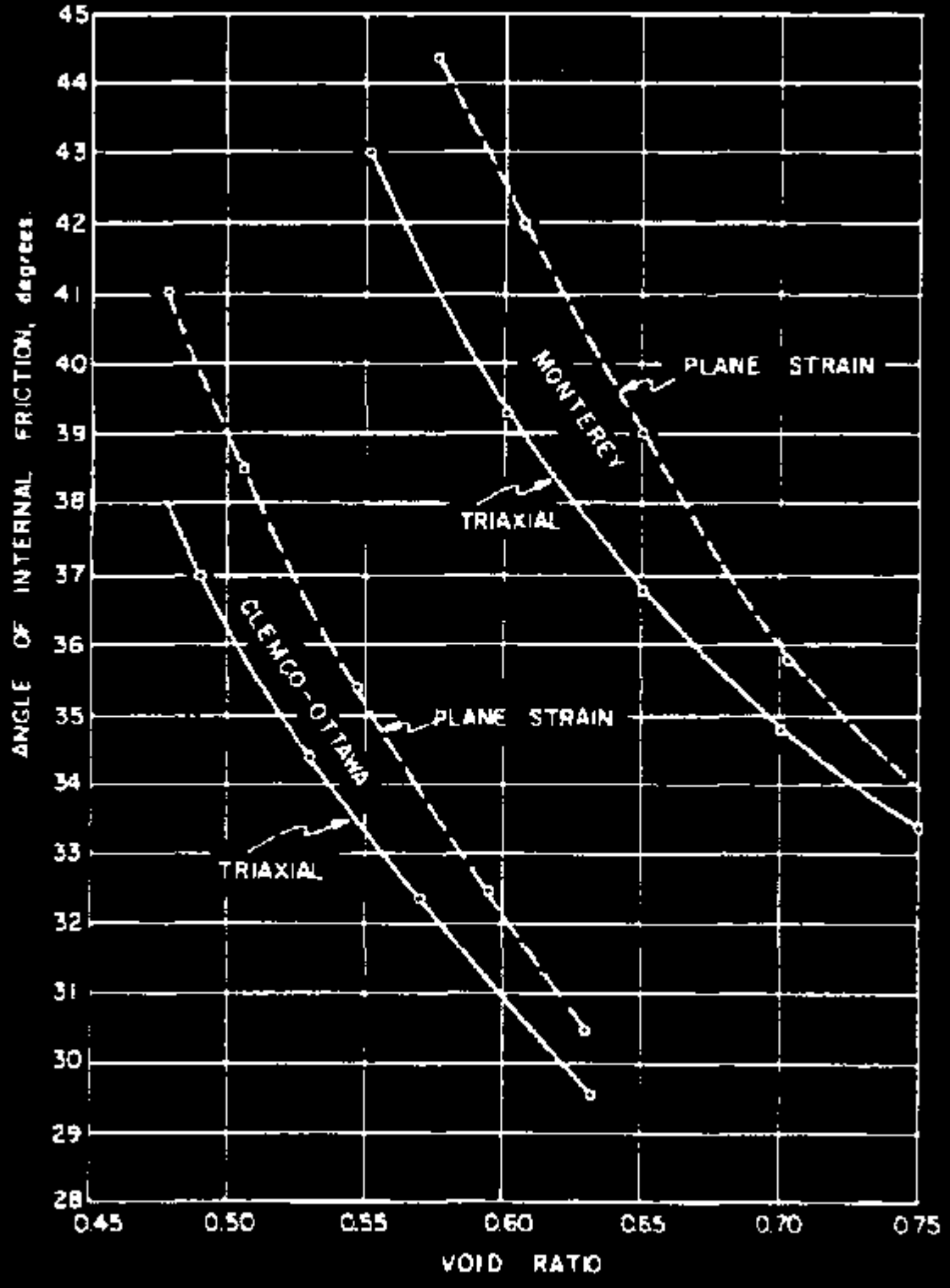

Figure 2-11. Peak Strengths From Drained Vertical Plane Strain Tests and Triaxial compression Tests on Rectangular Samples. (Green and Reades 1975)

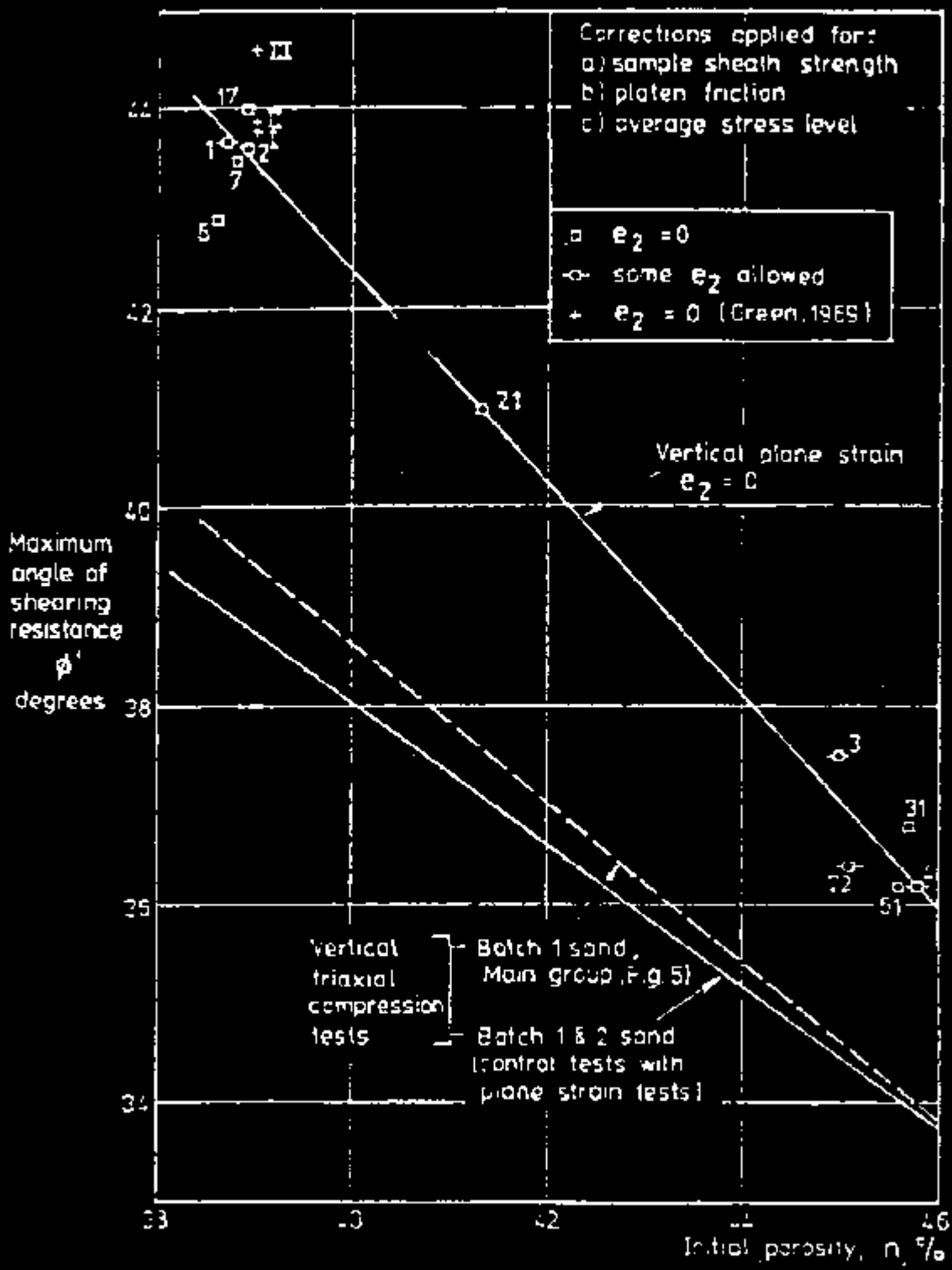

Figure 2-12. Compiled Figure of the Mohr's Failure Envelopes in the Plane Strain and Triaxial Compression Tests. (Oda et al. 1978)

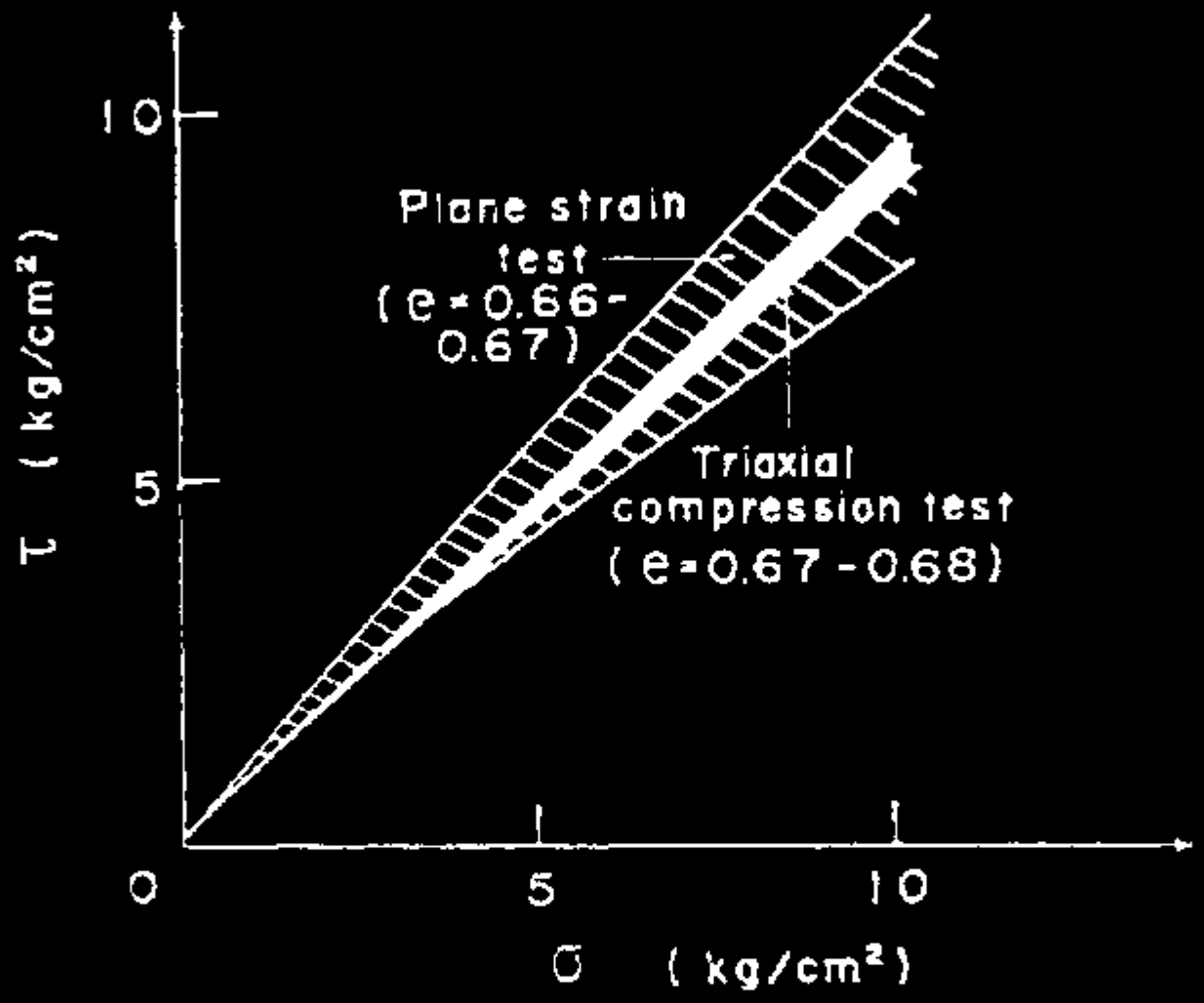

Compiled figure of the Mohr's failure envelopes in the plane strain and triaxial compression tests

Marachi et al. (1981) conducted a comprehensive series of experiments on a medium to coarse uniform sand to examine the effects of a number of soil and test specimen variables on the plane strain test results. Of interest to this project are the results shown in Figure 2-13, that are very similar in appearance to those of Cornforth (1964), Figure 2-9. Both the peak strength and initial tangent moduli are greater in plane strain. Peak secant moduli were scaled from these figures, and the ratios of PS to TC moduli ranged from 3.7 to 1.9. In this case, however, the denser specimens apparently had the greater modulus ratios--opposite of what the Cornforth (1964) data showed.

Marachi et al. (1981) also verified that the PS friction angle is grater than the TC friction angle, especially for denser sands. These results are given in Figure 2-14 in terms of initial void ratio, and in Figure 2-15 versus confining pressure.

Peters et al. (1988), in an investigation of shear band formation in sands, conducted TC and PS tests on a uniform medium sand at 90 percent relative density. Because of different stress paths, the results of only one PS and one TC test can be meaningfully compared, and the PS modulus was about 1.25 higher than the corresponding TC modulus.

Boyle (1995) conducted a few PS and TC tests on very dense (D_r = 96-101 percent) specimens of uniform and rounded grained Ottawa sand and a slightly better graded, coarser, and very angular grained Rainier Avenue Sand from Seattle. The TC tests were conventional strain rate controlled (Figures 2-16 and 2-17), while the PS tests were conducted in a new "unit cell" device that used stress (incremental) controlled loading. The PS test results for the two sands are given in Figures 2-18 and 2-19. The PS to TC secant modulus ratios ranged from 0.9 to 2.1 for the Ottawa sand and from 2.9 to 4.2 for the Rainier Avenue Sand.

Boyle (1995) also summarized the test results for friction angle for both sands in Figure 2-20. The difference in PS versus TC friction angle is significant for the angular Rainier Avenue Sand, especially at low confining pressures.

SUMMARY

Based on the available experimental evidence, it is generally accepted that the PS friction angle is significantly greater than the friction angle measured in TC tests, especially for denser sands and sands with friction angles greater than about 35°.

Although the literature is somewhat inconsistent, it appears that the PS modulus at higher densities is between two and four times the TC modulus for most medium to coarse uniform sands.

Figure 2-13. Stress-Strain Relationship for Plane Strain and Triaxial Specimen. (σ_3 - 70 kPa [10 psi]) (Marachi et al. 1981)

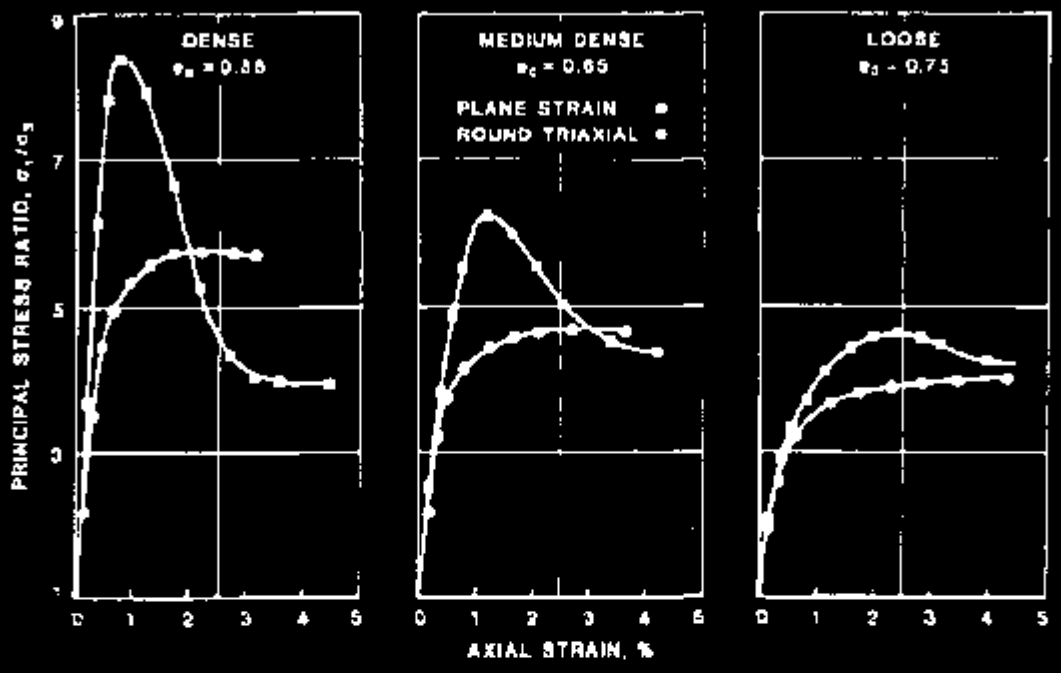

Figure 2-14. Angle of Internal Friction - Void Ratio Relationship for Plane Strain and Triaxial Tests. (σ_3 - 70 kPa [10 psi]) (Marachi et al. 1981)

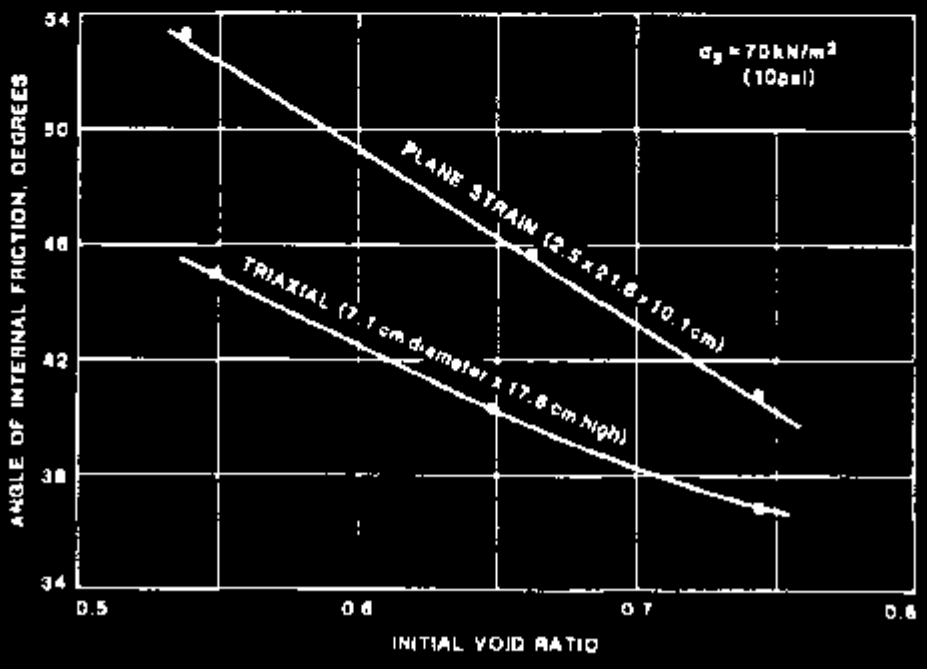

Figure 2-15. Variations of Angle of Internal Friction With Continuing Pressure. (Marachi et al. 1981)

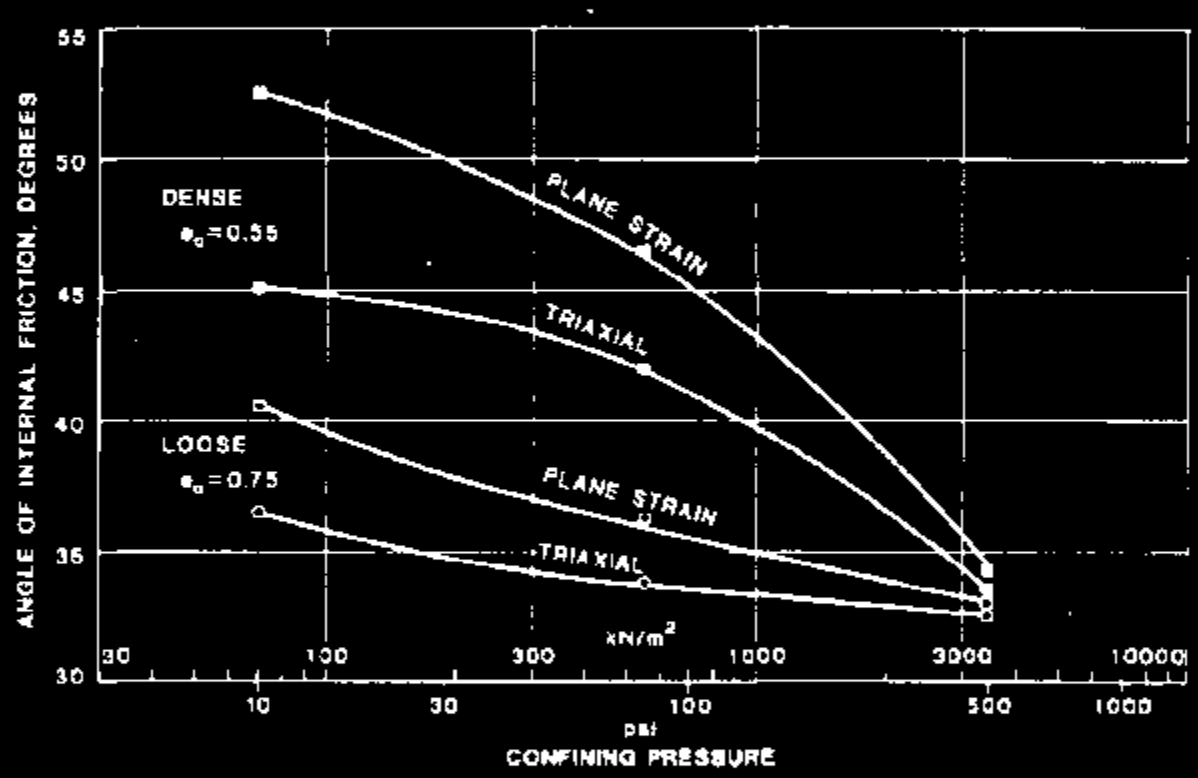

Figure 2-16. Triaxial Test Results for Ottawa Soil. (Boyle 1995)

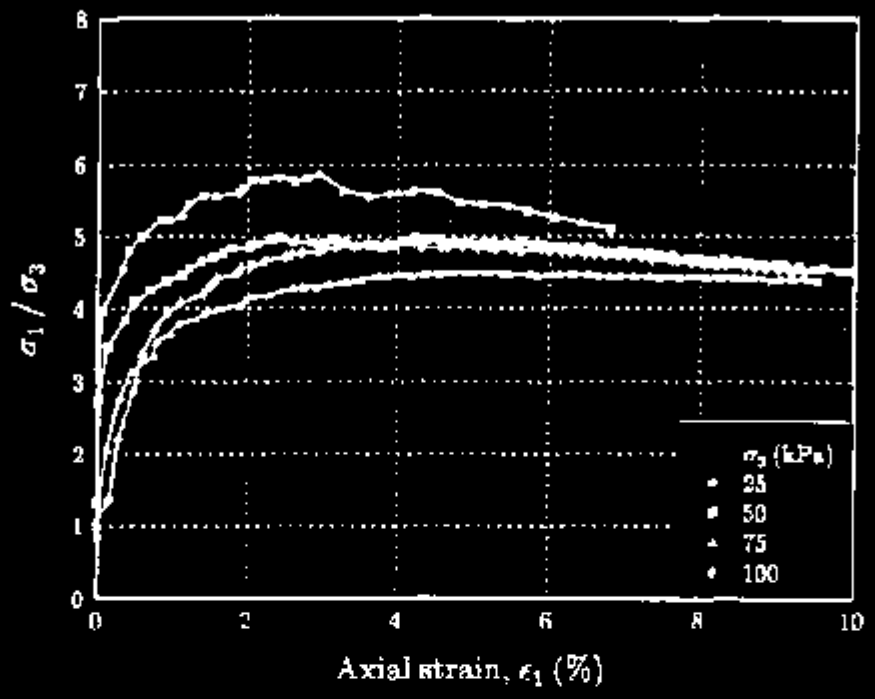

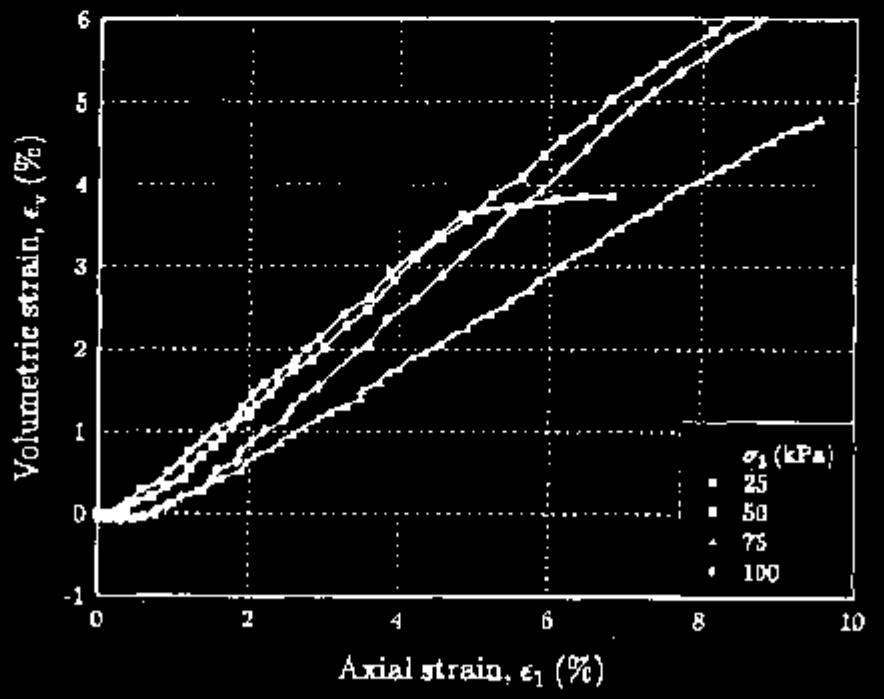

Figure 2-17. Plane Strain Test Results for Ottawa Soil. (Boyle 1995)

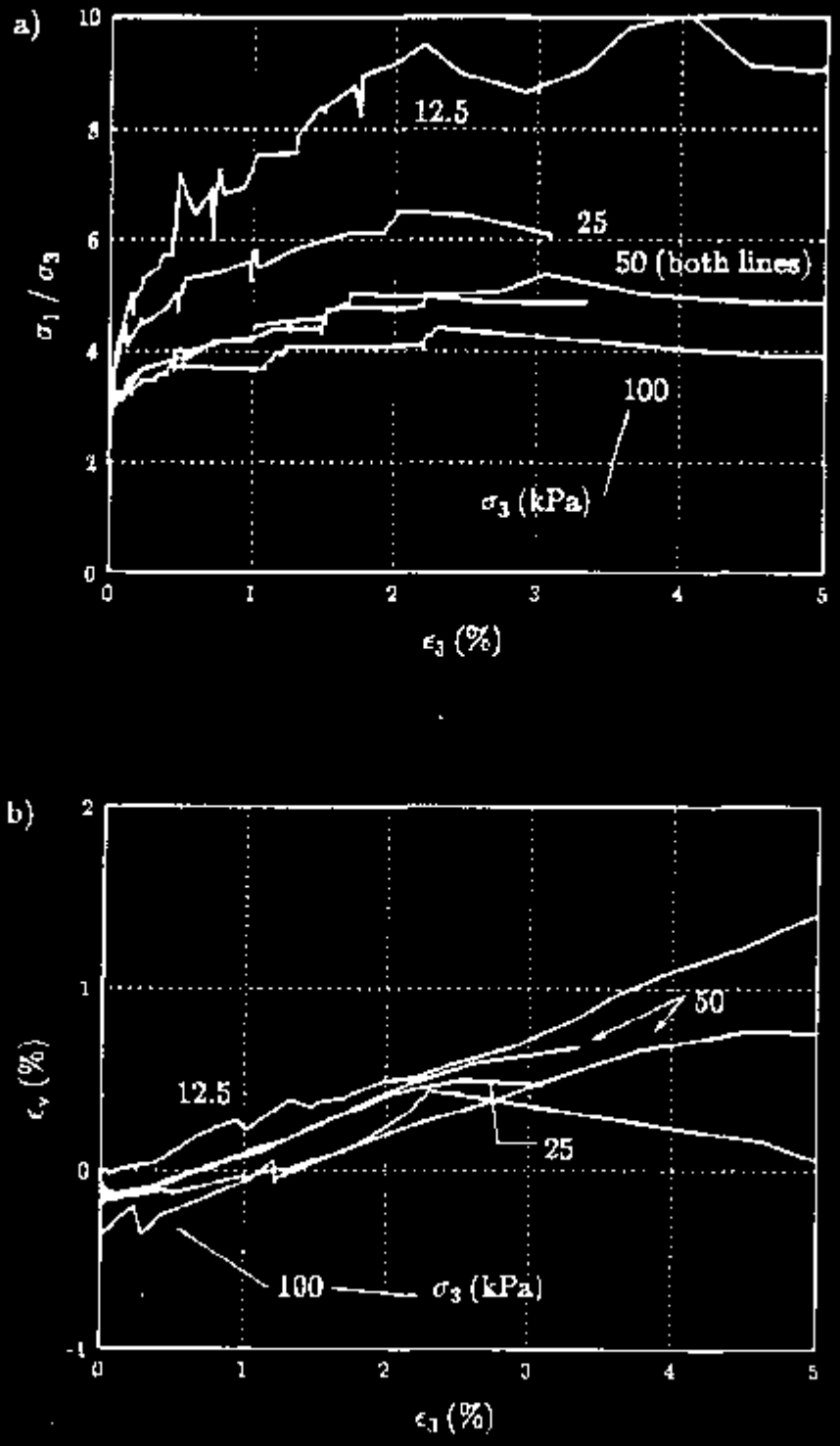

Figure 2-18. Triaxial Test Results for Rainer Avenue Soil. (Boyle 1995)

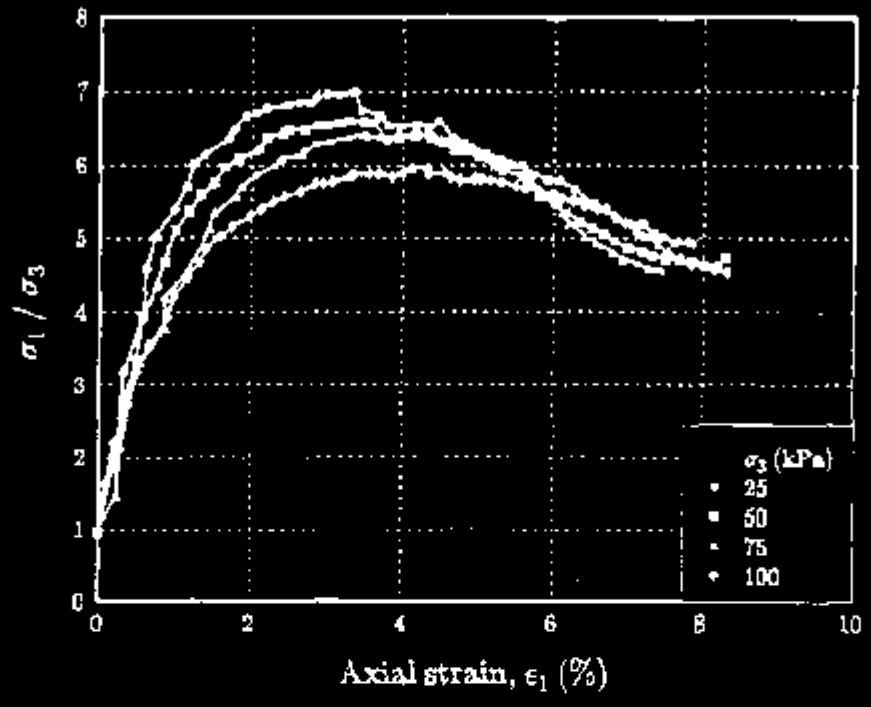

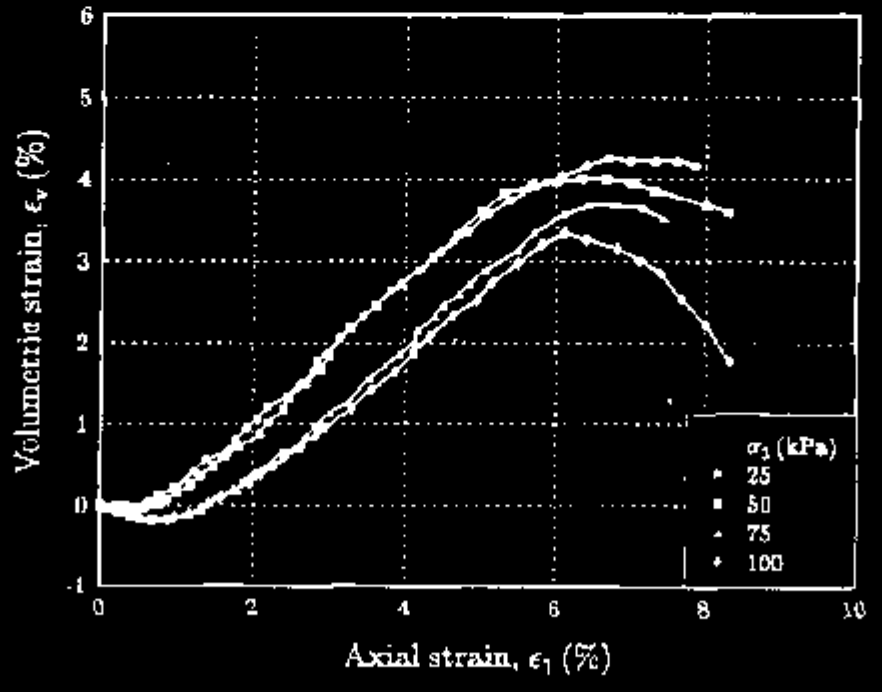

Figure 2-19. Plane Strain Test Results for Rainer Avenue Soil. (Boyle 1995)

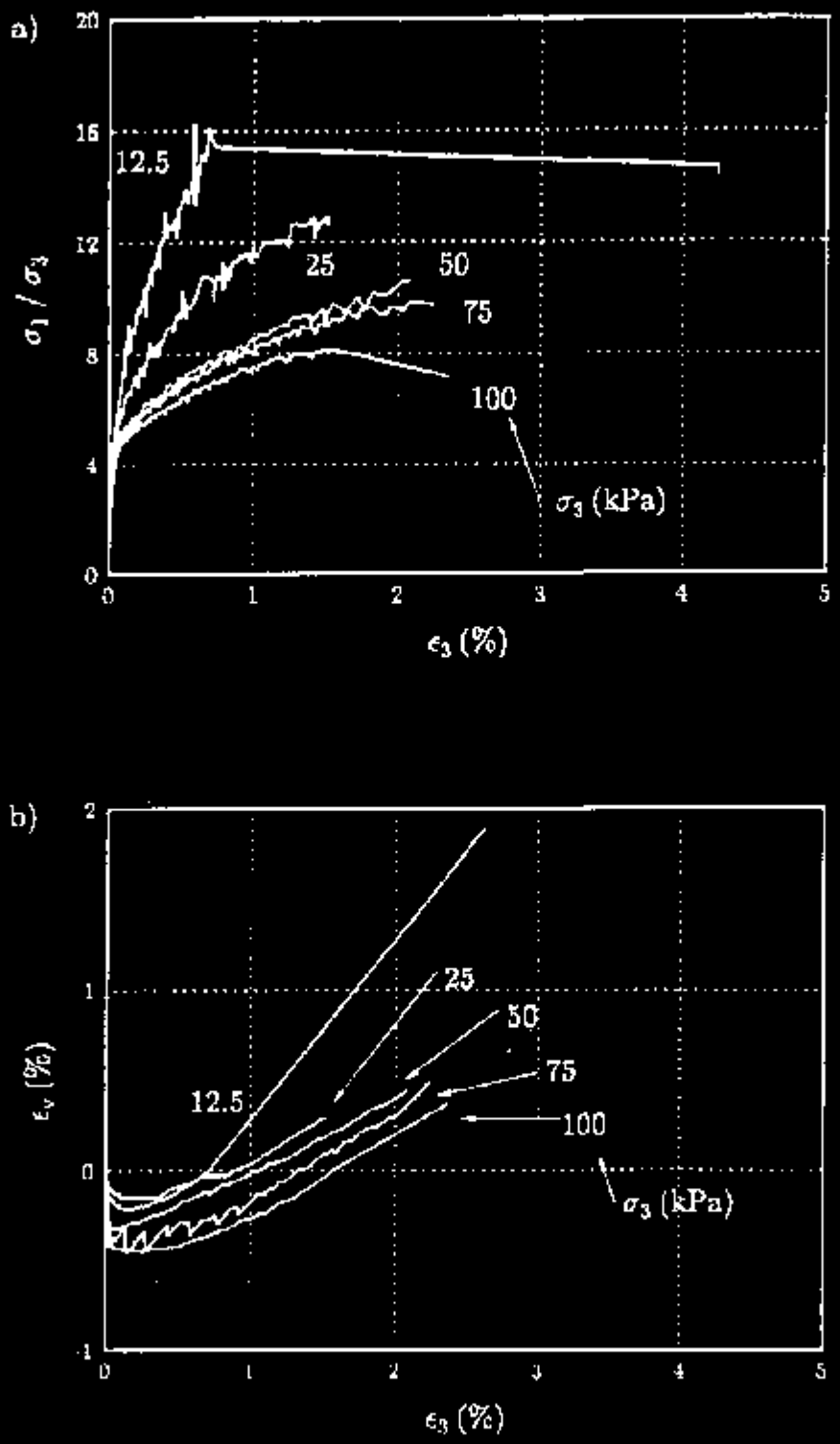

Figure 2 20. Plane Strain, Triaxial, and Direct Shear Friction Angles for Ottawa and Rainer Avenue Soils. (σ_{3c} - Confining Pressure, σ_N - Direct Shear Normal Pressure, kPa). Triaxial Results for Soil R at 70,190,260 and 310 kPa and STS (1990). (Boyle 1995)

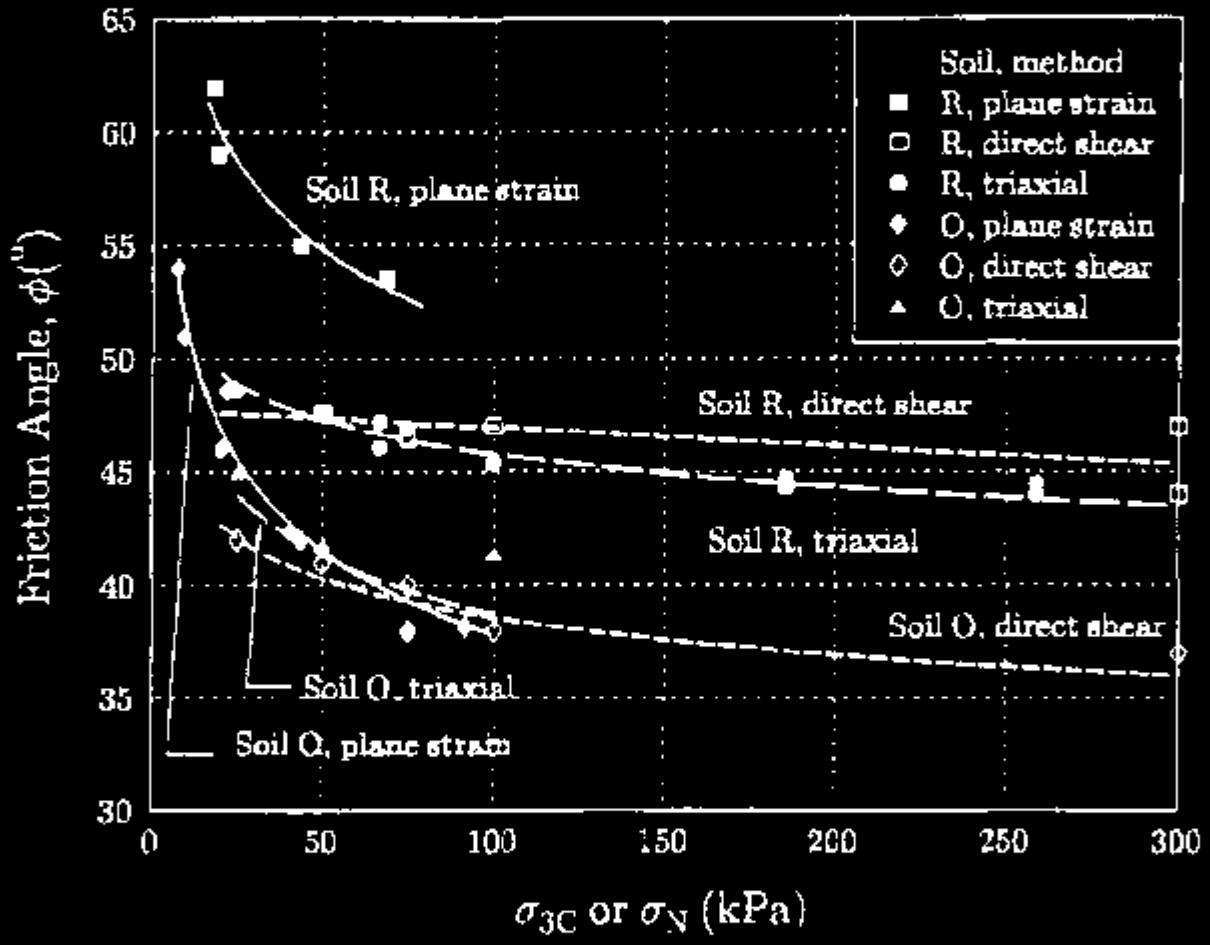

2.2.4 Application To The Drucker-Prager Constitutive Model

The following discussion is based on information extracted from the following references: Desai and Siriwardane (1984), Chen and Mizuno (1990), Chen and Saleeb (1994), and Chen (1994).

The Drucker-Prager constitutive model is basically an extension of the classical von Mises failure criterion to take into account the observed dependency of the strength of soils on the hydrostatic stress component. The Drucker-Prager criterion can be written in terms of the stress invariant as follows:

$$f(I_1, J_2) = \sqrt{J_2} - \alpha I_1 - k = 0 \qquad (2\text{-}4)$$

where α and k are positive material constants, I_1 is the first invariant of the stress tensor, and J_2 is the second invariant of the deviatoric stress tensor. The constants α and k must be determined from test results, and it is possible to relate these constants to the common Mohr-Coulomb strength parameters ϕ and c. For conventional triaxial compression, these equivalent parameters are

$$\alpha = \frac{2\sin\phi}{\sqrt{3}(3-\sin\phi)} \qquad (2\text{-}5)$$

and

$$k = \frac{6c\cos\phi}{\sqrt{3}(3-\sin\phi)} \qquad (2\text{-}6)$$

As the Mohr-Coulomb parameter c can be assumed to be zero in granular materials, the Drucker- Prager criterion for sands in triaxial compression is

$$\frac{2\sin\phi}{\sqrt{3}(3-\sin\phi)} I_1 + \sqrt{J_2} = 0 \qquad (2\text{-}7)$$

The advantages and limitations of the Drucker-Prager model have been discussed by Chen and Mizuno 1990) and Chen and Saleeb (1994). As shown by Chen and Saleeb (1994, pp 483-5), in any implementation of the Drucker-Prager model, it is imperative that proper selection of the matching conditions must be made in order to approximate the Mohr-Coulomb failure surface. For plane strain matching, the value of alpha is

$$\alpha = \frac{\tan\phi}{(9+12\tan^2\phi)^{1/2}} \qquad (2\text{-}8)$$

and the Drucker-Prager criterion for plane strain conditions is

$$\frac{\tan\phi}{(9+12\tan^2\phi)^{1/2}} I_1 + \sqrt{J_2} = 0 \qquad (2\text{-}9)$$

For the derivation of the incremental equations for the Drucker-prager model, see Desai and Siriwardane (1984, pp 246-251).

2.2.5 Alternate Approaches

Constitutive modeling of soils is not ordinarily easy nor straight-forward. Soils in general have a non-linear stress-strain relationship and this relationship is highly stress state dependent. Furthermore, soils are nonconservative, inhomogeneous, and anisotropic materials, and often their mechanical properties are time dependent. In the present case, however, the predominately granular soils at the Hanford Site permit us to ignore time dependency. Because natural soils were excavated and recompacted adjacent to the waste tank walls and on the tank domes, the soils can be reasonably considered to be homogeneous and isotropic for analysis purposes. In addition, the soils were compacted and therefore, preloaded or prestressed, so the use of the unload-reload modulus is appropriate--this modulus can be readily approximated by a linear average of the two curves, provided unload-reload cycles were done during the tests.

For limit state or failure type analyses, the Mohr-Coulomb failure criterion has been found to be the most suitable for predicting the failure of soils. It has a long history of successful use for the solution of many common problems in geotechnical practice. However, as noted by Desai and Siriwardane (1984) and Chen and Mizuno (1990), the Mohr-Coulomb criterion has serious limitations for generalized three-dimensional states of stress. The failure surface in stress space exhibits "corners" or singularities that lead to difficulties in numerical analyses such as the finite-element method.

Alternate failure criterion such as Drucker-Prager, even with its limitations and deficiencies, can potentially provide a better prediction of failure conditions, provided it is properly calibrated and its parameters appropriately determined for the soils at the site. A serious shortcoming however is the inability of the Drucker-Prager to consider strain softening, a typical behavior of dense sands during shear. As shown in Figures 2-9 and 2 13, for example, dense sands sheared in plane strain undergo significant strain softening after reaching their peak stress at rather small deformations.

Other soil failure models that could be considered include the (1) Cap model (Chen and Mizuno 1990, Chen 1994), (2) the Lade two parameter criterion (Chen and Saleeb 1994, Chen 1994), and (3) the Prevost and other "nested" models (Chen 1994). Although the Cap model has shown considerable success for some problems, it also cannot account directly for strain softening. The Lade model, however, can do this, but it has 14 model parameters determined apparently from three triaxial compression tests (at three different confining pressures). The Prevost model requires a triaxial extension test--but TE tests are not easy to do on granular materials.

Conventional Sampling and Laboratory Testing

It is always difficult to obtain reliable soil properties from laboratory tests on granular materials. First, it is almost impossible to obtain undisturbed samples of these types of materials, and unfortunately, sample disturbance tends to cause unconservative test results for most practical problems. Second, reconstituting disturbed samples of granular materials in the laboratory is not viable either because this process cannot recreate the natural or compacted structure of the material in situ. Laboratory tests on reconstituted samples are not very likely to yield the correct response or soil properties.

In Situ Tests

These difficulties with sampling and laboratory testing of sands has led to increased use of in situ tests in problems similar to the Hanford Site waste tanks. In situ tests using calibrated inflatable proves (pressuremeters), cone penetrometers, plate load tests carried out at depth (screw plate compressometer), and a number of geophysical techniques offer considerable promise for obtaining meaningful estimates of the pertinent deformation and strength properties of the granular backfill soils. Please refer to report Section 3.1.1.

Observations of the Performance of Other Nearby Structures

One of the most reliable sources of information about soil properties and foundation conditions at a particular site is settlement performance data on nearby structures constructed on similar soils. Provided the structural loads can be reasonably estimated, back-calculation of deformation moduli and other parameters necessary for settlement analyses can be performed. Unfortunately, performance date are often not available or difficult to obtain in most situations. However, the presence of a large number of structures at the Hanford Site

and all on similar foundation soils would appear to provide an excellent opportunity to utilize this variation of the "observational method" to obtain an additional piece of information about the deformation properties of the Hanford Site sands.

2.3 SPRING MODELING OF SOIL

The simplest and least costly method for analytical modeling of the Hanford Site waste tanks is to model the soil beneath the tanks as elastic springs. The initial evaluation of generic tanks has employed soil springs. The current ANSYS and ABAQUS[1] detailed modeling of reinforced concrete tanks has shown that the Hanford Site tank designs are sensitive to the soil modeling.

2.3.1 Determination of Soil Elastic Modulus Variation With Depth

The most important factor influencing the modulus of granular soils is the stress history, or more precisely, the strain history of the deposit. The construction sequence of the Hanford Site waste tanks began with removal of a sand and gravel overburden down to the level of the present tank foundation. Then the tanks were constructed and the tank farm buried under soil fill.

The tank foundation soil at the Hanford Site has already been subjected to vertical pressure loads greater than a tank filled with waste. Consideration of the history of the tank foundation soil led to an engineering judgment to employ soil unload-reload modulus derived from triaxial test data (Dames & Moore 1988).

Cylindrical samples of the Hanford Site soil are taken from bore holes at various depths (Dames & Moore 1988). The soil is a cohesionless sand and gravel mix. The cylindrical soil samples are wrapped in a rubber membrane for testing. These samples are subjected to radial confining pressures representative of the bore hole depth as they are also loaded in compression. The stress strain relation of the soil cylinders to failure is very nonlinear. Unloading and reloading of the samples before failure results in a nearly linear unload-reload modulus (see Figures 2.1-2 and 2.1-3, from Dames & Moore (1988). The Hanford Site test data were used to derive a simple relation for the variation of unload reload elastic modulus with confining pressure or depth.

---

[1]ABAQUS is software developed by Hibbitt, Karlsson & Sorensen, Inc., Pawtucket, Rhode Island.

ANSYS is a registered trademark of Swanson Analysis Systems, Inc., Houston, Pennsylvania.

The University of California at Berkeley has done considerable research on soil constitutive modeling including variation of the unload reload modulus with confining pressure (Wong and Duncan 1974, Duncan et al. 1980, Seed and Duncan 1983). The results show that the unload-reload soil modulus can be defined as in Equation 2 2 of section 2.1.1.

2.3.2 Schmertmann Estimation of Foundation Soil Springs

In 1970, J. H. Schmertmann proposed a new procedure for estimating elastic settlement of foundations on granular soils. The equivalent soil springs are calculated by dividing the foundation force by settlement displacement. Although the Schmertmann method is empirical, the procedure has a rational basis in the theory of elasticity, finite-element analyses, and observations from field measurements and laboratory model studies (Holtz 1991). The distribution of vertical strain within the linear-elastic half space subjected to a uniformly distributed load over an area at the surface can be determined by

$$\epsilon_z = \frac{\Delta q}{E} I_z, \qquad (2\text{-}10)$$

where

ϵ_z = the vertical strain
Δ q = the intensity of the uniformly distributed load
E = Young's modulus of the elastic medium
I_z = a strain influence factor, that depends only on the Poisson's ratio and the geometric location.

The distribution of strain within loaded granular masses has been observed to be very similar in form to that for a linear-elastic medium, based on the results of displacement measurements within sand masses loaded by model footings, as well as finite-element analyses and deformations of materials with nonlinear stress-strain behavior. Figure 2-21 shows some typical results of model tests and finite-element analyses reported by Schmertmann (1978 and 1970) and Perloff (1975). The settlement of a soil layer due to a uniformly distributed load is simply the vertical strain from equation (2-4) times the soil-layer thickness. The strain influence factor at various soil depths can be estimated from the results show in Figure 2 21 or by the simplified modification shown in Figure 2-22 (Schmertmann et al. 1978, Schmertmann 1978). The total foundation settlement S_i can be obtained by the following summation:

$$S_i = C_1 \, C_2 \, \Delta q \, \Sigma \left(\frac{I_z}{E} \right) \Delta Z_i, \qquad (2\text{-}11)$$

Figure 2-21. Comparisons of Vertical Strain Distributions From FEM Studies and From Rigid Model Tests.

(a) Hartman FEM axisymmetric, (b) Brown Model Test L/B=1, (c) Hartman FEM plane strain, (d) Brown Model Test L/B=4 (Schmertmann et al., 1978)

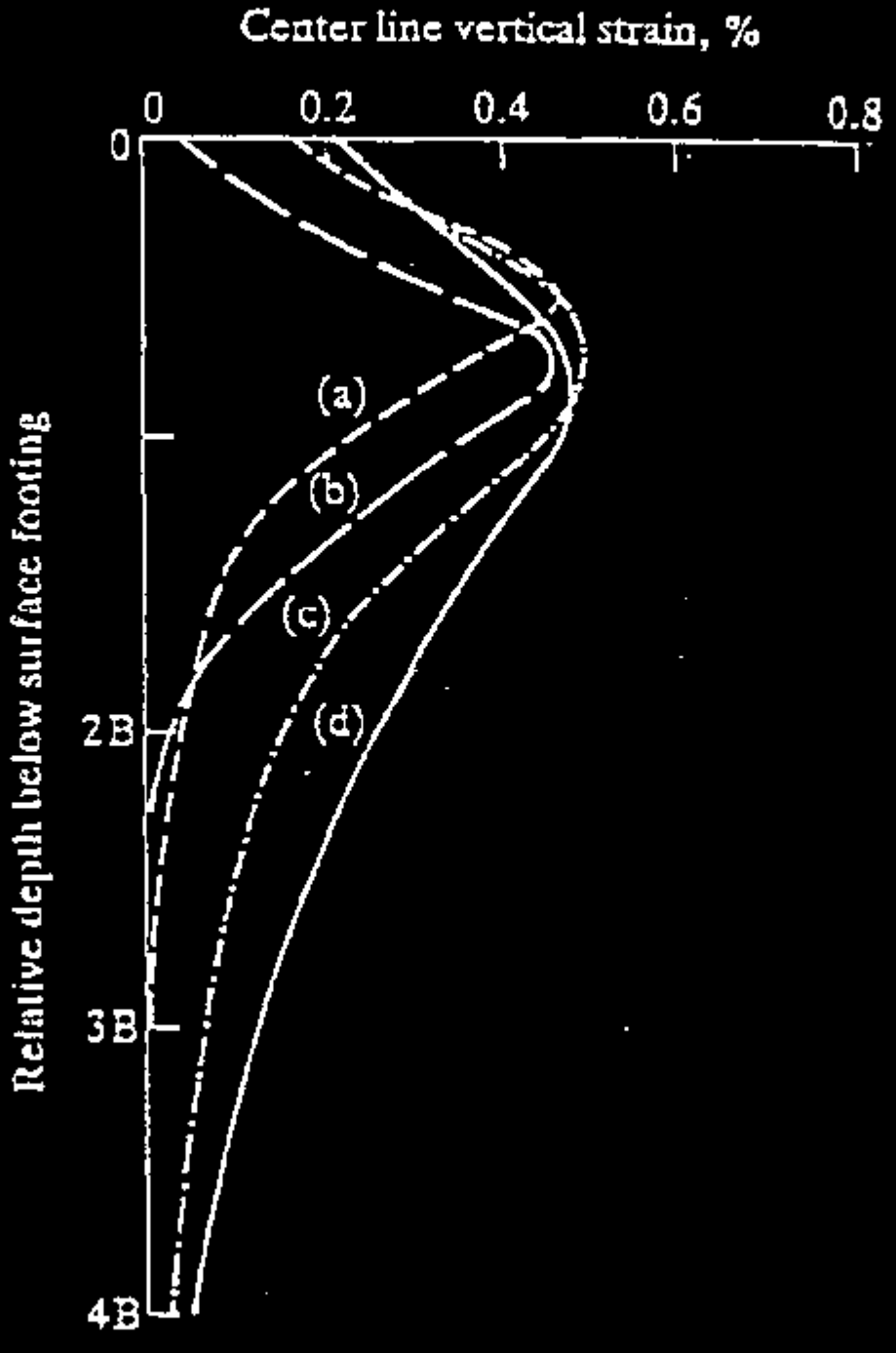

Figure 2 22. Modified Strain Influence Factor Diagrams For Use in Schmertmann Method for Estimating Settlement Over Sand (Schmertmann 1978).

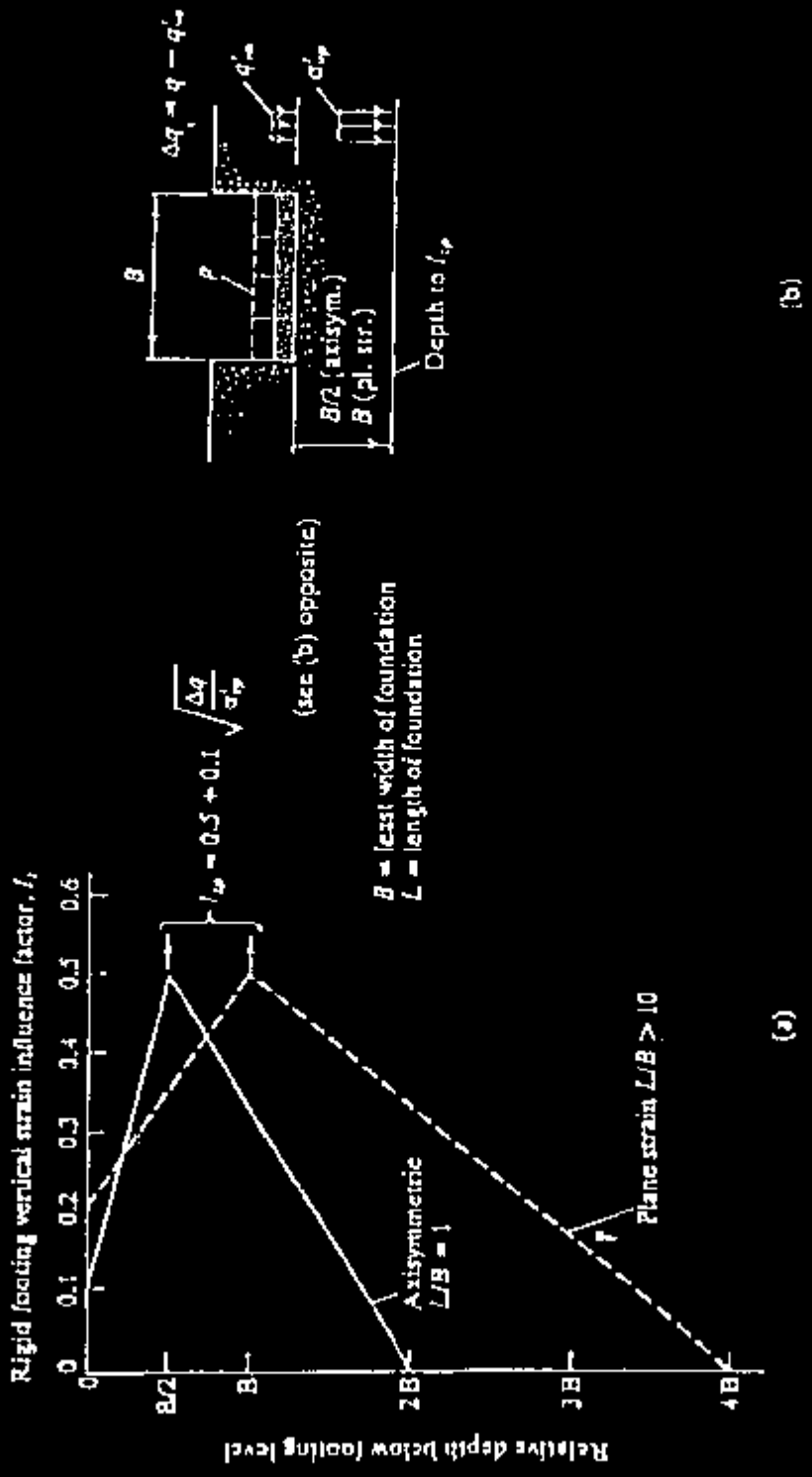

in which

S_i = total foundation settlement
Δq = net load intensity at the foundation depth
I_z = strain influence factor from Figure 2-22
E = appropriate Young's modulus from equation 2-2
C_1, C_2 = correction factors, as described below,

where

$$C_1 = 1 - 0.5 \left(\frac{\sigma'_{oB}}{\Delta q}\right) > 0.5, \qquad (2\text{-}12)$$

and

σ'_{oB} = effective in situ overburden stress at the foundation depth
Δq = net foundation pressure.

In all cases, the C_1 embedment correction factor should not be less than 0.5. Schmertmann also included the C_2 correction to account for some time-dependent increase in settlement. Holtz (1991) does not recommend using C_2; therefore C_2 is set equal to 1.0.

The soil spring value per unit area of foundation is obtained by dividing the soil beneath the foundation into layers with the corresponding strain influence factor and soil modulus (based on the unload/reload modulus power equation show in Equation 2-2). The summation of the soil layer settlements (Equation 2-11) was obtained and divided by the foundation pressure to obtain the equivalent spring per unit area of foundation.

The Schmertmann method could also be used to obtain an equivalent E (Young's Modulus) for the entire layer beneath the foundation. The summation of Equation 2-11 could be set equal to another similar summation with a constant E value. The equation would be solved numerically for an equivalent E (Young's Modulus).

2.3.3 Estimation Of Soil Layer Confining Pressure

The confining pressure of the soil layers should be estimated as being the depth of the soil multiplied by the soil density.

2.3.4 Results Of Schmertmann Soil Spring Estimation

If the Hanford Site 500,000 gallon waste tanks were considered to have a full-diameter rigid foundation and the corresponding uniform distributed load, Schmertmann method of soil foundation spring estimation results in springs of 100 lbf/in. for each square in. of foundation area (Note: This value compares to Dames & Moore 1988 recommendations). Initial ANSYS finite-element analyses with the spring values given above experienced nonlinear numerical problems and large-scale concrete cracking and crushing in the tank floor area. These problems may be solved using the updated version of the concrete element that allows for a gradual stress redistribution after cracking.

The 500,000 gallon tank footings carried the soil overburden, dome, and wall weight, while the center floor region carried only the waste load. The tank floor and footing do not act as a single rigid foundation for Hanford Site tanks. The footing region carried the largest load (Note: The load is greater for the footing than the overburden load at the foundation depth.). Calculations of soil springs assuming only the footing region as foundation resulted in estimated soil springs of 330 to 380 lbf/in (depending on confining pressures estimations for variation) for each square in. of area.

Additional investigation of 500,000 gallon tanks employed the Schmertmann method using a superposition of two problems. A rigid foundation with a uniform pressure equivalent to the center floor pressure gives an elastic settlement consistent with foundation springs of 100 lbf/in for each square in. of area. The delta pressure for the footing region also gives additional settlement, if only the active footing width is applied. The two settlements were added and the sum was divided into total footing pressure to obtain foundation springs of around 200 lbf/in for each square in. of area. An analysis with soil springs for the center floor and footing of 100 and 200 lbf/in per square in. of area, respectively, needs additional work and evaluation.

2.3.5 EPRI Foundation Soil Spring Estimation

The Electric Power Research Institute sponsored a report by Cornell University (Kulhawy and Mayne 1990) that recommended Equation 2-13 (Vesic 1961) for the determination of subgrade foundation springs:

$$k_s = \left(\frac{0.65}{B}\right)\left(\frac{EB^4}{E_f I_f}\right)^{1/12}\left(\frac{E}{1-\nu^2}\right) \qquad (2\text{-}13)$$

where

E = soil Young's Modulus (use unload/reload power equation),
ν = soil Poisson's Ratio,
B = foundation width, beam foundation
E_f = foundation Young's Modulus,
I_f = foundation moment of inertia.

A sample calculation was completed with Equation 2-13 for 6 ft wide 2 ft thick tank wall foundation at a 55 ft depth. Equation 2-13 resulted in estimated foundation springs of 273 lb/in/in^2.

2.3.6 Recommendations For Hanford Site Foundation Soil Spring Modeling

Either or both the Schmertmann soil spring calculation and the EPRI endorsed Vesic may be used for tank foundation soil springs. It is recommended for wall foundation spring calculations that the width of the foundation be limited to only the rigid portion of the footing that carries the wall and dome load weight. The thin nonstructural floors that carry only waste hydrostatic loads would be treated as a separate larger foundation with different stiffness springs. Please refer to Appendix A for formulation calculations.

The triaxial test data is, at this time, one of the best existing Hanford Site sources for soil properties at depth for spring calculation. The Hanford Site soil has been shown to have a linear unload/reload modulus behavior. The past loading or strain history can shift the Hanford Site soil into this linear unload/reload modulus region especially with compacted soil or soil that has not been disturbed but has had a large heavy overburden removed. As long as the new loads are not greater than the previous soil load and the soil is not disturbed it will act linearly. The range of the loads may need to be checked for extreme load case analyses.

The power equation relation for confining pressure can be used to interpolate and extrapolate triaxial test data as needed. This method was also recommended in the Cornell University report funded by EPRI.

Although the triaxial testing data base is important for Hanford Site soil characterization, plane strain soil testing data is probably more applicable for soil properties around the wall and wall foundation of very large buried tanks with axisymmetric loads. Published public domain research data has shown that plane strain test data versus triaxial data results in stiff modulii by factors or two to as much as four. In like manner the compression failure strength seems to increase by about 50 percent and the strain at failure decreases to 1/3. The stress-strain curves for plane strain testing and triaxial testing are significantly different.

Soil spring modeling on the outside of the tank walls should account for compaction with the unload/reload modulii used for small strains. Exact determination of the strain limit

for unload/reload moduli depends on the compaction history. Please refer to Appendix A for horizontal spring calculations.

It is recommended that the existing Hanford Site triaxial testing data base be used to establish the lower bound soil properties. The upper bound properties for buried tanks should be factored up from the triaxial testing to account for plane strain effects (For example moduli factored up by 2 or 3 times.). Triaxial versus plane strain testing needs additional investigation for the Hanford Site sandy soils. The actual stress and strain field of these sandy soil test samples need investigation.

2.4 FINITE-ELEMENT CONTINUUM MODELING OF SOIL

At this time the plasticity-based models are the most popular for modeling geotechnical materials (Chen 1994). The characterization of soil behavior by plasticity theories has become one of the most active research areas in solid mechanics. Significant advances in this area have led to the development of constitutive models that may accurately represent the behavior of soils subjected to general load paths. Technology has progressed to the extent that the monotonic loading response of the soil can be accurately represented by several existing constitutive models. But, when cyclic loading conditions have significant plastic response under both loading and reverse loads, very few existing models are capable of reproducing most of the observed soil responses, although some of their qualitative behaviors may be captured.

The wide variety of soils leads to the conclusion that no material model will be able to capture the behaviors of all soils under all conditions, and at the same time retain the necessary simplicity for practical implementation and use (Chen 1994). At this time the three most popular plasticity based constitutive models for cohesionless (sandy) soils are the Mohr-Coulomb, the Drucker-Prager, and the Lade Two-Parameter model. For past and present Hanford Site soil continuum modeling only the Drucker-Prager has been available. The Lade Two-Parameter or the Lade Fourteen-Parameter model would be preferred for nonlinear three dimensional static soil-structure analyses of Hanford Site waste storage tanks.

2.4.1 Mohr-Coulomb Plasticity

The Mohr Coulomb plasticity failure model defines a pressure or hydrostatic stress dependent failure surface or envelope. In the principal stress space, the Mohr-Coulomb failure surface represents an irregular hexagonal pyramid with straight meridians (Chen and Saleeb 1994, see Figure 2-23). The advantages and limitations of the Mohr-Coulomb plasticity model can be summarized as follows (Chen and Saleeb 1994):

- The Mohr-Coulomb failure criterion is a fair approximation of soil strength in most practical applications.

Figure 2-23. Mohr-Coulomb Criterion in Principal Stress Space and Mohr's Diagram.
(a) Principal Stress Space, (b) Mohr's Diagram.

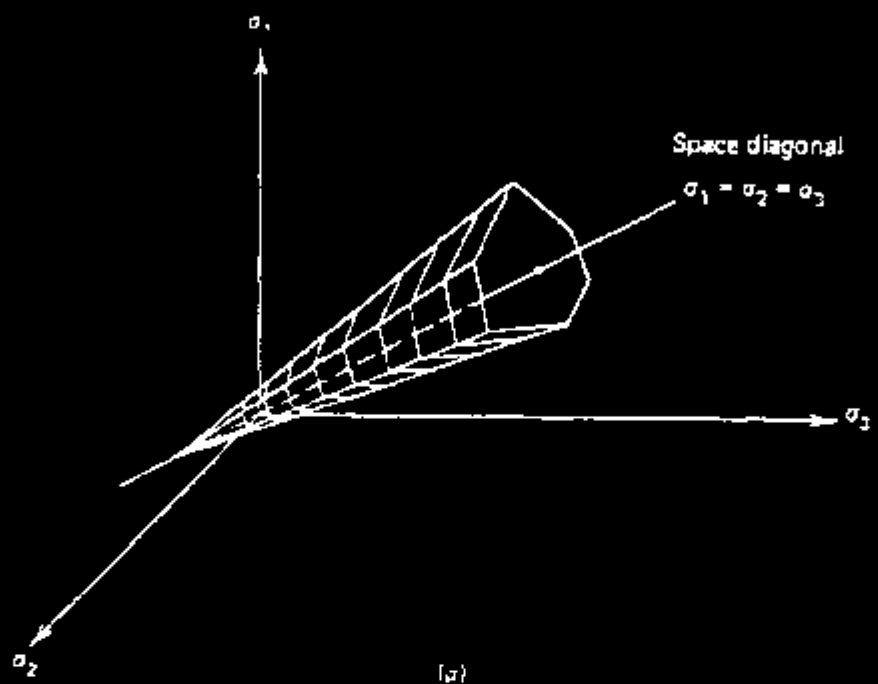

(a)

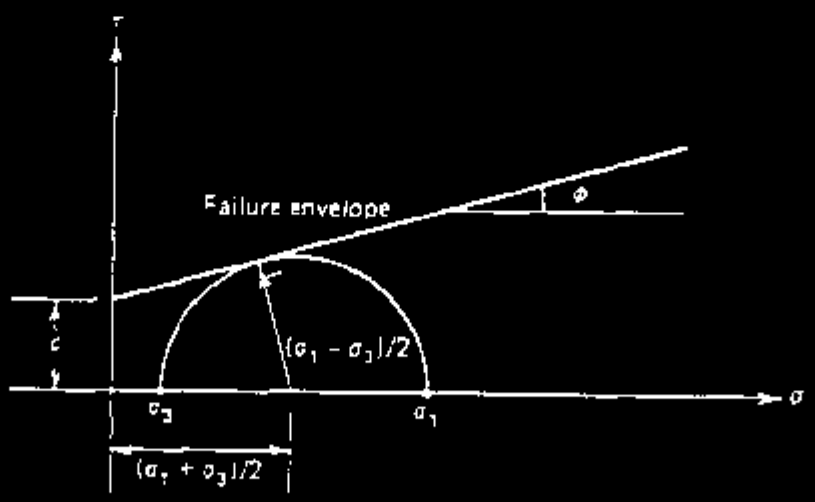

(b)

- It assumes that the intermediate principal stress has no influence on failure, which is contrary to experimental results.

- It assumes that the failure parameter of the soil friction angle does not change with confining or hydrostatic pressure.

- The failure surface has corners (singularities) that make it inconvenient numerically for three dimensional problems.

2.4.2 Drucker-Prager Plasticity

The Drucker-Prager can be simply understood as an extended or modified Von Mises failure criterion with a dependency on confining pressure or hydrostatic stress. The Drucker-Prager failure surface in the principal stress space is a right circular cone with the space diagonal hydrostatic stress axis as its axis (see Figure 2-24). The Drucker-Prager cone failure surface can be viewed as a smooth Mohr-Coulomb surface (Chen and Saleeb 1994). The advantages and disadvantages of the Drucker-Prager model can be summarized as follows (Chen and Saleeb 1994):

- The criterion is simple and has only two parameters that can be determined from conventional triaxial tests.

- The failure surface is smooth and mathematically convenient to use in three-dimensional analyses.

- The effect of hydrostatic pressure is addressed. However, since the traces of the cone failure surface are straight lines, reasonable results are expected only for a limited range of hydrostatic pressures, where the curvature in the failure envelope may be neglected.

- The trace of the failure surface on the deviatoric plane is circular, which does not match test results.

- The Drucker-Prager criterion does consider the influence of the intermediate principal stress. But if great care is not taken in selecting the material parameters from test results, this influence may not be correctly represented with serious discrepancies between predicted and experimental results.

It is generally observed that the use of the associated flow rule for conical yield surfaces results in excessive plastic dilation which is not observed during testing of soils (Chen 1994). The concept of adding a cap to conical failure surfaces was first proposed by Drucker et al. (1957). The proposed cap would allow consideration of compressive plastic

Figure 2-24. Drucker-Prager Failure Criterion - Failure Surface and Traces on the Meridian and Deviatoric Planes. (a) Principal Stress Space, (b) Meridian Plane (θ = constant), (c) Deviatoric Plane. (Chen and Saleeb 1994)

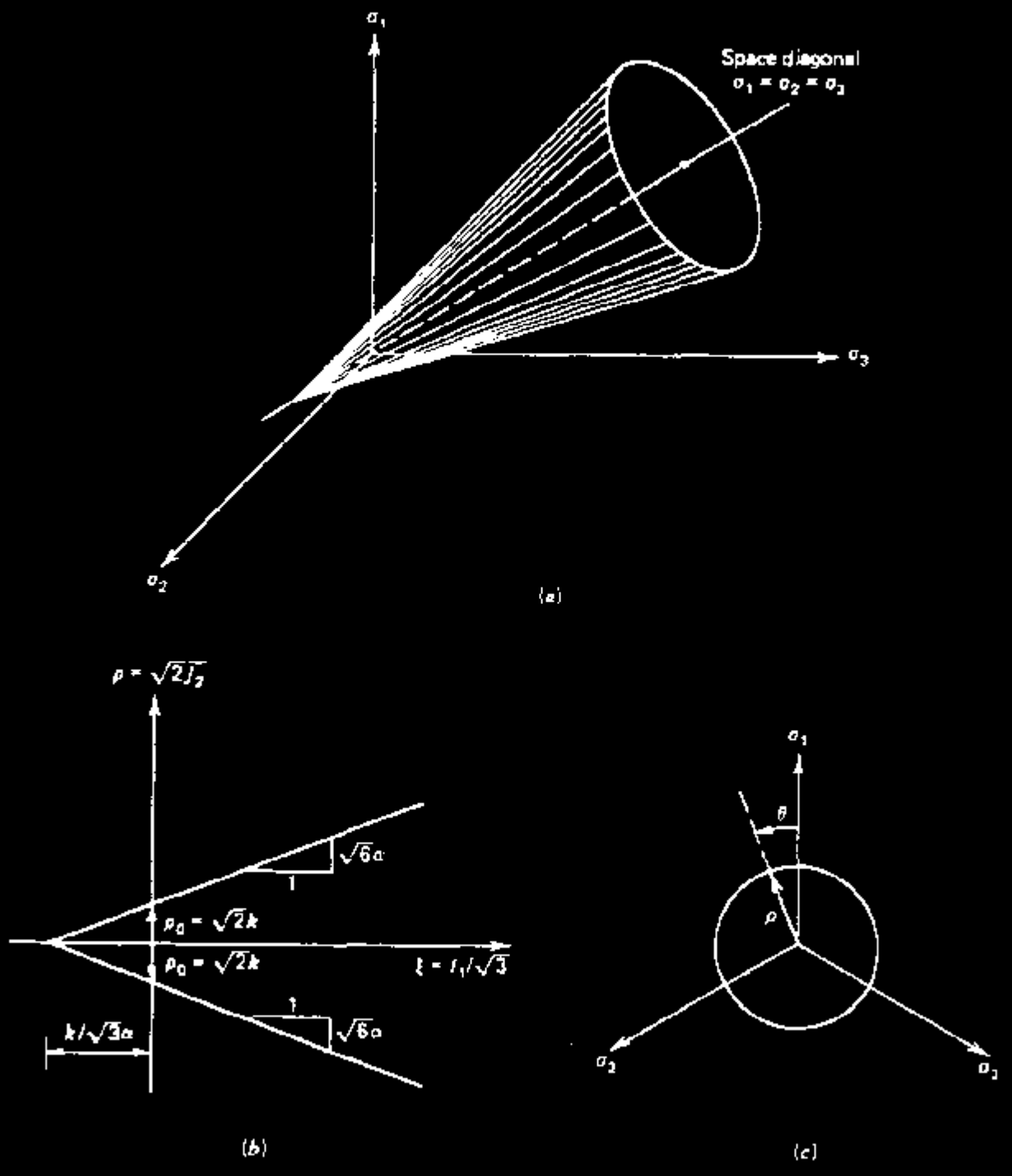

volumetric strains (or compaction) while at the same time limit the amount of plastic dilation that occurrs when loading on a conical limit surface. Although, increased hydrostatic pressure results more load carrying capability for granular cohesionless soils at extreme hydrostatic pressures the soil grains may crush or compact (thus the cap).

Figure 2-25 shows the Drucker Prager cap model. The model consists of a Drucker Prager surface with an elliptical cap positioned symmetrically about the hydrostatic axis at the open end. The capped Drucker-Prager model has not yet been used at the Hanford Site, because it was not available until recently.

2.4.3 Lade Two-Parameter and Fourteen-Parameter Plasticity

Experimental results have indicated that the failure envelopes of most soils are curved, particularly over a wide range of confining or hydrostatic pressures. The soil friction angle decreases with increased confining pressure. Lade (1977) has extended his simple one-parameter model to take into account the curvature of the failure envelope. In the principal stress space, the failure surface of the Lade Two-Parameter model is shaped like an asymmetric bullet with the pointed apex at the origin of the stress space (see Figure 2-26). The failure shape in the deviatoric plane is similar to the Mohr-Coulomb model but without the singularities or sharp points.

The advantages and disadvantages of the Lade Two-Parameter model can be summarized as follows (Chen and Saleeb 1994):

- The Lade (1977) model parameters may easily be obtained from the results of triaxial tests.

- The failure surface of the Lade (1977) model is always concave toward the hydrostatic axis. This implies that the friction angle is always decreasing with increasing hydrostatic pressure. This has been verified for a wide range of hydrostatic stresses, but at very high values of hydrostatic stress where crushing of soil grains becomes important, test results indicate that the experimental failure envelopes open up and become straight. Again the engineer must understand the range of proper application (depends on the sand -- its minerals, crystals, angularity, etc. -- experimentally determined).

- The Lade (1977) model has obtained reasonably good agreement with experimental results in all test cases for cohesionless and consolidated clays (Lade 1977, Lade and Musante 1977, and Chen and Saleeb 1994).

- The failure shape does not have the numerical singularities of the Mohr-Coulomb criteria.

Figure 2-25. Drucker-Prager Cap Model (a) I_1 - $J_2^{1/2}$ Plane, (b) Deviatoric Plane. (Chen and Saleeb 1994)

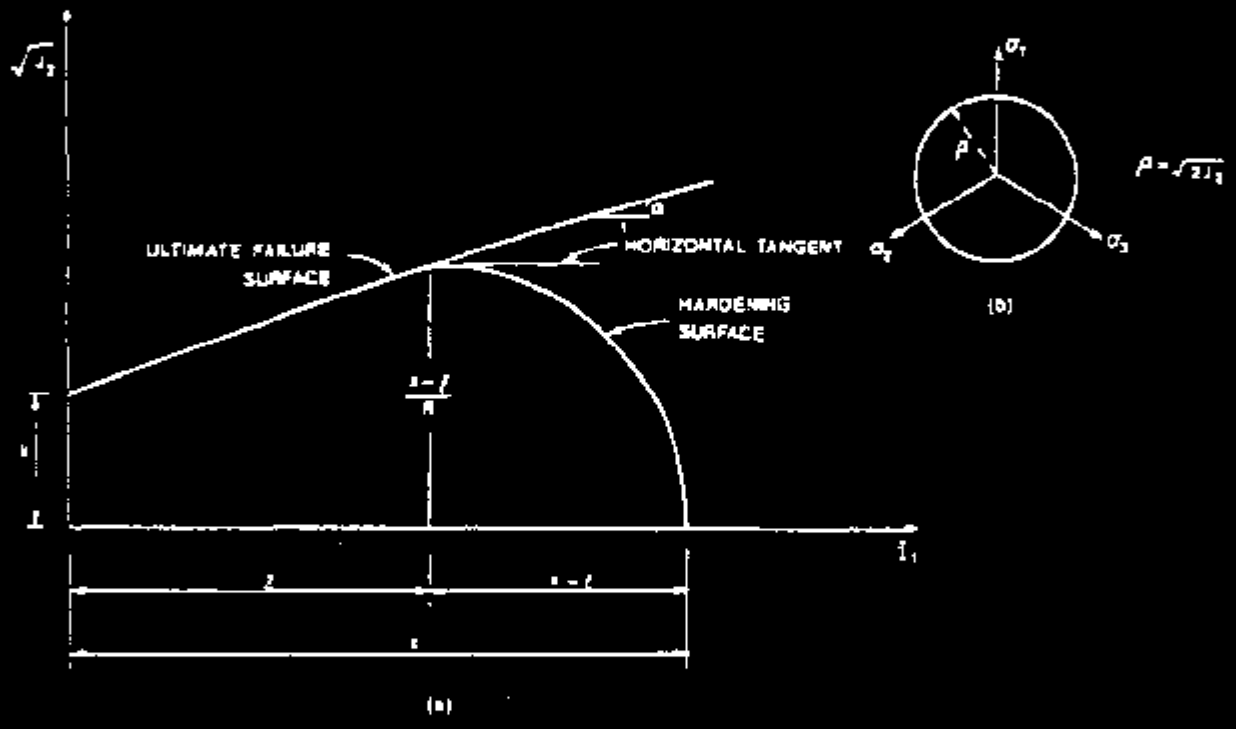

Figure 2-26. Traces of the Failure Surface in the Deviatoric, Triaxial, and Meridian Planes for Lade's Two-parameter Failure Model. (a) Deviatoric Plane. (b) Triaxial Plane. (c) Meridian. (Chen and Saleeb 1994)

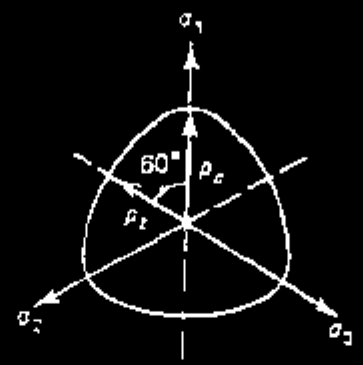

(a)

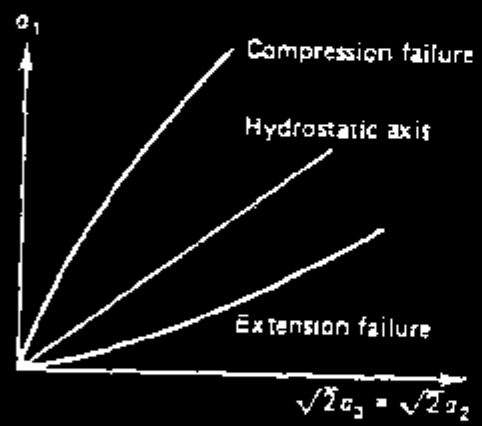

(b)

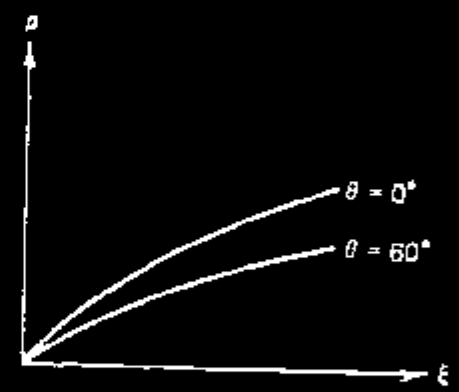

(c)

The Lade (1977) model also has a capped elastic-plastic work-hardening formulation for cohesionless soils. Fourteen parameters are required to fully characterize the capped model behavior. All of these parameters may be determined from the results of triaxial tests. The use of a nonassociative flow rule allows accurate representation of the observed plastic volumetric response of sands, but results in a larger demand on computational capacity because a full nonsysmetric system of equations must be solved (Chen 1994).

2.4.4 Hanford Site Application of Drucker-Prager Soil Plasticity

The purpose of explicitly modeling the soil is to model the soil-structure interaction. The Hanford Site tank farm soil has been characterized as **very coarse sand with some silt and pebbles** (Price and Fecht 1976). This type of soil is relatively cohesionless.

Several constitutive soil models are available within the ABAQUS finite-element code (HKS 1989) and many others are described in the literature (Duncan et al. 1980; Scott 1985). The soil interacts with the tank as the tank expands and contracts from changes in the waste level and heat generation within the waste. The soil also transfers loads from the surface to the tank and provides support by resisting radial displacement of the tank haunch. The soil constitutive model will affect the nature of the cracking predicted in the concrete tank and the magnitude of the collapse-load capacity of the tank. For example, as the tank expands, the soil places the tank in hoop compression. The hoop compression can prevent hoop cracks from developing even though radial thermal gradients of significant magnitude may be present. The soil also provides additional lateral support that affects the magnitude of the collapse load.

The past Hanford Site tank 241-C-106 structural analysis used the ABAQUS finite-element computer code. ABAQUS has several built-in material models suitable for modeling soil as a continuum. ABAQUS also allows user-defined constitutive relations. The Lade plasticity models are not available in ABAQUS. Thus the ABAQUS Drucker Prager plasticity model was selected for investigation in two numerical forms: as a strain-hardened plasticity model; and as an elastic, perfectly plastic material model.

The strain-hardening feature applied to the Drucker-Prager plasticity model is a workable way to use existing theory and features in ABAQUS to account for the cyclic unload-reload modulus behavior of Hanford Site soil and still model the proper monotonic stress strain behavior. The approach is to simply define the elastic modulus to be the unload reload modulus at a particular hydrostatic stress from triaxial testing or as interpolated using the power function based on research work completed by the University of California at Berkeley (Wong and Duncan 1974, Duncan et al. 1980, Seed and Duncan 1983, see section 2.1.1). The strain-hardening stress-strain curve is defined for the same unload/reload modulus compatible confining pressure. The strain-hardened Drucker-Prager is now dependent on hydrostatic strain because its defining parameters are also dependent. Thus, it is necessary for an ABAQUS implementation of the model to define multiple sets of hydrostatic parameters or multiple models that can be controlled during the analysis as

hydrostatic stresses develop. The multiple hydrostatic stress variable models also allow accurate approximation of the of the curved variation of the soil failure envelope with hydrostatic stress.

The above derived multiple strain-hardened Drucker-Prager ABAQUS model matched the triaxial experimental results including the unload/reload behavior. A numerical iteration effort required for the strain hardening became a problem when combined with a nonlinear ABAQUS user-defined concrete subroutine called ANACAP-U or ANACON[2]. When the Hanford Site tank 241-C-106 team set the Newton-Raphson iteration limit to three as specified by the developers of the concrete material model software, the strain-hardened Drucker-Prager soil model went unstable resulting in run termination without completion of the load case.

The final soil constitutive model selected for the tank 241-C-106 structural analysis was the ABAQUS Drucker-Prager elastic, perfectly plastic model because it was the most stable numerically. The perfectly plastic model does not model the correct cyclic behavior but only approximates the behavior to a simple monotonic load.

An additional word or reminder of caution with regard to the Drucker-Prager soil model is as follows: The trace of the failure surface on the deviatoric plane is circular. Although the onset of plastic deformation or failure will duplicate triaxial test results, the failure of the soil under other deviatoric load conditions may only be approximate. To date (June 1995) at the Hanford Site the Drucker-Prager soil model has only been used for soil around the sides and top of the tank 241-C-106 analyses. (The soil under 241 C-106 was modeled as linearly elastic with no failure criteria.)

Calibration of ABAQUS Drucker-Prager Soil Constitutive Parameter

The ABAQUS version of the Drucker-Prager plasticity model contains several parameters. One of these parameters, β, is described as the angle of internal friction. This angle is not equivalent to the Mohr-Coulomb friction angle. The Drucker-Prager friction angle determines the slope of the material yield line in the (p-t) plane as shown in Figure 2-27 (HKS 1989), where p is the equivalent pressure stress (mean stress) and t is a deviatoric stress measure (HKS 1989). The parameter denoted by K in the ABAQUS documentation (HKS 1989) helps define the response of the constitutive model in tension and is defined by the ratio of the yield stress in triaxial tension to the yield stress in triaxial compression. A third parameter is ψ, the dilation angle. The dilation angle is related to the magnitude of the change in material volume during plastic deformation. For example, a dilation angle of zero corresponds to incompressible plastic flow. If ψ is equal to β, the plastic flow is fully associated, i.e., the plastic potential and the yield function have the same stress dependence (HKS 1989). Additional parameters determine the uniaxial yield stress and the elastic

[2] ANACAP-U and ANACON are software developed by ANATECH Research Corporation of San Deigo, California.

Figure 2-27. Drucker-prager Soil Model (a) Schematic Diagram of the p-5 Plane and (b) Schematic Diagram of the Mohr-Coulomb Relation (HKS 1989).

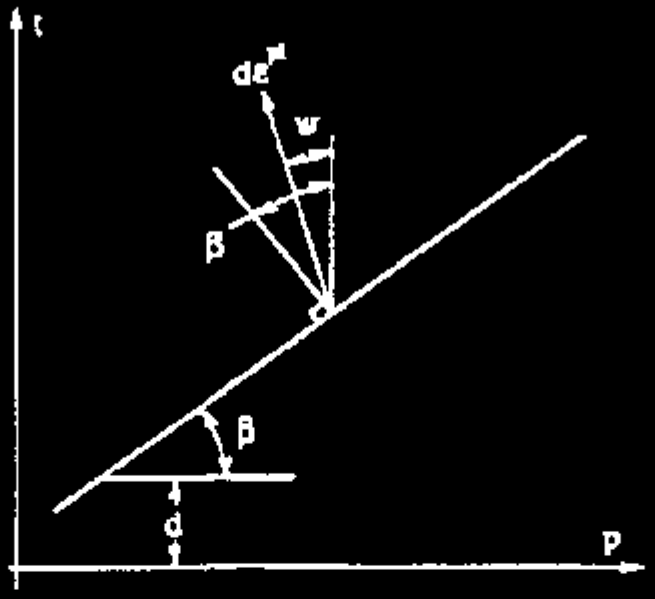

(a) Schematic Diagram of the p-t plane

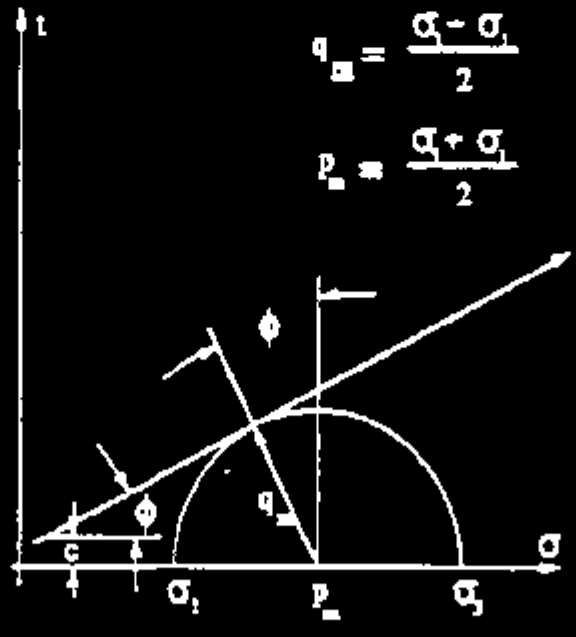

(b) Schematic Diagram of the Mohr-Coulomb Relation

behavior of the model. The general form of the ABAQUS extended Drucker-Prager constitutive soil model is written as

$$t - p\tan(\beta) - d = 0 \qquad (2\text{-}14)$$

where

$$t = \frac{1}{2} q\left[1+\frac{1}{K}-\left(1-\frac{1}{K}\right)\left(\frac{r}{q}\right)^3\right]$$

q = *von Mises equivalent stress*

$$d = \left[1-\frac{1}{3}\tan(\beta)\right]\sigma_c$$

σ_c = *uniaxial compression stress*

r = *third invariant of deviatoric stress*

K = *yield stress ratio* $\frac{\text{triaxial tension}}{\text{triaxial compression}}$

β = *friction angle in p-t space.*

When $\Psi = \beta$ and K = 1, the classical Drucker-Prager model is recovered. Note that if K = 1, then t becomes q, the von Mises stress. The yield line in the p-t plane (Figure 2-27) shows a striking similarity to the Mohr-Coulomb yield surface. The Drucker-Prager and Mohr-Coulomb yield surfaces are equivalent in triaxial compression and tension if ϕ, β, K, c, and d are given as:

$$Tan\beta = \frac{6\sin\phi}{3-\sin\phi}$$

$$d = c\left[\frac{6\cos\phi}{3-\sin\phi}\right] \qquad (2\text{-}15)$$

$$K = \frac{3-\sin\phi}{3+\sin\phi}.$$

All constitutive models contain parameters that must be calibrated from test data. A minimum of two triaxial compression tests at different confining pressures are required to define the Drucker-Prager soil parameters. Dames & Moore (1988) conducted triaxial compression tests on Grout Vault soil and provided graphs of stress versus strain at three different confining pressures (see Figures 2-1, 2-2 and 2-3). The Drucker-Prager parameters were chosen specifically so that finite-element simulations of these tests closely matched the experimental results.

To complete the Drucker-Prager constitutive model description requires volume-change data to determine the dilation angle and Poisson's ratio. Such data are not included in the Dames & Moore report. However, the test reports do contain enough information to define the internal angle of friction, Young's modulus, and the material yield stress. These parameters, along with Poisson's ratio, completely describe the classical Drucker-Prager plasticity model (Drucker and Prager 1952).

ABAQUS Drucker-Prager Strain-Hardened Soil Model

The Dames & Moore (1988) triaxial test data must be transformed into true stress and logarithmic (true) strain, as these are quantities used by ABAQUS. The transformed data and the transformation equations are shown in Table 2-1. The data given in Table 2-1 were used to derive the Drucker-Prager strain-hardened soil model. The transformation of the engineering stress to true stress assumes a Poisson's ratio of 0.5. Because of the lack of volume-change data specific to the Hanford Site soil, the assumption of Poisson's ratio of 0.5 may not result in the greatest accuracy for plastic deformation strains. As stated previously, the angle of internal friction is related to the slope of the material yield line in the (p,q) plane. Specifically, the angle of internal friction is the inverse tangent of the slope of the yield line. The best-fit line through the three yield points derived from the Dames & Moore triaxial test data has the equation

$$q_y = 0.71\ p + 3.41. \qquad (2\text{-}16)$$

Thus, the internal angle of friction is 35.4°. The best-fit line and the three yield points are shown in Figure 2-28.

The point at which the best-fit yield line intersects the q axis is the uniaxial yield stress value. The uniaxial yield stress value is one of the parameters required in the ABAQUS implementation of the Drucker-Prager plasticity model. In the present case, from Equation 2-9 with p set equal to zero, the uniaxial yield stress value is 3.41 lbf/in^2.

The granular soil is an extremely nonlinear material that exhibits plastic strain hardening at lower strains (both loose and dense) and plastic softening at large strains (if dense). The degree of hardening and softening depends on the confining pressure and density. The soil stiffness (tangent modulus and unload-reload modulus) is related to the confining pressure through a power function as given by Equations 2-1 and 2-2 (Duncan et al. 1980). An engineering evaluation of the Dames & Moore triaxial test data has shown agreement with this trend. The soil models have been derived for the actual triaxial test results with power function interpolation and extrapolation of the soil data for different confining pressures.

Figure 2 28. Best-Fit Yield Line for Triaxial Test for Grout Vault Soil. (Julyk et al. 1993)

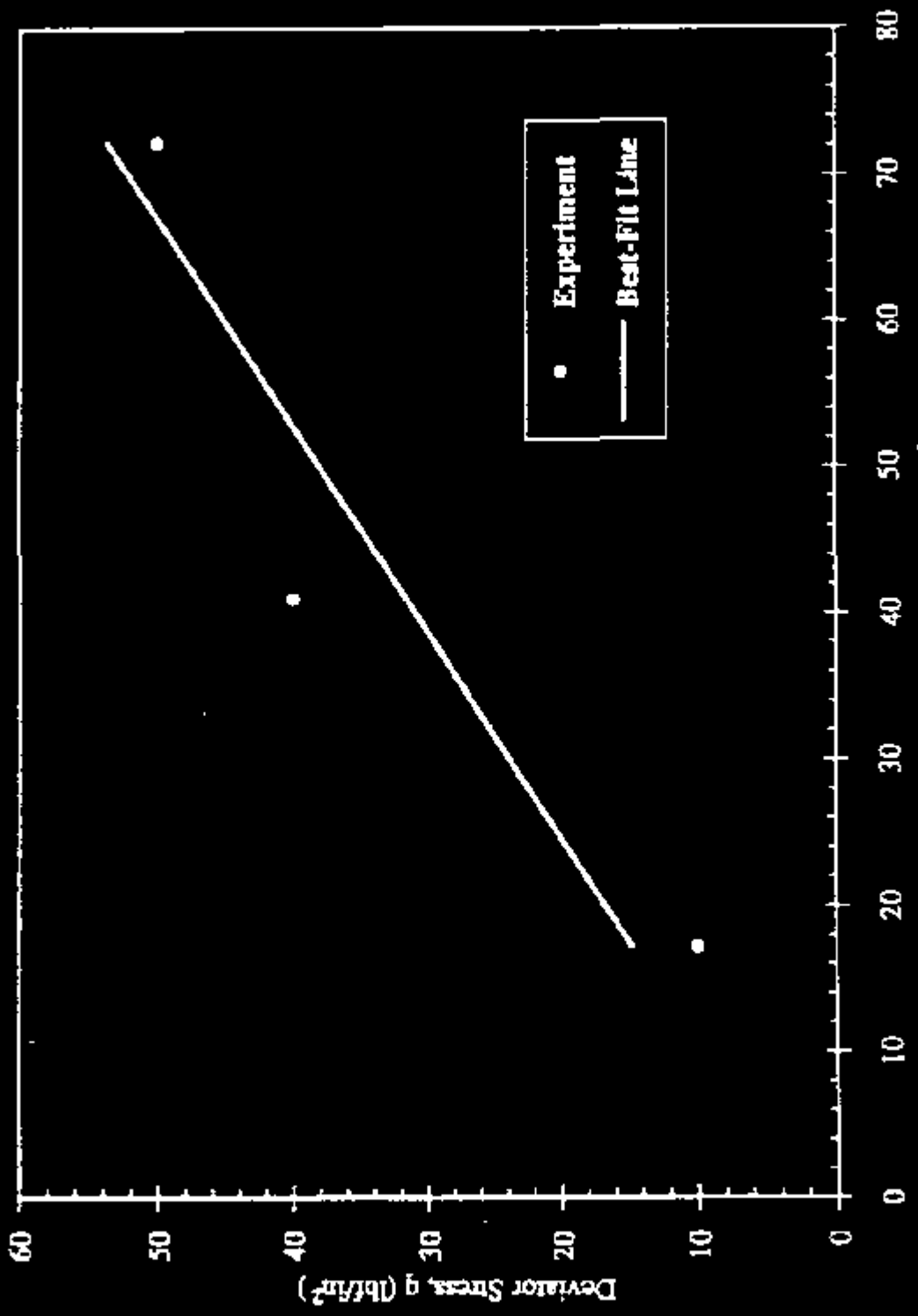

Table 2-1. True Stress versus Logarithmic (True) Strain for Triaxial Test Data from Grout Vault Soil. (Dames & Moore 1988)

Confining Pressure, p_c (lbf/in^2)	13.9	27.8	55.6
True Axial Strain (in/in)	True Axial Stress (lbf/in^2)	True Axial Stress (lbf/in^2)	True Axial Stress (lbf/in^2)
0.0000	23.9	27.8	55.6
0.0101	47.4	82.0	133.8
0.0202	54.5	115.6	173.2
0.0305	58.9	127.8	203.4
0.0408	61.3	132.9	220.6
0.0513	62.3	134.1	228.3
0.0619	62.7	132.9	232.9
0.0726	62.5	130.9	234.1
0.0834	61.6	126.8	234.3
0.0943	60.5	123.1	231.8
0.1054	58.6	--	228.3
0.1165	55.6	--	224.8
0.1278	52.6	--	221.3

The true strain and the true stress are determined from the triaxial test data by

$$\textit{True axial strain} = -\log(1-\epsilon)$$
$$\textit{True axial stress} = \sigma(1-\epsilon) + p_c$$

where σ denotes the engineering deviator stress from the test data, and ϵ denote the corresponding engineering strain from the test data. These are taken as positive quantities.

The soil-model confining pressures are specified in ABAQUS by field variables that can be updated at any analysis step. The field variables can be adjusted manually to account for changes in confining pressure that result from changes in stress state. This process is an iterative one in which the analyst compares mean-stress contour plots from results of the current analysis load step with the current field-variable values. If the values do not agree within a specified tolerance then the field-variable values are adjusted accordingly.

ABAQUS Drucker-Prager Elastic, Perfectly Plastic Soil Model

ABAQUS analyses using the Drucker-Prager strain-hardened soil model rely heavily on automatic load incrementation and many cycles of iteration for convergence of the plasticity algorithm. The requirement to deactivate the ABAQUS automatic incrementation and limit iteration to three cycles when the ANACAP-U concrete constitutive model is invoked motivated the implementation of the simpler Drucker-Prager elastic, perfectly plastic model with reduced Young's modulus. The reduced Young's modulus accounts for the stiffness reduction associated with plastic deformation. The elastic, perfectly plastic soil model was easier to run and, in a verification case, gave essentially the same results as the full elastic plastic model when the field variables to account for the changing mean stress were updated.

The triaxial test data from Dames & Moore (1988) indicate that the elastic Young's modulus as well as the post-yield behavior depends on the confining pressure. The dependence of soil material properties on the confining pressure has been recognized for some time (Wong and Duncan 1974, Seed and Duncan 1983, Scott 1985). The pressure dependence is modeled by defining the Young's modulus and the yield stress in terms of a predefined field variable representing the expected confining pressure at a material point. Because the confining pressure is not known a priori, the static field variable approach is inherently approximate and iterative. If the actual pressures at the end of an analysis are similar to those at the beginning, the results can be judged favorably. Even in the case where the beginning and ending pressure fields are not equivalent, the analysis may be valid as long as the pressure changes are generally small or highly localized where load redistribution will tend to diminish their effects. The static field-variable approach is reasonable for this effort because only small pressure changes are expected to occur throughout the soil during the concrete creep analysis with the possible exceptions of local regions below the footing or during the collapse-load analysis for surcharge loading.

The elastic modulus for this soil model is taken to be the unload-reload modulus that varies with confining pressure. If a triaxial soil specimen is unloaded during a test, the stress-strain curve followed during the unloading is steeper than the curve followed during primary loading, as shown in the plots from Dames & Moore (see Figures 2.1-2 and 2.1-3). If the soil sample is reloaded, the stress-strain curve followed is also steeper than the trend for primary loading and is quite similar in slope to the unloading curve. The soil behavior is inelastic, because the strains occurring during the initial loading are only partially recoverable on unloading. On reloading there is always some hysteresis, but the Hanford

Site Grout Vault test results show that reasonable accuracy can be obtained by assuming a single unload-reload modulus that ignores hysteretic effects for static analyses. Again the interpolation and extrapolation of the unload-reload modulus employs a power equation relating modulus to confining pressure.

In introducing the elastic, perfectly plastic model, the uniaxial yield stress must be modified to produce the correct stress-strain behavior. The yield stress must be increased greatly beyond the 3.41 lbf/in^2 level or else the perfectly plastic portion of the stress-strain curve will lie far below the maximum experimental stress level. The increased yield stress changes the tensile response of the material model significantly. However, the soil deformation from tank expansion is small, and superficial loading places the soil in compression.

2.4.5 Recommendations for Hanford Site Finite-Element Soil Modeling

Based on Chen (1994) the best finite element plasticity based constitutive material model for granular soils is the fourteen-parameter Lade formulation. At the present time this model is not available at Hanford Site and is not a part of the Hanford Site structural analysis programs (such as ABAQUS and ANSYS).

A more commonly used model that is available at Hanford Site is the Drucker-Prager model. The Drucker-Prager does have limitations in the failure region but it is numerically more stable than the Mohr-Coulomb model. Because the Lade model is not available currently (July 1995) at Hanford Site the Drucker-Prager Capped model should be used for Hanford Site soils modeling.

The triaxial test data is at this time the one of the best existing Hanford Site sources for soil properties at depth for finite-element model material definition. The Hanford Site soil has been shown to have a very linear unload/reload modulus behavior. The past loading or strain history can shift the Hanford Site soil into this linear unload/reload modulus region especially with compacted soil or soil that has not be disturbed but has had a large heavy overburden removed. As long as the new loads are not greater than the previous soil load and the soil is not disturbed it will act very linear. The range of the loads may need to be checked for extreme load case analyses.

The power equation relation for confining pressure can be used to interpolate and extrapolate triaxial test data as needed. This method was also recommended in the Cornell University report funded by EPRI.

Although the triaxial testing data base is important for Hanford Site soil characterization, plane strain soil testing data is probably more applicable for soil properties around the wall and wall foundation of very large buried tanks with axisymmetric loads. Published public domain research data has shown that plane strain test data versus triaxial data results in stiff modulii by factors of two to as much as four. In like manner the

compression failure strength seems to increase by about 50 percent and the strain at failure decreases to 1/3. The stress-strain curves for plane strain testing and triaxial testing are significantly different.

Soil finite-element modeling on the outside of the tank walls should account for compaction with the unload/reload modulii used for small strains. Exact determination of the strain limit for unload/reload moculii depends on the compaction history.

It is recommended that the existing Hanford Site triaxial testing data base be used to establish the lower bound soil properties. The upper bound properties for buried tanks should be factored up from the triaxial testing to account for plane strain effects (For example modulii factored up by 2 or 3 times.).

2.5 RECOMMENDATIONS FOR SOIL FAILURE EVALUATION

The Hanford Site sandy soil does not have a failure problem when it is properly compacted. Soil failure is not a concern for operational loads or code case factored loads. Checks for soil failure would be based on existing Hanford Site triaxial soil testing. The Berkeley hyperbolic model (Wong and Duncan 1974, Duncan et al. 1980) has been used at the Hanford Site to interpolate and extrapolate limited triaxial test data to provide soil strength data at various depths and confining pressures. The hyperbolic model was also recommended for similar use for foundation design in a Cornell University report funded by the Electric Power Research Institute (Kulhawy and Mayne 1990).

Although the triaxial testing data base is important for Hanford Site soil characterization, plane strain soil testing data is probably more applicable for soil properties around the wall and wall foundation of very large buried tanks with axisymmetric loads. Published public domain research data has shown that plane strain test data versus triaxial data results in stiff modulii by factors of 2 to as much as 4. In like manner the compression failure strength seems to increase by about 50 percent and the strain at failure decreases to 1/3. The stress-strain curves for plane strain testing and triaxial testing are significantly different.

It is recommended that the existing Hanford Site triaxial testing data base be used to establish the lower bound soil failure (strength) properties. The upper bound failure (strength) properties for buried tanks should be factored up 50 percent (with modulus factored up also) from the triaxial testing to account for plane strain affects.

3.0 SEISMIC SOIL MODELING

3.1 DYNAMIC SOIL MODELING PROPERTIES

The effect of dynamic earth pressure is considered in the design of Safety Class 1 and Safety Class 2 below-grade structures. Safety Class 3 and 4 structures are not required to be evaluated for dynamic soil loads.

The subsurface conditions shall be determined by means of borings, test pits, triaxial shear tests, or other approved field and laboratory methods that adequately disclose soil and groundwater conditions. Data and other information obtained from prior subsurface investigations at nearby sites are used, supplemented by additional investigations at the specific location as deemed necessary by the design professional. Subsurface investigations are made for critical facilities. A bibliography and brief summary of geotechnical studies performed at Hanford Site have been documented by Giller (1992).

Values defining the dynamic properties of the native soils and backfill materials are required in the dynamic analysis of tank structures and their foundations. Parameters required for these analyses include soil depth related properties of Poisson's ratio, shear wave velocity and shear moduli and strain-dependent relationships for shear moduli reduction and damping. These properties were developed for the MWTF project based upon site-specific studies that included both field testing and laboratory measurements and correlations with testing done at nearby facilities including the vitrification plant and the grout vault in the 200 East area.

3.1.1 Shear Wave Velocity

Shear wave velocity is commonly used in ground response analyses and soil structure interaction studies. Shear wave velocities for the in situ soils at the MWTF sites were largely based upon field measurements from a large-strain geophysical crosshole test. Limited results from field pressuremeter tests were also used to collaborate the results of the crosshole velocity measurements. Velocity data were augmented with velocity measurements from the nearby vitrification plant and grout vault sites.

The shear wave velocity data show excellent agreement among the testing procedures used at the site (crosshole and pressuremeter) and the test results from the vitrification plant and the grout vault. This correlation of the velocities that were derived using different measurement techniques provides a high confidence level in the crosshole test results at the MWTF 200 West site. The only exceptions are the lower velocities determined for the WNP-1 and WNP 4 sites. The lower velocities at the WNP 1 and WNP-4 sites may be attributed to differing subsurface conditions that exist for locations closer to the Columbia river.

The velocity data also suggest that the vertical stratigraphy at the MWTF 200 West site is relatively uniform because of the small scatter (+/- 200 ft/sec) in the data at adjacent test depths. Additionally, the shear wave velocity suggest continuity in the horizontal stratigraphy at Hanford Site because similar velocities were obtained in the 200 East sites including the MWTF site, the vitrification plant, and the grout vaults. However, the shear wave velocities at the 200 West area are about 200 ft/sec higher than the 200 East area. This small difference is consistent with the underlying soil conditions that are more dense at the 200 West area.

Shown on Figure 3-1 is the recommended shear wave velocity, compression wave velocity, and computed Poisson's ratio distribution profile for the MWTF sites. This recommended distribution is largely based on the results of the crosshole geophysical test data.

The soil density and shear wave velocity data for both the 200 East and 200 West Areas are shown in Table 3-1 and Table 3-2 respectively.

3.1.2 Compression Wave Velocity

Measurements of compression wave velocities obtained at the MWTF 200 West site and at nearby sites are also presented in Figure 3-1. Compression wave velocities derived at the 200 West site were determined from the large-strain geophysical crosshole tests. Figure 3-1 also includes velocities determined for the MWTF 200 East site, the vitrification plant, the grout vault, WNP-1 and WNP-4.

The compression wave velocities determined for the MWTF 200 West site compare favorably with the results for the 200 East site which includes both crosshole and downhole measurements. This agreement in the velocities that were derived using different testing procedures provides a high level of confidence in the results.

The compression wave velocities for the MWTF sites are approximately 800 ft/sec greater than at WNP-1 and WNP-4 which may again be attributed to differing geologic conditions for locations closer to the Columbia river.

The compression wave velocities for both the MWTF 200 East and West sites are approximately half the values reported for the vitrification plant and the grout vault. The compression wave velocities at the vitrification plant and the grout vault are suspect because of their unusually high values and the resulting unusually high values of Poisson's ratio that are not consistent with published values. The higher compression wave velocities and Poisson's ratio at the grout vault and vitrification plant may be attributed to the use of water-filled casings in the field measurements. Specifically, it may be that the measured

Figure 3-1. Dynamic Soil Properties Velocities and Poisson's Ratio. (Shannon & Wilson, Inc. 1994)

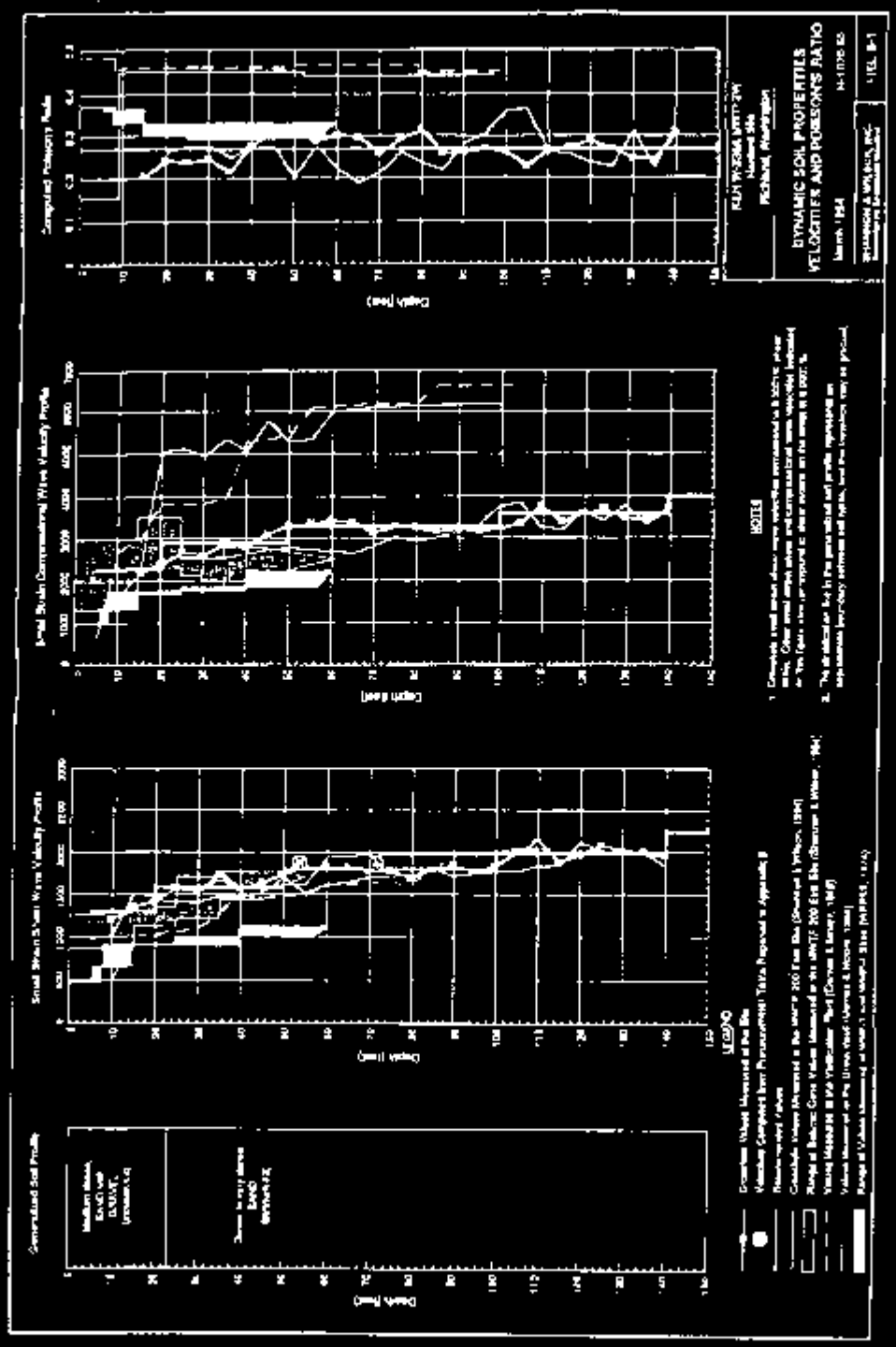

Table 3 1. Summary of Dynamic Soil Properties.

200 East Area Table 2, Shannon & Wilson 1994a			
Material	Depth Below Grade (ft)	Moist Density (lbf/ft^3)	V_s (ft/sec)
Stratum 2 (Gravel) El.727 to 706	0 to 21	112	1200
Stratum 3 (Sand) El.706 to 663 El.663 to 613 El.613 to 477 El.477 to 250	21 to 64 64 to 114 114 to 135 135 to 250 250 to 477	113 113 113 113 113	1500 1750 2000 2000 2500
Bedrock	477	140	4000
Backfill	0 to 60	130	1000

Table 3-2. Summary of Dynamic Soil Properties.

200 West Area Table 8-2, Shannon & Wilson 1994b			
Material	Depth Below Grade (ft)	Moist Density (lbf/ft^3)	V_s (ft/sec)
Stratum 2 (Sand,Gravel) El.685 to 670	0 to 15	113	1300
Stratum 3 (Sand) El.670 to 640 El.640 to 590 El.590 to 550 El.550 to 440 El.440 to 135	15 to 45 45 to 95 95 to 135 135 to 245 245 to 550	113 113 113 113 113	1600 1800 2000 2250 2500
Bedrock	550	140	4000
Backfill	0 to 60	130	1000

compression wave velocities were from the water inside the casings as opposed to the compression wave velocity in the unsaturated soil outside of the casing. This is substantiated in that the recorded velocities at both locations below a depth of 20 feet were typically on the order of 5,000 to 6,000 ft/sec and is very close to the compression wave velocity of water. Therefore, the reported compression wave velocities and the calculated Poisson's ratio are artificial and do not reflect the in situ dry soil conditions. However, since soil structure interaction analyses are typically insensitive to these parameters, the interaction studies conducted using these values may not have been significantly affected by the use of these properties.

The recommended compression wave velocity distribution was largely based on the results from the large-strain crosshole geophysical testing.

3.1.3 Dynamic Poisson's Ratio

Poisson's ratio is defined by a relationship between shear wave velocity and compression wave velocity. Shear and compression wave velocities determined from the large-strain crosshole testing at the MWTF site were used to compute the Poisson's ratio at each 5 ft test depth interval. On the average, these measurements support a constant Poisson's ratio of 0.27. This average value for the Poisson's ratio is substantiated by data presented in Fang (1991) which indicates that a nearly dry sand, similar to Hanford Site soils, would have a Poisson's ratio of 0.25. The Poisson's ratio of 0.27 also agrees with the 0.30 Poisson's ratio that was calculated from the soil velocity measurements at WNP-1 and WNP-4. Therefore, a constant Poisson's ratio of 0.27 to characterize the soils is recommended.

Different values of Poisson's ratio have not been assigned for static and dynamic conditions. Existing research (Shannon and Wilson and Agbabian Associates, 1972; Fang 1991) shows Poisson's ratio to be independent of strain and loading conditions (i.e., static or dynamic) for soil strains in the range expected at Hanford Site during an earthquake. Poisson's ratio may change at strain levels approaching the failure limit of the soil. While soil strain may result in a change to the Poisson's ratio, soil strains expected under earthquake loading will be much less than those of the failure limit and therefore, a single constant value of Poisson's ratio of 0.27 is applicable for modeling the site soils.

3.1.4 Strain Dependent Shear Modulus Curve

The strain-dependent shear moduli reduction data derived for the in situ soils are presented in Figure 3-2. This plot contains data from all of the large-strain crosshole geophysical tests conducted at the MWTF site (depth range of 10 to 140 ft). All of the site data is plotted on a single curve. No significant differences could be detected in the computed results for intermediate depth ranges of 10 to 50 ft, 50 to 100 ft, and 100 to 140 ft.

The figure also contains shear moduli reduction curves derived by Seed and Idriss (1970) for sands and relationships recently published by the Electric Power Research Institute (EPRI, 1993) for generic soils. The Hanford Site data typically lie between the Seed and Idriss sand curve and the EPRI generic soil curve. Therefore, the data from the crosshole testing of the in situ soils are in reasonable agreement with published data.

Shear moduli reduction data derived from the results of dynamic laboratory tests are also presented in Figure 3-2. The data was derived from the results of resonant column and cyclic triaxial tests performed on reconstituted materials obtained from site explorations. It was necessary to test reconstituted samples of the site soils because it was not possible to obtain undisturbed samples of the sand for laboratory testing. The samples were reconstituted to dry densities of 110 and 116 lb/ft^3. Because the reconstituted samples cannot account for the slight cementation characteristics of the in situ native soils, some differences are expected between the results of the dynamic laboratory tests and the actual behavior of the site soils. The normalized moduli were not significantly different at confining pressures ranging from 0.5 to 1.5 times the overburden stress at the bottom of the tank foundation. These findings are similar to the data derived from the crosshole tests.

There is good correlation between the results of the crosshole tests of the in situ native soils and the laboratory tests of the backfill soils. The relationship defining the results of the crosshole testing may be used to model the dynamic behavior of the in situ site soils.

3.1.5 Strain Dependent Damping Curve

Data characterizing the dynamic damping properties are presented in Figure 3-2. The data was obtained exclusively from the results of the resonant column and cyclic triaxial testing because damping values are not measured in the large-strain geophysical crosshole tests. The damping relationship is for both the site in situ soils and the backfill material. This relationship was largely based on the results of the laboratory resonant column test data that provided more consistent and reproducible results. Although the recommended damping curve falls below the Seed and Idriss (1970) and EPRI (1993) curves, the recommended damping relation is reasonable and consistent with published values.

3.2 TANK SOIL-STRUCTURE INTERACTION

Seismic loads and reactions may be amplified due to the effect of soil-to-structure interaction (SSI).

SSI analyses generally involve significant uncertainties in soil and structural stiffness. To account for these uncertainties, it is a common practice to perform parametric SSI studies. See, for example, Section 3.4 of Bandyopadhyay, 1993 and Section 3.3.1.7 of ASCE, 1986. Three-dimensional analyses are necessary. Since three-dimensional dynamic

Figure 3-2. Dynamic Soil Properties Shear Moduli and Damping. (Shannon & Wilson, Inc. 1994)

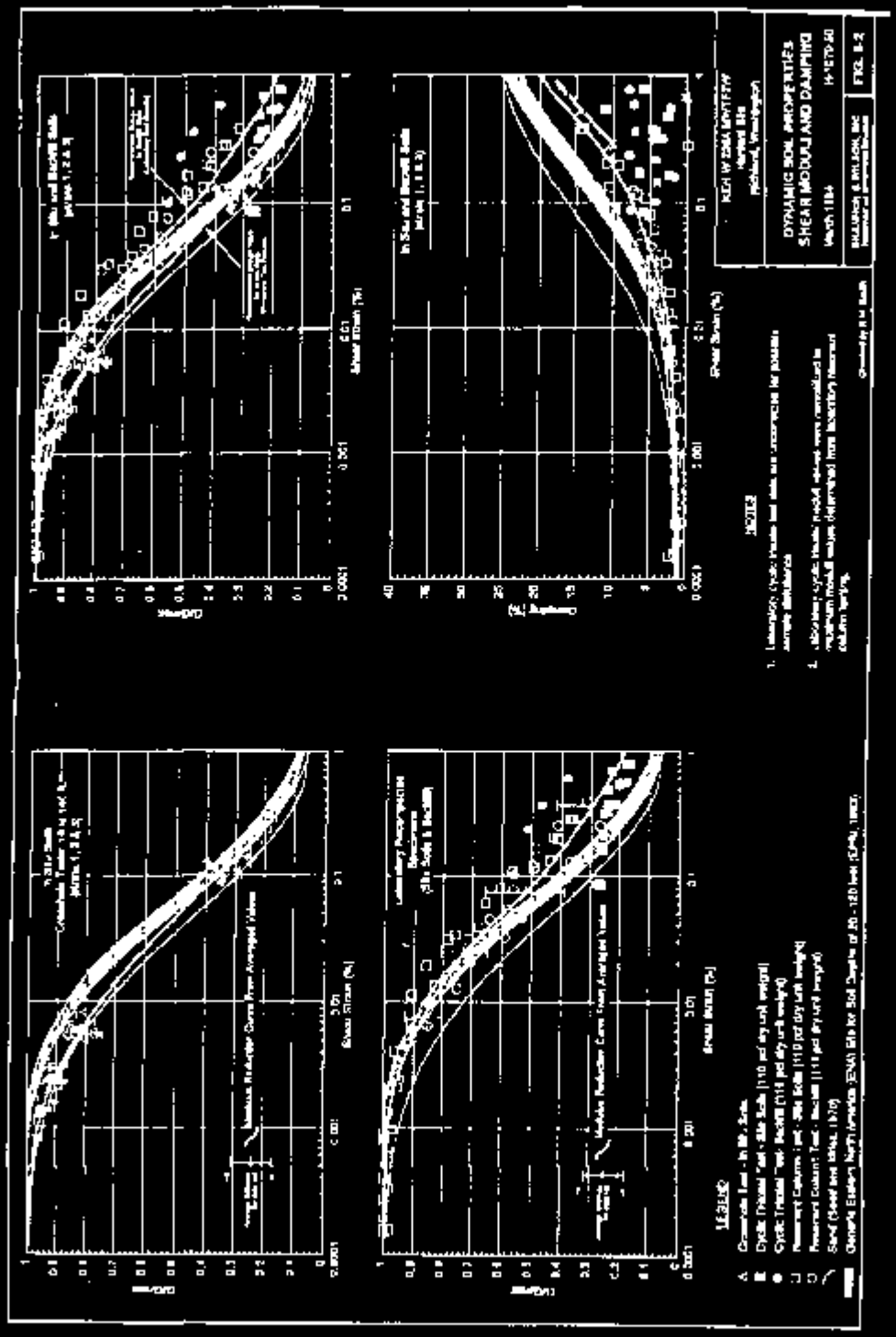

SSI analyses can be relatively expensive to run and cumbersome to process, simplified static models should be developed to perform the parametric studies. The dynamic analyses can then be limited to a few critical combinations of parameters.

In order to obtain the seismic response of the concrete structure to provide seismic inputs for the seismic analysis of the primary tank and the associated components, it is necessary to perform seismic SSI analysis of the tank-soil system. Objectives of the SSI analyses effort are to perform simplified evaluations of the tank-soil system in order to identify critical combinations of tank and soil stiffness parameters for further, more detailed evaluation. Studies to evaluate the effects on the seismic response of parameters such as steel liner stiffness, fluid mass content, concrete cracked-section stiffness, and soil stiffness variation, should be performed. Bandyopadhyay (1993) recommends a simplified one dimensional lumped parameter spring/damper model evaluation of buried waste tanks in lieu of the more rigorous three-dimensional finite-element (FE) evaluation. No justification of this simplified evaluation technique for tanks of small height to radius ratios is provided. Applicability of the simplified spring/damper model was addressed for the MWTF project.

Parametric models consisting of lumped-parameter spring/damper stick models were evaluated. Inadequacy of the lumped-parameter model approach was demonstrated by comparing results with a relatively rigorous three-dimensional dynamic model. Based upon the results from these comparisons, significant reservations developed in the ability of the stick models to adequately predict the three dimensional response of the buried tanks.

A three-dimensional model of the tank and surrounding soil was developed. The model was loaded by using static lateral acceleration of the soil column. The magnitude of the static lateral acceleration loading was selected such that the peak soil strains obtained from the free field dynamic analysis of the soil column were approximated. This approach yielded results that were more consistent with the three-dimensional dynamic response.

3.2.1 SHAKE

In order to provide seismic inputs for the seismic analysis of the concrete structure, the primary tank, and the associated components, it is necessary to perform seismic free field soil analyses. The primary objective of the free field soil analysis is to perform free field soil evaluations to obtain the iterated seismic strain compatible dynamic soil properties (damping and shear modulus) and acceleration time-histories to be used as input to fixed base SSI evaluations, and soil layer strains to be used during the simplified model parametric evaluations.

In order to perform soil free field analyses, industry accepted, quality assurance qualified, and efficient computer analysis codes are required. The following is a brief description of SHAKE, the computer code selected for the soil free field analysis and the rationale behind the selection.

The program SHAKE is a FORTRAN[3] computer code developed to calculate the earthquake response in a horizontal layered semi-infinite soil/rock system subjected to transient, vertically propagating shear waves through the base-rock motion. Developed by Schnabel, Lysmer, and Seed at the University of California, Berkeley, the program is based on the continuous solution to the wave-equation adapted for use with transient motions through the fast fourier transform algorithm.

The program SHAKE is selected for use because it has been in use by the engineering profession since 1972, and is one of the most popular and widely used programs in the field of SSI. The program is well recognized in the industry, and it provides all the necessary analysis options required for SSI evaluations. Verification of the SHAKE program has been performed. The program has sixteen (16) run options. However, only a few of the options will normally be used.

In general, two of the main usages of the SHAKE program are:

- Generate iterated strain-dependent soil properties for input into SSI analysis programs such as SASSI.

- Compute new control motions at the top of specified soil layer produced from a control ground motion. The new control motion is then used for input to SSI analyses.

The formulation of the SHAKE program is based on certain assumptions that translates into limitations in the modeling. The following are a few of the major limitations:

- The soil system must extend infinitely in the horizontal direction.

- Each layer in the soil system must be completely defined by its value of shear modulus (or shear wave velocity), critical damping ratio, density, and thickness.

- The responses in the system are caused by the upward propagation of shear waves from the underlying rock formation.

SOIL PROFILE

The SHAKE evaluation shall be run for site specific soil data. Structural properties of clay and rock are generally not used in the SHAKE evaluations at Hanford Site because Hanford Site is a deep granular soil site. The site-specific soils reports shall provide

---

[3]FORTRAN is a registered tradename of International Business Machines (IBM), Corporation.

non-linear relationships to be used for all soil depths. The soil data should also include site-specific shear wave velocities and dynamic Poisson's Ratio.

Bandyopadhyay (1993) recommends that bounding values of the soil shear moduli be used. Three soil profiles representing the best estimate, lower bound and upper bound of the final site-specific soil investigation must be used in the evaluation. The lower-bound soil shear moduli is equal to the best-estimate moduli divided by a constant factor. The upper bound soil shear moduli is equal to the best-estimate moduli multiplied by the constant factor. In the absence of site specific data quantifying the variability of the soil shear modulus, the constant factor shall of 2.0 shall be used. When site specific soil data is obtained showing actual soil variability, a lower value may be used but shall not be less than 1.5. The moduli are adjusted before running the SHAKE program.

Soil layer thicknesses should be selected to match soil layers used in the SASSI evaluation. Soil layer thicknesses shall be derived in accordance with ASCE (1986) for proper transmission of high frequency content of seismic motion and in accordance with Bandyopadhyay (1993) which recommends that soil layer thicknesses need not transmit frequencies greater than 25 hertz.

Total depth of soil column is derived in accordance with ASCE (1986) as the lesser of bedrock depth, depth of soil having a shear modulus of 10 times that at the foundation, or a depth below the foundation of no greater than three times the foundation width.

A frequency cutoff of 20 hertz should be used. As discussed in the SHAKE 1972 manual, page 17, frequencies above 10 to 15 hertz carry relatively little energy. For the MWTF project, the lower bound soil condition was evaluated using cutoff frequencies of 25 hertz and 20 hertz. The difference in maximum soil strains was less than 2 percent. The difference in maximum ground acceleration was less than 5 percent in the top 140 feet and less than 12 percent at depths greater than 140 feet. The difference in response spectral values at the base of the tank were less than 3 percent.

The input motion specified in SDC 4.1 is a surface motion. The control point for the input motion shall be selected as a rock outcropping at the top of the uppermost competent soil layer. Bandyopadhyay (1993) states that soil sites where a soft (shear wave velocity less than 750 feet per second) soil overlays a stiffer soil, the motion control point shall be specified at the free surface of an outcropping of the stiffer material.

SEISMIC INPUT

The acceleration time-history used for the evaluation shall be derived to match the site-specific response spectra of SDC 4.1. Synthetic earthquake time histories have been developed that adequately match, with appropriate scale factors, the design response spectra of SDC 4.1. These time histories may be used for SSI evaluation. These time histories are presented for standard use site wide. The time histories are documented in Weiner (1995)

which describes the development and review of the time histories and describes where the digitized files of the time histories may be accessed. Digitized files of the small-magnitude near-field time history and the small-magnitude near-field response spectra are also available in the same location. The analyst is not restricted, however, to the use of these time histories. Any time history that is adequately documented to match the design response spectra may be used.

The response spectra accelerations and the time-history accelerations may be scaled to obtain response spectra and time histories at zero period accelerations other than the 0.20 *g*.

Time histories found in Weiner (1995) shall be scaled in accordance with the following table for application at various damping levels to ensure enveloping of the design response spectra.

Table 3-3. Time Histories Scaling.

Damping %	geoh.ht	geov.ht
2	1.13	1.08
5	1.05	1.01
7	1.	1.
10	1.01	1.03
12	1.02	1.07

3.2.2 SASSI

Detailed three-dimensional finite-element analyses are necessary for reliable results. The SSI response of the concrete structure due to vertical and horizontal seismic excitation shall be evaluated. The seismic results from the vertical analysis shall be combined with those from the horizontal analysis to obtain the total seismic SSI response. These seismic results can then be combined with other applicable loads to form the final design loads for the design/evaluation of the concrete tank structure. Other seismic results such as acceleration time-histories and amplified response spectra may be obtained for analysis of other structures, components or equipments.

The SHAKE results of the iterated strain compatible soil properties from those of the horizontal analysis are applicable for both the horizontal and vertical SASSI analyses. This is based on the assumption that seismic effects on soil properties are similar for both vertical

and horizontal orientations and is primarily controlled by the horizontal earthquake excitation.

In order to perform sophisticated FE or SSI analyses, industry accepted, quality assurance (QA) qualified, and efficient computer analysis codes are required. The following is a brief description of the computer code SASSI selected for SSI analysis and the rationale behind the selection:

SASSI

The SASSI (a System for Analysis of Soil Structure Interaction) program is a special purpose computer code that can be used to solve a wide range of dynamic SSI problems in two or three dimensions. It contains nine inter-related modules. The program treats SSI problems with the flexible-volume substructuring method. In this approach, the problem is subdivided into a series of simple problems. Each problem is solved separately and the results are combined in the final step of the analysis to provide the complete solution, based on the principle of superposition.

SASSI is extensively used in the field of SSI analysis. It has been used in the analysis of structures for many commercial nuclear facilities. The program was developed at the University of California at Berkeley, by a research team consisting of four (4) doctoral students under the direction of Prof. John Lysmer who is a highly recognized expert in the field of SSI. The SASSI program is selected for use based on its accepted use in the nuclear industry and its special capability in the 3D analysis of SSI problems with FE modeling of the structure.

MODEL DESCRIPTION

Three-dimensional dynamic soil-structure interaction (SSI) seismic analyses have only become practical in the last decade. Only two seismic analyses of buried tanks have been performed on the Hanford Site employing SSI techniques. A review of the tank seismic work and consulting with a DOE tank seismic experts panel has reinforced the conviction that detailed SSI is a prudent way to evaluate single or multiple buried structures.

SASSI 3D QUARTER-TANK SHELL MODEL

The SASSI quarter-tank shell model uses four node quadrilateral shell elements having bending and membrane capabilities to model the concrete tank walls, dome, and base slab. The secondary liner and the supporting concrete pad were not modeled. The primary metal tank was modeled using beam elements having a moment connection at the base of the tank and a roller connection at the top of the tank.

Eight node solid elements were used to model the backfill soil elements. The size of the soil elements in the base and dome areas was selected to satisfy the guidance in ASCE (1986), paragraph 3.3.3.4 to have at least eight horizontal elements over the foundation width. Soil layer thickness were specified so that frequencies of 23 hertz were transmitted through soil having a lower bound stiffness. Soil element size above and below the tank was approximately 10 feet by 10 feet horizontal. Soil element size beside the tank was approximately 11 feet circumferential by 3 feet radial. Soil layer thicknesses are approximately 5.4 feet above the tank, 8.2 feet beside the tank, and 10 feet below the tank.

The shell elements used to represent the concrete tank have aspect ratios of approximately 1.

The soil element nodes are attached to the structural element nodes at every structural element node.

The quarter-tank shell model uses the global x and y axis for the plan and the global z axis for elevation. The origin is located at the centerline of the axi-symmetric tank at the bottom of the tank. One-quarter of the tank was modeled using one plane of symmetry and one plane of antisymmetry in the horizontal evaluation model and two planes of symmetry in the vertical evaluation model. Seismic motion was specified in the +/- x direction for the horizontal evaluation and in the +/- z direction for the vertical evaluation.

Degrees-of-freedom (DOF) were assigned to each node according to the type of element connected to it and according to the boundary conditions associated with the planes of symmetry and antisymmetry. Nodes used to define the shell elements depicting the reinforced concrete tank have six DOF, three translational (ux, uy, and uz) and three rotational (rotx, roty, and rotz). Nodes having $y=0$ lie on a plane of symmetry in both horizontal and vertical evaluation models. Nodes having $x=0$ lie on a plane of symmetry in the vertical evaluation model and on a plane of antisymmetry in the horizontal evaluation model.

Shell element nodes on a symmetry plane have the out-of-plane translation and the rotations about the in-plane axes set to zero. Shell element nodes on an antisymmetry plane have rotations about the out-of-plane axis and the in-plane translations set to zero. Shell element nodes having $x=y=0$ lie on the centerline axis of the tank and have DOF constrained according to the sum of the symmetry/antisymmetry conditions. The remainder of the shell element nodes not lying on a plane of symmetry or antisymmetry have all six DOF free to displace, no DOF set to zero.

Nodes used to define both shell elements and solid elements have the DOF set to the rules for the shell elements. Nodes used to define only solid elements have possible only three structural DOF, the three translational DOF. For all these nodes, the three rotational DOF are set to zero ($rotx=roty=rotz=0$). The translational DOF follow the rules for the shell elements.

Table 3-4. Element Nodes.

		Shell Element Nodes				Solid Element Nodes			
		x=0	y=0	x=0 y=0	x≠0 y≠0	x=0	y=0	x=0 y=0	x≠0 y≠0
Horiz. Model	sym type	asym	sym	℄	none	asym	sym	℄	none
	translation DOF	uy=0 uz=0	uy=0	uy=0 uz=0	none	uy=0 uz=0	uy=0	uy=0 uz=0	none
	rotation DOF	rotx=0	rotx=0 rotz=0	rotx=0 rotz=0	none	rotx=0 roty=0 rotz=0	rotx=0 roty=0 rotz=0	rotx=0 roty=0 rotz=0	rotx=0 roty=0 rotz=0
Vertical Model	sym type	sym	sym	℄	none	sym	sym	℄	none
	translation DOF	ux=0	uy=0	ux=0 uy=0	none	ux=0	uy=0	ux=0 uy=0	none
	rotation DOF	roty=0 rotz=0	rotx=0 rotz=0	rotx=0 roty=0 rotz=0	none	rotx=0 roty=0 rotz=0	rotx=0 roty=0 rotz=0	rotx=0 roty=0 rotz=0	rotx=0 roty=0 rotz=0

TESTING OF SYMMETRY CONDITIONS

The development of the most cost-effective buried-tank seismic analyses requires the use of symmetric and antisymmetric boundary conditions. For example, a single tank under a horizontal seismic acceleration can be modeled as a quarter-model with both symmetric and antisymmetric boundary conditions. In like manner two tanks subjected to horizontal seismic accelerations can be modeled with a single half-tank employing symmetric and antisymmetric boundary conditions.

The developed half-model tank (necessary for tank to-tank interaction studies) was run with a horizontal seismic acceleration and a single symmetric boundary condition. The half-model single-tank results were compared with the results from the same horizontal seismic excitation employing a quarter-tank model with two symmetry conditions (symmetric and antisymmetric). The results (as indicated by forces and moments in the tank shell elements) from the two single-tank models were identical. The SASSI antisymmetric boundary conditions and the use of these boundary conditions were verified to be correct.

The SASSI program defines the site soil as an infinite continuum with interaction nodes established throughout the structure of interest. The structural nodes and elements connect to the soil interaction nodes. The SASSI user manual allows the definition both of

The SASSI program defines the site soil as an infinite continuum with interaction nodes established throughout the structure of interest. The structural nodes and elements connect to the soil interaction nodes. The SASSI user manual allows the definition both of symmetry planes and of boundary conditions on all nodes. It was not clear whether the symmetry planes could be established outside the structural nodes and elements.

Two simple test cases were run to test the establishment of antisymmetric planes beyond the structural FE mesh. A buried half-tank was modeled with interface soil and interaction nodes out to the antisymmetric plane (center line between the two buried tanks). The model had the proper boundary conditions for antisymmetry defined for all nodes on the plane. A second half-tank was modeled having interface soil and interaction nodes around the tank but not out to the antisymmetric boundary at the two tank center line position. The antisymmetry nodes are outside the structural model.

The forces and moments in the buried tank shell for both models were the same. SASSI antisymmetric planes can be established outside the structural model.

PRIMARY TANK STICK MODEL

The methodology for modeling the primary metal tank and the fluid mass in the finite-element models of the concrete tank is discussed herein.

The concrete tank is explicitly modeled including the stiffness of the metal liner where appropriate. The primary tank is modeled as a stick connected to the concrete tank at the base and at the haunch. The primary tank stick has the stiffness of the average of the wall thickness over the lower two-thirds of the liquid height (Bandyopadhyay, 1993, Section 4.3.2.2).

In the SASSI 3D quarter-tank shell model, the base of the primary tank stick is connected to the concrete tank perimeter using stiff beams. These stiff beams are connected to the primary tank stick in translation and in bending about the horizontal axis. The beams are released such that they transmit no torsion or bending about the vertical axis. The beams are pinned to the concrete base slab approximately where the primary tank contacts the base slab. The top of the primary tank stick is connected to the concrete perimeter using stiff spars. The stiff spars are connected to the concrete dome approximately where the primary tank contacts the dome. In the horizontal evaluation, the fluid mass is connected to the primary tank stick using a spring. Only the impulsive mass as determined by Bandyopadhyay (1993) is included in the horizontal evaluation.

For the vertical analysis, the effect of the fluid mass was modeled with lumped masses connected and distributed to the nodes of the concrete tank base slab. As a conservative approach, one hundred per cent of the waste fluid mass was lumped to the base slab for the vertical evaluation.

The primary tank including the connecting beams and spars were modeled and tested to verify that the impulsive fluid mass was responding horizontally at the appropriate frequency and that the support reactions are properly distributed. The mass of the impulsive fluid (m_i), the frequency of the impulsive fluid (f_i), and the effective height of the impulsive fluid (h_i') shall be calculated in accordance with Bandyopadhyay (1993) Chapter 4. In accordance with Bandyopadhyay (1993), the support reactions are to be distributed 40 percent to the dome and 60 percent to the base. The stiffness of the fluid mass spring and the connecting beams and spars shall be varied until the proper impulsive fluid mass frequency and support reactions were achieved. The primary tank model can then incorporated into the SASSI models.

ANALYSES INPUT

SOIL PROFILE

Soil property inputs of shear wave velocity at seismic strain, density, and poisson's ratio shall be taken from the site-specific SHAKE analysis. The SHAKE results of the iterated strain compatible soil properties shall be used as input for both the horizontal and vertical SASSI analyses. This is based on the assumption that seismic effects on soil properties are similar for both vertical and horizontal orientations and is primarily controlled by the horizontal earthquake excitation. Seismic evaluations shall be based on site-specific soil shear modulus reduction and damping curves.

SEISMIC INPUT

The acceleration time-histories used for the horizontal and vertical seismic SSI evaluation shall be the same as used in the SHAKE evaluation.

SEISMIC SSI EVALUATION

For the SSI analysis of the concrete tank, the most significant parameters that affect the overall results are : dynamic soil property (i.e. Lower Bound properties (LB); Best Estimate properties (BE); and Upper Bound properties (UB)) and the level of waste fluid content in the tank (empty or full). For the SSI analysis, six (6) cases were analyzed and identified as follows:

Seismic results from the horizontal and the vertical earthquake directions for each load case shall be combined using the square-root of-the-sum of-the squares (srss) method.

IN-STRUCTURE RESPONSE SPECTRA

Enveloped horizontal and vertical response spectra is developed for points on the tank base and the tank dome for subsequent evaluation of tank mounted equipment.

Response spectrum results from the horizontal and the vertical earthquake directions need be combined only for the horizontal response at the haunch. Only the tank haunch has any appreciable horizontal response to the vertical earthquake. This can be explained by considering that the haunch is the tension ring at the base of the dome arch. As the dome flexes vertically, the haunch flexes horizontally. Response spectrum results from the horizontal and vertical earthquake directions at all other tank locations need not be combined. Typically, the vertical response due to the horizontal earthquake and the horizontal response from the vertical earthquake (except at the haunch) are not significant.

TRANSFER FUNCTIONS

The SASSI evaluation is performed at user selected frequencies from which SASSI interpolates results for intermediate frequencies. In performing the SASSI SSI analysis, an initial set of frequency points (approximately 15) shall be specified for the analysis. Based on the transfer functions for the initial set of frequency points, additional frequency points shall then be selected to produce smooth transfer functions whose peaks are well defined by calculated frequencies.

3.2.3 ANSYS Equivalent Static

SSI analyses generally involve significant uncertainties in such parameters as soil and structural stiffness. To account for these uncertainties, it is a common practice to perform parametric SSI studies. See, for example, Section 3.4 of Bandyopadhyay, 1993 and Section 3.3.1.7 of ASCE, 1986. Since three-dimensional SSI analyses can be relatively expensive to run and cumbersome to process, simplified models should be developed to perform the parametric studies. The detailed three-dimensional analyses can then be limited to a few critical combinations of parameters.

The basis for using a static evaluation of the buried tank-soil system to approximate the dynamic seismic response of the buried tank is that the inertial effects of the buried tank are not significant when compared to the reaction of the tank to the deformation of the soil column during the earthquake. By simulating the maximum deformation of the soil column in the range of the depth of the buried tank, the maximum strain and stress of the buried tank can be approximated.

Seismic strains of the soil column shall be obtained from the SHAKE evaluation for the three sets of soil properties: best estimate, lower bound, and upper bound. The soil strains for the top 130 feet of soil occurring at the time of maximum soil strain at the base of the buried tank shall be compared to soil strains computed by ANSYS by applying a lateral acceleration to the soil-tank system and checking the soil strain in the soil elements on the perimeter of the soil column to verify that the SHAKE soil strains were duplicated in the depth of the buried tank. The maximum ground acceleration for the soil layer at the base of the buried tank may be used as an initial static lateral acceleration of the soil-tank system. Lateral ground acceleration can then be adjusted until soil strains from the SHAKE and the

ANSYS evaluations agree for the elevations of interest over the depth of the tank. The static soil strains at depths below the tank need not match the dynamic soil strains and will not affect the maximum strain and stress of the buried tank.

ANSYS

In order to perform sophisticated FE or SSI analyses, industry accepted, quality assurance (QA) qualified, and efficient computer analysis codes are required. The following is a brief description of the computer code ANSYS selected for simplified SSI analysis and the rationale behind the selection.

ANSYS is a general purpose finite-element analysis computer code that has been used in the nuclear industry for decades. The program has an extensive element library with over 70 element types and many analysis options. It also has extensive graphic, preprocessing and postprocessing capabilities.

It is a well documented and proven FE program. With the availability of an extensive element library, it provides flexibility in terms of modeling. The program comes with a well documented theoretical manual and verification manual. It is QA approved by ICF Kaiser Hanford Company (ICF/KH) and has a good error reporting system maintained by Swanson Analysis System, Inc.

MODEL DESCRIPTIONS

This section provides general descriptions of the various computer models used for the seismic parametric study.

ANSYS 3D HALF-TANK MODEL

The ANSYS 3D half-tank model is similar to the SASSI quarter-tank shell model described above, but with half (i.e. 180 degrees) of a single tank modeled. The shell elements representing the reinforced concrete tank, the solid elements representing the soil that is immediately below, beside, and above the tank, and the beam elements representing the primary steel tank are identical in geometry and properties to the SASSI model. Additional soil beside and below the tank is modeled in the ANSYS model using eight node solid elements. As this model would be used for static evaluations, the size of the added soil elements were allowed to exceed the ASCE-4-86 guidelines for dynamic evaluations. The ANSYS model is a 180-degree tank model including about two tank-radii of adjacent soil on the bottom of the tank and three tank-radii of soil on the sides. Above the tank, the soil extends to the surface. Symmetry boundary conditions were applied. The soil was fixed at the bottom of the soil column. The ANSYS model uses the global x and z axis for the plan and the global y axis for elevation. Seismic motion was specified in the +/- x direction.

TESTING OF SYMMETRY CONDITIONS

The developed half-model tank (necessary for soil-structure-structure-interaction studies) was run with a horizontal seismic acceleration and a single symmetric boundary condition. The half-model single-tank results were compared with the results from the same horizontal seismic excitation employing a quarter-tank model with two symmetry conditions (symmetric and antisymmetric). The results (as indicated by forces and moments in the tank shell elements) from the two single-tank models were identical. The SASSI antisymmetric boundary conditions and the use of these boundary conditions were verified to be correct.

SOIL PROFILE

Soil property inputs of shear wave velocity at seismic strain, density, and poisson's ratio shall be taken from the site-specific SHAKE analysis.

3.2.4 Tank-to-Tank Interaction

Bandyopadhyay (1993) recommends that for multiple tank installations, tank-to tank interaction effects are not significant unless the spacing between the tanks is less than one-half tank radius, and that tank-to-tank interaction effects should be evaluated for spacings closer than one-half tank radius.

Two studies of seismic tank-to-tank interaction were completed at Hanford. One study evaluated seismic tank-to-tank interaction for an existing reinforced concrete tank design used during construction of the Hanford Site in the 1940's. These existing tanks are separated by approximately two-thirds tank radius. The other study evaluated seismic interaction and radius of separation for newly designed double shelled buried waste tanks. The new tanks are scheduled to be installed at a spacing of one tank radius. A detailed three-dimensional finite-element SSI study to determine the tank-to-tank interaction effects for the multiple tank installations was performed for tank separations of one tank radius, one-half tank radius, and one-quarter tank radius. The SSI seismic analysis for single and two-tank interaction were completed with the computer program SASSI.

The two tank to-tank interaction evaluations conclude that interaction effects for tanks separated by one-half tank radius or more have no significant increases in stress levels in the concrete tanks. Maximum in-plane shear stresses at the base of the wall are relatively uncharged for the one-tank-radius-separation and reduced by 4 percent for the one-half- and one-quarter-tank radius separation. Tank-to-tank interaction decreases the peak vertical membrane stress in the walls by 1 percent at one-tank-radius separation and increases the peak vertical membrane stress in the walls by 2 percent at one-half-tank-radius separation and 30 percent at one-quarter-tank-radius separation. Many other peak stress components have larger percentage increases or decreases as a result of tank-to-tank interaction, but because of the low stress magnitudes the changes are considered insignificant. The largest shear stress increase is 30 lbf/in^2. The largest membrane stress increase is 32 lbf/in^2. Thus, the effects

of tank-to-tank interaction are generally minor. The computation of tank-to-tank interaction considered the effect of only one adjacent tank and assumed the two tanks to be identical (no difference in contents, in situ loads, or materials).

DESCRIPTION OF THE DOUBLE-SHELL TANK MODEL

The 3D model used a vertical plane of symmetry parallel to the excitation direction and a vertical plane of antisymmetry perpendicular to the excitation direction. The reinforced concrete base, wall, and dome of the tank are modeled with thin-shell elements. The primary steel tank is modeled with vertical beam elements at the centerline of the tank. The vertical beam elements have the section properties of the primary steel tank. The near-field soil, that is considered part of the structural model, is modeled with solid elements. The near-field soil mesh extends 36 in. radially outward from the tank wall and to the ground surface above the dome apex. No soil is modeled beneath the tank base. Eight-node brick elements as well as degenerate eight-node elements (wedges) are used in modeling the near-field soil. All brick elements use fourth-order integration. Nodes are shared by the tank and near-field soil at the tank-soil interface.

Soil is modeled as a viscoelastic material using site-specific data. Soil density as a function of depth, shear modulus as a function of depth and effective strain, percentage of critical damping as a function of effective strain, and a horizontal control motion at the ground surface are provided as input to the computer program SHAKE. The variation of density and shear modulus with depth and the variation of shear modulus and damping with effective strain are taken from EPRI. A synthetic acceleration time history based on the 5 percent-damped, 0.35-g anchored site specific response spectrum is used as the horizontal control motion in SHAKE.

Poisson's ratio of the soil, taken as a constant equal to 0.27, is based on wave speeds reported in Shannon and Wilson (1994b). Because Poisson's ratio is assumed to be a constant, compression wave speed is directly proportional to shear wave speed.

The damping ratios of the soil calculated by SHAKE and used in SASSI are typically within a range of 0.01 to 0.06 (1 percent to 6 percent of critical damping) and thus are well within the maximum damping value of 15 percent allowed by Bandyopadhyay (1993). Free-field soil and near-field soil (fill) are assumed to have the same fundamental material properties. Further, the effective strain profile in the near-field soil used in developing strain-compatible shear moduli and damping ratios is approximated as being equal to the effective strain profile in the free-field soil.

The reinforced concrete tank is modeled with shell elements of elastic, isotropic material. The thickness of shell element and Young's modulus of the elastic material are prescribed to approximate the uncracked, undegraded concrete properties. The weight density of 150 lbf/ft^3 was used to approximate the density of reinforced concrete.

Results from the study of single tank configurations indicate that empty tanks have greater SSI effects than do full tanks (full tanks more closely duplicate the mass of the excavated soil). For this reason, only the empty tank configuration was evaluated for TTI.

TESTING OF SASSI SYMMETRY CONDITIONS

The development of the most cost-effective buried-tank seismic analyses requires the use of symmetric and antisymmetric boundary conditions. For example, a single tank under a horizontal seismic acceleration can be modeled as a quarter-model with both symmetric and antisymmetric boundary conditions. In like manner two tanks subjected to horizontal seismic accelerations can be modeled with a single half-tank employing symmetric and antisymmetric boundary conditions.

The developed half-model tank (necessary for tank-to-tank interaction studies) was run with a horizontal seismic acceleration and a single symmetric boundary condition. The half-model-generated single-tank results were compared with the results from the same horizontal seismic excitation employing a quarter-tank model with two symmetry conditions (symmetric and antisymmetric). When boundary conditions consistent with standard engineering practice were used, the results (as indicated by forces and moments in the tank shell elements) from the two single tank models were identical. The SASSI antisymmetric boundary conditions and the use of these boundary conditions were verified to be correct.

TESTING OF THE TANK-TO-TANK ANTISYMMETRIC PLANE

The SASSI program defines the site soil as an infinite continuum with interaction nodes established around the structure of interest. The structural nodes and elements connect to the site interaction nodes. The SASSI user manual allows the definition both of symmetry planes and of boundary conditions on all nodes. It was not clear whether the symmetry planes could be established outside the structural nodes and elements.

Two simple test cases were completed to test the establishment of antisymmetric planes beyond the structural finite-element mesh. Results from a buried half-tank shell with interface soil and interaction nodes modeled out to the antisymmetric plane (center line between the two buried tanks) were compared to results from a second half-tank model having interface soil and interaction nodes modeled around the tank but not out to the antisymmetric boundary at the two tank center line position.

The forces and moments in the buried tank shell for both models were the same. SASSI antisymmetric planes can be established outside the structural model.

4.0 THERMAL SOIL MODELING

The average and dry values of sandy soil thermal conductivity and specific heat are shown in Table 4-1 (P/THERMAL 1991). Bouse (1975) measured the thermal conductivity of several samples of backfill soil from SX tank farm. His values ranged from 0.13 Btu/h-ft-°F for loosely poured dry soil at 79 °F to 0.51 Btu/h-ft-°F for vibrated soil at 215 °F. A more realistic thermal conductivity for dry, sandy soil is approximately 0.30 Btu/h-ft-°F (Julyk et al., 1993).

5.0 SOIL DENSITY

Typical site soil densities are 100 to 112 lb/ft^3 down to 34 feet depth with an average of approximately 110 lb/ft^3 on to 120 ft with approximately 125 lb/ft^3 at greater depths. Please refer the overview of Hanford Site soil data reports by Giller (1992).

6.0 REFERENCES

American Society of Civil Engineers (ASCE), 1986, *Seismic Analysis of Safety-Related Nuclear Structures and Commentary on Standard for Seismic Analysis of Safety Related Nuclear Structures*, ASCE 4-86, American Society of Civil Engineers, New York, New York.

Bandyopadhyay, K., et al., 1993, *Seismic Design and Evaluation Guidelines for the Department of Energy High-Level Waste Storage Tanks and Appurtenances*, BNL 52361, Department of Nuclear Energy, Brookhaven National Laboratory, Associated Universities, Inc., Upton, New York. (DOE Tank Seismic Experts Panels-TSEP).

Bouse, D. G., July 1975, *Thermal Conductivity of Hanford Waste Tank Solids and SX Tank Farm Soil Samples*, ARH-CD-378, Atlantic Richfield Hanford Company, Richland, Washington.

Boyle, S.R., 1995, *Deformation Prediction of Geosynthetic Reinforced Soil Retaining Walls*, Ph.D. Dissertation, University of Washington, 391 pp.

Chen, W. F., and E. Mizuno, 1990, *Nonlinear Analysis in Soil Mechanics*, Developments in Geotechnical Engineering 53, Elsevier, 661 pp.

Chen, W. F., 1994, *Constitutive Equations for Engineering Materials Volume 2: Plasticity and Modeling*, Pub. Elsevier Science B. V., Amsterdam, The Netherlands.

Chen, W. F. and A. F. Saleeb, 1994, *Constitutive Equations for Engineering Materials Volume 1: Elasticity and Modeling*, Pub. Elsevier Science B. V., Amsterdam, The Netherlands.

Cornforth, D. M. 1964, *Some Experiments on the Influence of Strain Conditions on the Strength of Sand*, Geotechnique, Vol. XIV, No. 2, pp 143-167.

Dames & Moore, 1988, *Report, Geotechnical and Corrosion Investigation, Grout Vaults, Hanford, Washington*, Contract No. 87059-255-001, Dames & Moore, Seattle, Washington.

Desai, C. S. and H. J. Siriwardane, 1984, *Constitutive Laws for Engineering Materials--With Emphasis on Geologic Materials*, Prentice-Hall, Inc., 468 pp.

Drucker, D. C., R. E. Gibson, and D. J. Henkel, 1957, "Soil Mechanics and Work-Hardening Theories of Plasticity," *Transactions*, ASCE, Vol. 112, pp. 338-346.

Drucker, D. C. and W. Prager, 1952, "Soil Mechanics and Plasticity Analysis or Limit Design," *Quarterly Journal of Applied Mathematics*, Vol. 10, pp. 157 165.

Duncan, J. M., P. Byrne, K. S. Wong, and P. Mabry, 1980, *Strength, Stress-Strain and Bulk Modulus Parameters for Finite-Element Analyses of Stresses and Movements in Soil Masses*, Report No. UCB/GT/80-01, University of California, Department of Civil Engineering, Berkeley, California.

Electric Power Research Institute (EPRI), 1993, *Guidelines for Determining Design Basis Ground Motions, Volume 1, Method and Guidelines for Estimating Earthquake Ground Motion in Eastern North America*, EPRI TR-102293, Electric Power Research Institute, Palo Alto, California.

Fang, H. Y. ed, 1991, *Foundation Engineering Handbook*, 2nd edition, Van Nostrand, New York, New York.

Giller, R. A., 1992, *Bibliography and Summary of Geotechnical Studies at the Hanford Site*, WHC-SD-GN-ER-30009, Westinghouse Hanford Company, Richland, Washington.

Green, G. E. and D. W. Reades, 1975, *Boundary Conditions, Anisotropy, and Sample Shape Effects on the Stress-Strain Behavior of Sand in Triaxial Compression and Plane Strain*, Geotechnique, Vol. 25, No. 2, pp. 333-356.

Hanford Plant Standards SDC-4.1, *Standard Arch-Civil Design Criteria - Design Loads for Facilities*, Revision 12. Department of Energy, Richland, Washington.

HKS, 1989, *ABAQUS User's Manual*, Version 4.8 with 4.9 Supplement, Hibbitt, Karlsson & Sorensen, Inc., Pawtucket, Rhode Island.

Holtz, R. D., 1991, *Stress Distribution and Settlement of Shallow Foundations*, Foundation Engineering Handbook, Second Edition, H. Y. Fang, Editor, Chapter 5, Van Nostrand Reinhold, New York, New York, pp. 179-180.

Julyk, L. J.,T. J. Bander, J. P. Day, A. D. Dyrness, R. S. Marlow, C. J. Moore, E. W. Pianka, and M. P. Weis, 1993, *Tank 241-C-106 Structural Integrity Evaluation For In Situ Conditions*, WHC-SD-W320-ANAL-001, Westinghouse Hanford Company, Richland, Washington.

Kitamura, R. and M. Haruyama, 1988, "Compression and Shear Deformation of Soil Under Wide-Ranging Confining Pressure," *Advanced Triaxial Testing of Soil and Rock*, ASTM STP 977, R. T. Donaghe, R. C. Chaney, and M. L. Silver, Eds., American Society for Testing and Materials, Philadelphia, 1988, pp. 501-511.

Kulhawy, F. H. and P. W. Mayne, 1990, *Manual on Estimating Soil Properties for Foundation Design*, prepared for Electric Power Research Institute, by Cornell University, Geotechnical Engineering Group, Ithaca, New York.

Lade, P. V., 1977, "Elasto-Plastic Stress-Strain Theory for Cohesionless Soil with Curved Yield Surfaces," International Journal of Solids and Structures, Vol. 13, pp. 1019-1035.

Lysmer, J., et al., 1972, *" SHAKE " A Computer Program for Earthquake Response Analysis of Layered Sites*, University of California, Berkeley, California.

Lysmer, J. et al., 1991, *User's Manual - SASSI : A System For Analysis of Soil-Structure Interaction*, University of California, Berkeley, California.

Marachi, N. D., J. M. Duncan, C. K. Chan, and H. B. Seed, 1981, *Plane-Strain Testing of Sand*, Laboratory Shear Strength of Soil, ASTM STP 740, R. N. Yong and F. C. Townsend, Editors, American Society for Testing and Materials, pp 294-302.

Oda, M., I. Koishikawa, and T. Higuchi, 1978, *Experimental Study of Anisotropic Shear Strength of Sand by Plane Strain Test*, Soils and Foundations, Vol. 18, No. 1, pp. 26-38.

Perloff, W. H., 1975, *Pressure Distribution and Settlement*, Foundation Engineering Handbook, H. F. Winterkorn and H. Y. Fang, Eds., Chapter 4, Van Nostrand Reinhold, New York, New York, pp. 148-196.

Peters, J. F., P. V. Lade and A. Bro, 1988, *Shear Band Formation in Triaxial Testing of Soil and Rock*, ASTM STP 977, R. T. Donaghe, R. C. Chaney, and M. L. Silver, Editors, American Society for Testing and Materials, pp. 604-627.

Price, W. H. and K. R. Fecht, 1976, *Geology of the 241-C Tank Farm*, ARH-LD-132, Atlantic Richfield Hanford Company, Richland, Washington.

P/THERMAL, April 1991, *P/THERMAL Release 2.5 Notes*, PDA Engineering, PATRAN Division, Costa Mesa, California.

Schmertmann, J. H., 1970, *Static Cone to Compute Static Settlement Over Sand*, Journal of Soil Mechanics and Foundation Division, ASCE, 96, No. SM3, New York, New York, pp. 1011-1043.

Schmertmann, J. H., 1978, *Guidelines For Cone Penetration Test Performance and Design*, Federal Highway Administration, Report FHWA-TS-78-209, Washington D.C.

Schmertmann, J. H., J. P. Hartman, and P. R. Brown, 1978, *Improved Strain Influence Factor Diagrams*, Journal of the Geotechnical Engineering Division, ASCE, 104, No. GT8, pp. 1131-1135.

Scott, R. F., 1985, "Plasticity and Constitutive Relations in Soil Mechanics," Journal of Geotechnical Engineering, Vol. 111, No. 5, pp. 563-595.

Seed, H. B. and Idriss, I. M., 1970, *Soil Moduli and Damping Factors for Dynamic Response Analysis*, Earthquake Engineering Research Center report EERC 70-10, Berkeley, California, University of California.

Seed, R. B., and J. M. Duncan, 1983, *Soil-Structure Interaction Effects of Compaction-Induced Stresses and Deflections*, Report No. UCB/GT/83-06, University of California, Department of Civil Engineering, Berkeley, California.

Shannon & Wilson and Agbabian Associates, 1972, *Soil Behavior Under Earthquake Loading Conditions, State of the Art Evaluation of Soil Characteristics for Seismic Response Analysis*, Shannon & Wilson Inc, Seattle, Washington and Agbabian Associates, Los Angeles, California.

Shannon & Wilson Inc., 1994a, *Geotechnical Investigation KEH W236A, Multi-Function Waste Tank Facility - Hanford Site, Richland, Washington*, Submittal Number 8002A-10-AE1-011, (H-1053-05). ICF Kaiser Hanford Company, Richland, Washington.

Shannon & Wilson Inc., 1994b, *Geotechnical Investigation KEH W236A, Multi-Function Waste Tank Facility 200 West Area Addition, Richland, Washington*, Submittal Number 8008-1-AE2-008, (H-1070-50), ICF Kaiser Hanford Company, Richland, Washington.

Swanson, 1992, *ANSYS User's Manual For Revision 5.0*, UpdO DN-R300:50-1, Swanson Analysis System, Inc., Houston, Pennsylvania.

Vesic, A. S., 1961, "Beams on Elastic Subgrade and the Winkler Hypothesis", Proceedings, 5th International Conference on Soil Mechanics and Foundation Engineering, Vol. 1, Paris, pp. 845-850.

Weiner, E. O., 1995, *Design Basis Earthquake Time Histories*, WHC-SD-GN-DA-30018, Rev.0-A. Westinghouse Hanford Company, Richland, Washington.

Wong, K. S. and J. M. Duncan, 1974, *Hyperbolic Stress Strain Parameters for Non Linear Finite-Element Analyses of Stresses and Movement in Soil Masses*, Report No. TE-74-3, University of California, Department of Civil Engineering, Berkeley, California.

APPENDIX A

SPRING CALCULATIONS

This page intentionally left blank.

Horizontal Springs

From Timoshenko's, Strength of Materials, 1956, the elastic solution to a thick cylinder yields the following equation for radial stress.

$$\sigma_r = \frac{E}{1-\nu^2}\left[C_1(1+\nu) - \frac{C_2}{r^2}(1-\nu)\right]$$

@ $r = \infty$; $\sigma_r = 0$

@ $r = R_0$; $\sigma_r = -p_0$

Solving for C_1 and C_2

$C_1 = 0$

$$C_2 = p_0\left(\frac{1+\nu}{E}\right)R_0^2$$

Thus

$$\sigma_r = -\frac{p_0 R_0^2}{r^2}$$

The deflection of the soil at the tank wall for a given wall pressure, p_0, was determined by intergrating the strain over the distance along the radius.

$$\delta = \int_{R_0}^{\infty} \epsilon\, dr$$

Let

$$\epsilon = \frac{\sigma_r}{E}$$

Use the power relation of Section 2.1.1 for the unload reload modulus ($E = E_{ur}$).

$$E_{ur} = K_{ur} P_a \left(\frac{P_c}{P_a}\right)^n$$

$$\delta = \int_{R_0}^{\infty} \frac{P_0 R_0^2}{E r^2}\, dr = \frac{P_0 R_0^2}{E}\left[-\frac{1}{r}\right]_{R_0}^{\infty}$$

$$\delta = \frac{P_0 R_0}{E}$$

The equivalent horizontal soil spring is as follows:

$$S_h = \frac{F_0}{\delta} = \frac{P_0}{\frac{P_0 R_0}{E}} = \frac{E}{R_0}$$

$$S_h = \frac{K_{ur} P_a \left(\frac{P_c}{P_a}\right)^n}{R_0}$$

Double shell tank foundation soil-spring calculations
E.O. Weiner 9/14/95

Scope:

Soil spring stiffness relating to foundation settlement is estimated with the Schmertmann method. The basic case is axisymmetric for a uniform load over the full diameter of the foundation. Effects of the more concentrated wall load are estimated by separating outer rings of the foundation and treating them with plane strain criteria.

Default units: ft, kip

$t_c := 1.25$ dome thickness, ft

$h_c := 8.1$ soil height above crown, ft

$\gamma_s := .125$ soil density, kcf

$\gamma_c := .145$ concrete density

Weight calculations:

$a := 40$ $b = 15$ Inside dome ellipse major/minor axes

$V_s := 0.5 \cdot \frac{4}{3} \cdot \pi \cdot a^2 \cdot b$ $V_s = 5.027 \cdot 10^4$ half spheroid volume

$V_c := \pi \cdot 41.5^2 \cdot (h_c + t_c + b)$ $V_c = 1.317 \cdot 10^5$ cylinder above springline

$V_d := 1.5 \cdot 2 \cdot \pi \cdot 27.50$ $V_d = 1.272 \cdot 10^4$ estimate concrete portion

$V_w := 2 \cdot \pi \cdot 40.75 \cdot 1.5 \cdot 32.5$ $V_w = 1.248 \cdot 10^4$ wall

$W_{af} := (V_c - V_s) \cdot \gamma_s + V_d \cdot (\gamma_c - \gamma_s) + V_w \cdot \gamma_c$

$W_{af} = 1.225 \cdot 10^4$ wt above foundation, thru wall, extended outer wall cylinder

$q_w := .0624 \cdot 1.7 \cdot 35.17$ $q_w = 3.731$ Waste q, sp gr = 1.7, h=35.17

Other constants and functions:

$D = 59$ Depth of foundation

$E_{ur}(H) := 726.2 \cdot 2.12 \cdot \left(\frac{\gamma_s \cdot H}{2.12}\right)^{.73}$ ASA-I unload-reload modulus

Settlement estimates are based on Holtz 1991. Calculations simplify the integration of the influence curve by a centroidal estimate utilizing the mild E vs depth relation and infinite depth.

Axisymmetric case

$B := 89$ Full diameter of foundation

$\Delta q := .001$ Dq is negative, use small

$\sigma_{vp}(B) := \gamma_s \cdot (D + B)$ $\sigma_{vp}(B) = 18.5$

$q_{vo} := \sigma_{vp}(0)$

$C_{1t} := 1 - 0.5 \cdot \left| \frac{q_{vo}}{\Delta q} \right|$ $C_1 := if(C_{1t} < .5, .5, C_{1t})$ $C_1 = 0.5$

$I_{sp} := .5 + .1 \cdot \sqrt{\frac{\Delta q}{\sigma_{vp}(B)}}$ $I_{sp} = 0.501$

$I_{sa}(I_{sp}) := \frac{.1 + I_{sp}}{2} \cdot .5 - \frac{I_{sp}}{2} \cdot 1.5$ Axisymmetric L/B=1, integrate influence curve normalized to B=1 and constant E.

$I := I_{sa}(I_{sp})$ $I = 0.526$

$H_a(B) := D + 0.7 \cdot B$ Locate influence curve centroid depth

$E := E_{ur}(H_a(B))$ $E = 6.473 \cdot 10^3$

$k := \frac{E}{C_1 \cdot I \cdot B}$ $k = 276.696$ Subrade modulus, kcf

$q_{axf} := q_w + 2 \cdot \gamma_c$ $q_{axf} = 4.021$ $k_{axf} := k$ Save q and k, full tank

$q_{axe} := 2 \cdot \gamma_c$ $q_{axe} = 0.29$ Save q, empty tank

Plane strain case, B=6'

$B := 6$

$q_{vo} := D \cdot \gamma_s$ $q_{vo} = 7.375$

$R_a := 40 + 1.5 + \frac{3.25}{2}$ $R_a = 43.125$

$A := 2 \cdot \pi \cdot R_a \cdot 3.25$ $A = 880.628$

$W_{tot} := -q_{vo} \cdot A - W_{af}$ $W_{tot} = 1.874 \cdot 10^4$

$A_B := 2 \cdot \pi \cdot \left(44.75 - \frac{B}{2}\right) \cdot B$

$q := \frac{W_{tot}}{A_B} + q_w$ $q = 15.64$ $\Delta q := q - q_{vo}$ $\Delta q = 8.265$

$\sigma_{vp}(B) := \gamma_s \cdot (59 + B)$ $\sigma_{vp}(B) = 8.125$

$I_{sp} := .5 + .1 \cdot \sqrt{\frac{\Delta q}{\sigma_{vp}(B)}}$ $I_{sp} = 0.601$

$I_{sps}(I_{sp}) := \frac{.2 + I_{sp}}{2} \cdot 1 + \frac{I_{sp}}{2} \cdot 3$

$I := I_{sps}(I_{sp})$ $I = 1.302$

$C_{1t} := 1 - 0.5 \cdot \left(\frac{q_{vo}}{\Delta q}\right)$ $C_1 := if(C_{1t} < .5, .5, C_{1t})$ $C_1 = 0.554$

$H_{ps}(B) := 59 + 1.5 \cdot B$ Locate influence curve centroid depth

$E := E_{ur}(H_{ps}(B))$ $E = 4.243 \cdot 10^3$

$k := \frac{E}{C_1 \cdot I \cdot B}$ $k = 980.818$ Subgrade modulus, kcf

$k_{ps6f} := k$

Empty tank:

$q := \frac{W_{tot}}{A_B}$ $q = 11.909$ $\Delta q := q - q_{vo}$ $\Delta q = 4.534$

$I_{sp} := .5 + .1 \cdot \sqrt{\frac{\Delta q}{\sigma_{vp}(B)}}$ $I_{sp} = 0.575$

$I_{sps}(I_{sp}) := \frac{.2 + I_{sp}}{2} \cdot 1 + \frac{I_{sp}}{2} \cdot 3$

$I := I_{sps}(I_{sp})$ $I = 1.249$

$C_{1t} := 1 - 0.5 \cdot \left(\frac{q_{vo}}{\Delta q}\right)$ $C_1 := if(C_{1t} < .5, .5, C_{1t})$ $C_1 = 0.5$

$H_{ps}(B) := 59 + 1.5 \cdot B$ Locate Schmertmann centroid depth

$E := E_{ur}(H_{ps}(B))$ $E = 4.243 \cdot 10^3$

$k := \frac{E}{C_1 \cdot I \cdot B}$ $k = 1.132 \cdot 10^3$ Subgrade modulus, kcf

$q_{ps6} := q$ $k_{ps6e} := k$ Save

Plane strain case, B=12'

$B := 12$

$q_{vo} := D \cdot \gamma_s$ $\quad q_{vo} = 7.375$

$R_a := 40 + 1.5 + \frac{3.25}{2}$ $\quad R_a = 43.125$

$A := 2 \cdot \pi \cdot R_a \cdot 3.25$ $\quad A = 880.628$

$W_{tot} := q_{vo} \cdot A + W_{af}$ $\quad W_{tot} = 1.874 \cdot 10^4$

$A_B := 2 \cdot \pi \cdot \left(44.75 - \frac{B}{2}\right) \cdot B$

$q_w := .0624 \cdot 1.7 \cdot 35.17$ $\quad q_w = 3.731$ Waste q, sp gr = 1.7, h=35.17

$q := \frac{W_{tot}}{A_B} + q_w$ $\quad q = 10.146$ $\quad \Delta q := q - q_{vo}$ $\quad \Delta q = 2.771$

$\sigma_{vp}(B) := \gamma_s \cdot (59 + B)$ $\quad \sigma_{vp}(B) = 8.875$

$I_{sp} := .5 + \sqrt{1 - \frac{\Delta q}{\sigma_{vp}(B)}}$ $\quad I_{sp} = 0.556$

$I_{sps}(I_{sp}) := \frac{.2 + I_{sp}}{2} \cdot 1 + \frac{I_{sp}}{2} \cdot 3$

$I := I_{sps}(I_{sp})$ $\quad I = 1.212$

$C_{1t} := 1 - 0.5 \cdot \left(\frac{q_{vo}}{\Delta q}\right)$ $\quad C_1 := if(C_{1t} < .5, .5, C_{1t})$ $\quad C_1 = 0.5$

$H_{ps}(B) := 59 + 1.5 \cdot B$

$E := E_{ur}(H_{ps}(B))$ $\quad E = 4.646 \cdot 10^3$

$k := \frac{E}{C_1 \cdot I \cdot B}$ $\quad k = 638.97$ Subgrade modulus, kcf

$k_{ps12f} := k$

Empty tank:

$q := \frac{W_{tot}}{A_B}$ $q = 6.416$ $\Delta q := q - q_{vo}$ $\Delta q = -0.959$ $\Delta q := .001$

$I_{sp} := .5 + .1 \cdot \sqrt{\frac{\Delta q}{\sigma_{vp}(B)}}$ $I_{sp} = 0.501$

$I_{sps}(I_{sp}) := \frac{2 + I_{sp}}{2} \cdot 1 + \frac{I_{sp}}{2} \cdot 3$

$I := I_{sps}(I_{sp})$ $I = 1.102$

$C_{1t} := 1 - 0.5 \cdot \left(\frac{q_{vo}}{\Delta q}\right)$ $C_1 := if(C_{1t} < .5, .5, C_{1t})$ $C_1 = 0.5$

$H_{ps}(B) := 59 + 1.5 \cdot B$

$E := E_{ur}(H_{ps}(B))$ $E = 4.646 \cdot 10^3$

$k := \frac{E}{C_1 \cdot I \cdot B}$ $k = 702.535$ Subgrade modulus, kcf

$q_{ps12} := q$ $k_{ps12e} := k$

Pressure-deflection calculations. Purpose is to estimate soil springs. First case is an axisymmetric uniform waste pressure over the full foundation diamenter. Then, the foundation is assumed broken at B from the outer edge, and and the excess of the wall and soil ledge pressure (figured from loads over B) above the waste pressure is treated as a plane stain increment and superposed with the axisymmetric solution. The B=12' case resembles the 2' thick foundation section without rotation. The B=6' case is used to estimate how higher pressures from foundation rotation might behave.

$\delta q_{ps12e} := q_{ps12} - q_{axe}$ $\quad \delta q_{ps12e} = 6.126$ Excess wall load over waste extended to plane strain region

$\delta q_{ps12f} := q_{ps12} - q_{axf}$ $\quad \delta q_{ps12f} = 2.395$

$\delta q_{ps6e} := q_{ps6} - q_{axe}$ $\quad \delta q_{ps6e} = 11.619$

$\delta q_{ps6f} := q_{ps6} - q_{axf}$ $\quad \delta q_{ps6f} = 7.888$

$i := 1..3$

$qf_1 := q_{axf}$ $\quad sf_1 := \frac{qf_i}{k_{axf}}$ Settlement under waste pressure, full tank

$qf_2 := qf_1 + \delta q_{ps12f}$ $\quad sf_2 := sf_1 + \frac{\delta q_{ps12f}}{k_{ps12f}}$ Adding plane strain settlement, B=12'

$qf_3 := qf_1 + \delta q_{ps6f}$ $\quad sf_3 := sf_1 + \frac{\delta q_{ps6f}}{k_{ps6f}}$ Adding plane strain settlement, B=6'

$qe_1 := q_{axe}$ $\quad se_i := \frac{qe_1}{k_{axf}}$ Settlement with empty tank

$qe_2 := qe_1 + \delta q_{ps12e}$ $\quad se_2 := se_1 + \frac{\delta q_{ps12e}}{k_{ps12e}}$

$qe_3 := qe_1 + \delta q_{ps6e}$ $\quad se_3 := se_1 + \frac{\delta q_{ps6e}}{k_{ps6e}}$

sf_i	qf_i	se_i	qe_i
0.015	4.021	0.001	0.29
0.018	6.416	0.01	6.416
0.023	11.909	0.011	11.909

Pressure-settlement relations, no load factors:

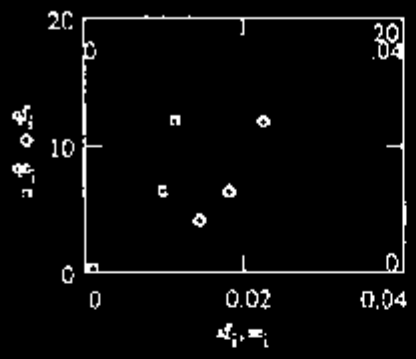

Repeat pressure-deflection calculations with load factors

$\delta q_{ps12e} := 1.4 \cdot q_{ps12} - 1.4 \cdot q_{axe}$ $\quad \delta q_{ps12e} = 8.576$

$\delta q_{ps12f} := 1.4 \cdot q_{ps12} - 1.7 \cdot q_{axf}$ $\quad \delta q_{ps12f} = 2.146$

$\delta q_{ps6e} := 1.4 \cdot q_{ps6} - 1.4 \cdot q_{axe}$ $\quad \delta q_{ps6e} = 16.267$

$\delta q_{ps6f} := 1.4 \cdot q_{ps6} - 1.7 \cdot q_{axf}$ $\quad \delta q_{ps6f} = 9.837$

$i := 1..3$

$qf_1 := 1.7 \cdot q_{axf}$ $\quad sf_1 := \frac{qf_1}{k_{axf}}$ Settlement under waste pressure, full tank

$qf_2 := qf_1 + \delta q_{ps12f}$ $\quad sf_2 := sf_1 + \frac{\delta q_{ps12f}}{k_{ps12f}}$ Adding plane strain settlement, B=12'

$qf_3 := qf_1 + \delta q_{ps6f}$ $\quad sf_3 := sf_1 + \frac{\delta q_{ps6f}}{k_{ps6f}}$ Adding plane strain settlement, B=6'

$qe_1 := 1.4 \cdot q_{axe}$ $\quad se_1 := \frac{qe_1}{k_{axf}}$ Settlement with empty tank

$qe_2 := qe_1 + \delta q_{ps12e}$ $\quad se_2 := se_1 + \frac{\delta q_{ps12e}}{k_{ps12e}}$

$qe_3 := qe_1 + \delta q_{ps6e}$ $\quad se_3 := se_1 + \frac{\delta q_{ps6e}}{k_{ps6e}}$

sf_i	qf_i	sc_i	qc_i
0.025	6.835	0.001	0.406
0.028	8.982	0.014	8.982
0.035	16.673	0.016	16.673

Pressure-settlement relations - with load factors

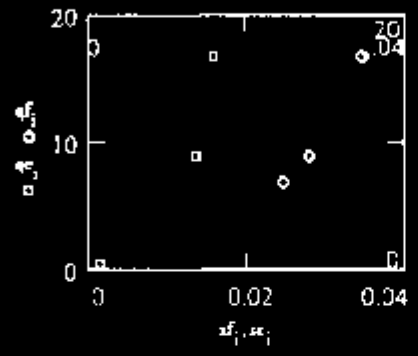

Conclusions:

Soil springs for the DST foundation are based on the full axisymmetric settlement condition without load factors, namely,

$$k_{axf} = 276.696 \quad \text{kcf} \qquad \frac{k_{axf}}{1.728} = 160.125 \quad \text{pci}$$

This corresponds to the first diamond on the plots of q vs s. The plots suggest that the full-tank condition with B=12' plane strain incremental loading (wall and soil ledge loads over B) is reasonably represented with this modulus. The situation is progressively worse for B=6' loading and the tank empty. The full-tank cases (diamonds) might be represented by a nonlinear spring, but the tank-empty cases (squares) would still be misrepresented. This is a limitation of soil spring modeling. A complete representation of soil behavior requires modeling the soil around the foundation or providing a substructure representation for the soil. In either case, the wavefront is increased substantially. Loading of the outer foundation is expected to be basically spread out over 12' and most severe for the empty tank case. Using the plane strain full condition subgrade modulus is a little conservative as opposed to the empty case. Consequently, the outer foundation will have

$$k_{ps12f} = 638.97 \quad \text{kcf} \qquad \frac{k_{ps12f}}{1.728} = 369.774 \quad \text{pci}$$

This value is tapered down to the axisymmetric full-condition value where the foundation thickness is tapered from 2' to 1'. For convenience of modification, the soil spring stiffnesses are modelled with a temperature dependent Young's modulus. Temperatures can be entered with the BE command.

Reference:

Holz, R.D., 1991, "Stress Distribution and Settlement of Shallow Soundations", Chapter 5 in Fang, "Foundation Engineering Hdbk", Van Nostrand.

Subject Side Soil Stats

Originator Edwards Date 9/27

Side Soil Pressure

Model side soil pressure for the DST using at-rest lateral pressure coefficient plus soil-springs for active-passive pressure effects.

From Grout vault soils report, Plate 7:

$K_o = 0.36$ (at-rest coeff)

$K_p = 3.0$ with 1.5 Safety factor

Use $K_p = 3.0/1.5 = 2.0$

$\Delta K = K_p - K_o = 2.0 - 0.36 = 1.6$

Passive pressure develops as follows (Plate 7)

δ/H	% Passive ΔK	$H = 38'$
.001	33	
.002	50	
.005	75	
.01	90	

Estimate δ (wall displacement) reqd'd)

Thermal $\delta = \alpha T R = 3.7e\text{-}6/°F\,(350-70°F)\times 4'$

$= 0.04' = 0.49"$

Dome load: use dome/wall ratio from A105 test report Figs 39 & 27 at 200 psf

$\delta_{wall} / \delta_{dome} = .024/.09 = .27$

ASME Fig 1 $\Rightarrow \delta_{dome} = 0.70"$

$\delta_{wall} = 0.27 \times 0.70" = 0.26"$

Subject 241-SY Soil Spring

Originator _____ Date _____

Include creep effect with 2x factor:

$\delta_{soil} = 0.26" \times 2 = 0.52"$

Thermal: $\frac{\delta}{H} = \frac{.04'}{36'} = .001$

Soil wt: $\frac{\delta}{H} = \frac{.52/12}{36'} = .001$

Use $\delta/H = .001$ data, likely overlying soft soil

σ_h Passive = 2.33 $\Delta K_s = 1.6$

Spring constant k (sym units)

$k' = \frac{P}{D Y_s} = \frac{2.33 \times 1.6}{.001 \times 22'} = \underline{\underline{13.9 \text{ kcf} = 1.16 \text{ kci}}}$

D = depth Y_s = soil density = 125 pcf

Evaluate soil springs:

Haunch D = 17.3' k = 13.9 x (18.3 x .125 = 32 kcf

Footing D = 56.7' k = 13.9 x 56.7 x .125 = 98. kcf

Compare footing soil-spring with thick cylinder result (Roarke Hired Table 13.3):

$\delta = \frac{pR}{E}(1+\nu)$

$\nu = 0.3$

For Phase I' $E_{ur} = K_{ur} P_a \left(P_3/P_a\right)^n$

$K_{ur} = 726.2$ $P_a = 14.7$ psi $= 2.12$ ksf

$P_3 = D\gamma_s = 57' \times .125 = 7.1$ $n = .72$

$E_{ur} = 726.2 \times 2.12 \left(7.1/2.12\right)^{.72} = 3730$ ksf

Page ____ of ____

Subject Side Soil Springs

Originator ____ Date ____

$E = E_{sec}$ $R = 41.5'$

$$K = \frac{P}{\delta} = \frac{E}{R(1+\nu)} = \frac{3330}{41.5 \times 1.3} = 69 \text{ kcf}$$

which compares with 98 kcf OK (Conc)

Soil Spring Elements

Use the SHELL membrane shell element. Nodes on the radial plane are coupled to one another, so the soil element need only be input in the θ plane.

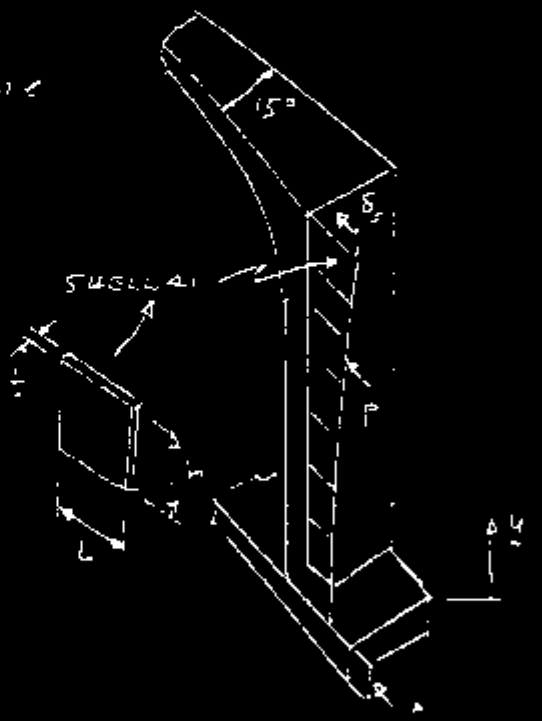

Vary L to get proper K vs depth:

$$K = \frac{EA}{L} \qquad A = Lh$$

$$K\ (\text{sqm}) = \frac{K}{A} = \frac{E}{L}$$

Top point (crown of dome) $y = 584.8$

Total $\Delta y = 8.1 \times 12 = 97.2"$

$\therefore D = 0 \Rightarrow y = 584.8 + 97.2 = 682" \equiv y_0$

$$K = K' D \gamma_s = \frac{E}{L} \qquad D = y_0 - y$$

$$L = \frac{E}{K'(y_0 - y)\gamma_s}$$

Subject 5.6 - Soil Effects

Originator _____ Date _____

Choose $L = 1'$ at haunch where $D = D_h = 18.5'$

$$E = L k' D \gamma_s = 1.0 \times 13.9^{\#}/_{ft^3} \times 18.5 \times .125$$
$$= 31.5 \text{ ksf} = 221 \text{ psi}$$

If the wall were stiff, then a uniform displacement δ_s would suffice to implement K_a:

$$p = K_a \gamma_s D = E \frac{\delta_s}{L}$$

$$\therefore \quad \delta_s = \frac{K_a \gamma_s D}{E/L} = \frac{K_a}{k'} = \frac{0.26}{1.16\ ^{\#}/_{in^3}} = 0.31''$$

The wall, however, gives somewhat, so apply the pressure

$$q = K_a (\gamma_a - \gamma_w) \gamma_s T \qquad [^{\#}/_{in}]$$

$$t = (9.5 \times 12 - 8) \frac{15^{\circ}}{57.3} = 1.72''$$

$\uparrow$ Lave

and then find δ_s vs $\frac{L}{D}$ and apply as a constraint. Attached are the plots showing the result. For convenience, the path includes some air in order to pick up the outside of the foundation. Minor readjustment of δ_s was done on the foundation.

Subject _____

Originator _____ Date _____

Reference

Dames & Moore, 1989, Report, Geotechnical and Corrosion Investigation, Grout Vaults, Hanford, Washington, Contract No. 87059-255-001, Dames & Moore, Seattle, Washington.

Lateral Earth Pressures as Function of Magnitude of Wall Movement

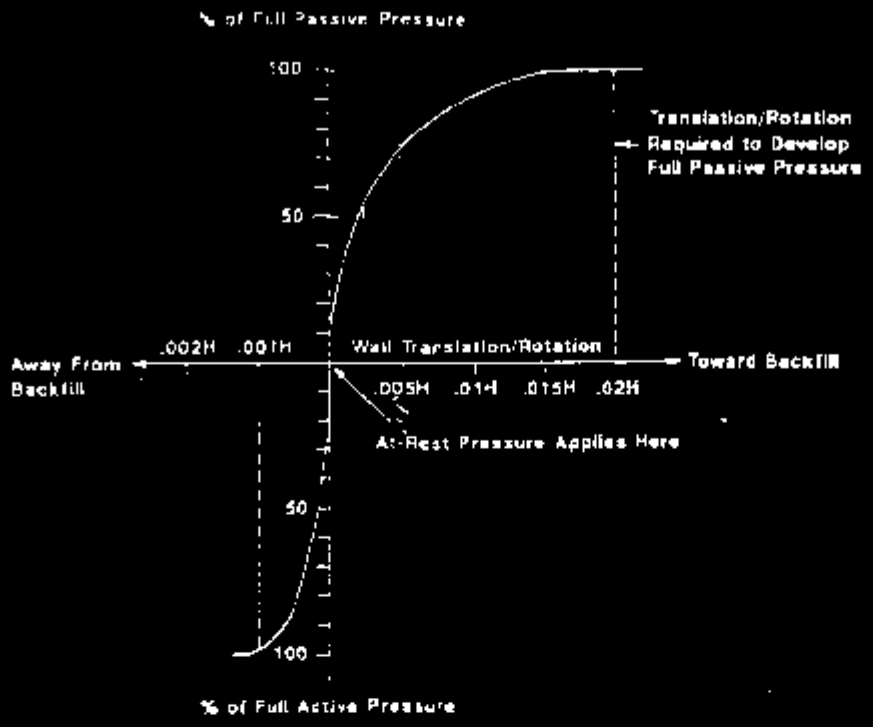

Lateral Earth Pressure Coefficients for Fully Developed Pressures

	AT-REST		ACTIVE		PASSIVE*	
	Static	Dynamic	Static	Dynamic	Static	Dynamic
Horizontal Backfill	0.36	0.60	0.23	0.39	3.0	2.5
Sloping Backfill (1.5 : 1)	0.43	0.72	0.41	0.65		

*Factor of safety = 1.5 applied

Wall Movement Required to Develop Full Lateral Earth Pressures

	TRANSLATION OR WALL ROTATION**		WALL DEFORMATION***	
	Active	Passive	Active	Passive
Horizontal or Sloping Backfill	.001	+.02	-.42"	+8.4"

**Wall rotation or translation = δ/H, where δ is horizontal deformation of the wall (- values indicate movement away from backfill, + values indicate movement toward backfill), H is the wall height.

***Indicates horizontal wall deformation of 28 foot high wall.

Lateral Earth Pressure Recommendations
Grout Vaults - Hanford, WA

October 10, 1988

Dames & Moore

Job No. 10805-282-016

Plate 7

ANSYS 5.1
SEP 21 1995
19:40:55
POST1
STEP=1
SUB =17
TIME=1
PATH PLOT
NOD1=4C3
NOD2=4810

ZV =1
DIST=0.75
XF =0.5
YF =-0.5
ZF =0.5
CENTROID HIDDEN

1
ANSYS 5.1
SEP 19 1995
17:16:29
POST1
STEP=1
SUB =20
TIME=1
PATH PLOT
NOD1=403
NOD2=4810
ZV =1
DIST=0.75
XF =0.5
YF =0.5
ZF =0.5
CENTROID HIDDEN
-5
-6.5
-8
-9.5
-11
-12.5
-14
-15.5
-17
-18.5
-20
SX, psi
SX
0
55
110
165
220
275
330
385
440
495
550
DIST, in from bearmch
DST soil pressure application

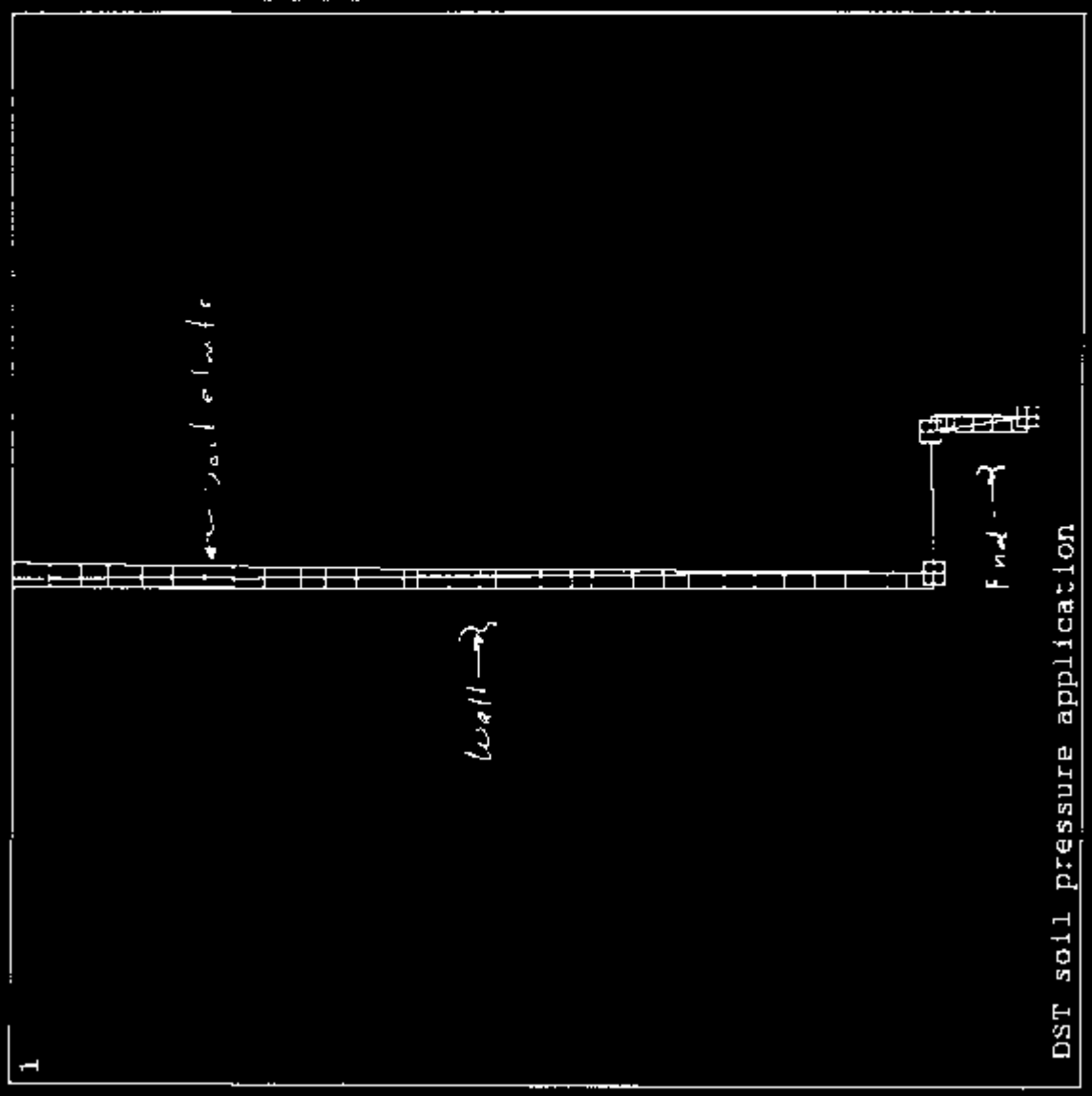
ANSYS 5.1
SEP 19 1995
12:23:27
ELEMENTS
TYPE NUM
PATH
ZV =1
*DIST=132.765
*XF =507.95
*YF =96.295
*ZF =-69.493
1
DST soil pressure application